

**Functional studies of yeast mutants reveal mechanisms for
TRAPP-complex integrity**

Stephanie Brunet
A Thesis in
The Department
of
Biology

**Presented in Fulfillment of the Requirements
For the Degree of Doctor of Philosophy at
Concordia University
Montreal, Quebec, Canada**

March 2015

© Stephanie Brunet, 2015

**CONCORDIA UNIVERSITY
SCHOOL OF GRADUATE STUDIES**

This is to certify that the thesis prepared

By: Stephanie Brunet

Entitled: Functional studies of yeast mutants reveal mechanisms for TRAPP-complex integrity

and submitted in partial fulfillment of the requirements for the degree of

Doctor of Philosophy (Biology)

complies with the regulations of the University and meets the accepted standards with respect to originality and quality.

Signed by the final examining committee:

_____ Chair
Dr. C. Wilds

_____ External Examiner
Dr. J. Presley

_____ External to Program
Dr. P. Joyce

_____ Examiner
Dr. A. Piekny

_____ Examiner
Dr. R. Storms

_____ Thesis Supervisor
Dr. M. Sacher

Approved by: _____
Dr. S. Dayanandan, Graduate Program Director

March 16, 2015 _____
Dr. A. Roy, Dean
Faculty of Arts and Science

Abstract

Functional studies of yeast mutants reveal mechanisms for TRAPP-complex integrity

Stephanie Brunet, PhD

Concordia University, 2015

Proteins and lipids are packaged into membrane bound vesicles and transported throughout the cell in a highly regulated process called membrane trafficking. Several categories of proteins including tethering factors, cooperate to ensure fidelity in this process that function as a physical link between a vesicle and the correct target membrane. The transport protein particle (TRAPP) complex is a multisubunit tethering complex that has been well characterized in yeast and is highly conserved in mammals. In yeast, three isoforms of the complex (TRAPPI, TRAPPII and TRAPPIII) have been described each acting in different membrane trafficking pathways. My research has focused on studying yeast TRAPP mutants to understand how specific subunits contribute to TRAPP-complex integrity and how each complex regulates distinct membrane trafficking pathways.

Several mutations in the human TRAPPC2 gene including a missense mutation of a highly-conserved aspartic acid residue (TRAPPC2D47Y), are linked to the skeletal disorder spondyloepiphyseal dysplasia tarda (SED), Chapter 2 discusses how the analogous mutation in the yeast homologue, *TRS20*, destabilizes the TRAPPIII complex and disrupts TRAPPIII-regulated membrane trafficking pathways, providing insight into the etiology of SED.

Chapter 3 of this thesis describes a mutational study that I conducted on the essential yeast TRAPP subunit, Trs23p. When a non-essential *Saccharomycotina*-specific (SMS) domain within this protein is deleted, TRAPPI, the smallest of the complexes, is destabilized however processes regulated by TRAPPI are not compromised. TRAPPII and TRAPPIII contain all the subunits of the smaller TRAPPI complex and I propose that TRAPPI is a fragment or assembly intermediate of the larger complexes.

Finally, in Chapter 4 I present evidence for a direct interaction between the TRAPPII complex and Gyp6p, a GTPase accelerating protein (GAP) for the small Rab GTPase Ypt6p. In mutants that destabilize the TRAPPII complex this interaction is disrupted and Ypt6p localization to the late Golgi compartment is increased relative to wild type. Together these results indicate that the interaction between TRAPPII and Gyp6p is important for regulating the dynamic distribution of Ypt6p within the cell.

Acknowledgments

I have been fortunate to receive a tremendous amount of guidance, support and advice throughout my graduate studies. I would like to thank my supervisor Dr. Michael Sacher for mentoring me and providing invaluable feedback during my studies. Thank you for continually encouraging me and always having time to discuss my research. I would also like to thank my committee members Dr. Alisa Piekny and Dr. Reginald Storms for their helpful suggestions and critical feedback.

I was never at a loss when seeking help within the Biology Department at Concordia. I would like to especially thank Dr. Christopher Brett and Dr. Vladimir Titorenko for discussions and reagents. I would also like to thank CMCI for the use of equipment and Melina for your help and patience.

I would like to extend my gratitude to Dr. Charles Barlowe for collaborating with my research as well as Dr. Akihiko Nakano, Dr. Nava Segev and Dr. Ruth Collins for reagents.

Thank you to all of my colleagues and friends at Concordia for helping me with my research and creating such a wonderful work environment. I would like to especially thank Djenann, Benedeta, Nassim, Baraa, Miroslav, Daniela, Sari, James, Adrian, Sok, Audrey, Debora, Keshika, Hart, Rodney, Madhav and Qingchuan.

Finally, I would like to thank my family, Amanda, Mom, Dad, Andrea, Phil, Maria and Battista, for supporting me unconditionally in everything that I do.

I am grateful for the funding I received from Concordia University, CIHR, FQRNT and GRASP throughout my studies.

Table of contents

Chapter 1: Introduction	1
1.1 Membrane trafficking in yeast.....	1
1.1.1 The secretory pathway.....	1
1.1.2 The endocytic pathway	3
1.1.3 Autophagy	4
1.2 Several proteins cooperate to regulate membrane trafficking.....	6
1.2.1 Vesicle coats.....	7
1.2.2 Tethering factors	8
1.2.4. SNARES.....	11
1.3 TRAPP: a conserved multisubunit tethering complex.....	12
1.3.1 The discovery of three TRAPP complexes in yeast	12
1.3.2 Structure and composition of the three yeast TRAPP complexes	14
1.3.2.1 TRAPPI core crystal structure.....	14
1.3.2.2 TRAPPII EM structure	16
1.3.2.3 TRAPPIII EM structure.....	16
1.3.3 TRAPP as a GEF	17
1.3.3.1 TRAPPIs a GEF for Ypt1p:	17
1.3.3.2 TRAPPII may be a GEF for Ypt32	18
1.3.4 TRAPPI, II, and III act in different membrane trafficking pathways	18
1.3.4.1 TRAPPI is essential for ER-Golgi trafficking	18
1.3.4.2 TRAPPII carries out functions at the late Golgi	20
1.3.4.3 TRAPPIII regulates endocytosis and autophagy	22
1.3.5 Mammalian TRAPP complexes.....	25
1.3.6 Mutations in the human Trs20 homologue TRAPPC2 cause SEDT	26
1.4 The purpose of my thesis:.....	27
Chapter 2: A <i>trs20</i> mutation that mimics an SEDT-causing mutation blocks selective and non-selective autophagy: a model for TRAPPIII organization	29
2.1 Introduction	29
2.2 Materials and methods	31
2.2.1 Yeast strains and molecular biological techniques	31
2.2.2 Yeast two-hybrid analysis.....	32
2.2.3 Cell culture and immunoprecipitation	32
2.2.4 Yeast trafficking assays	32
2.2.5 Preparation of yeast cell lysates	33
2.2.6 Optiprep gradient assay.....	33
2.2.7 Recombinant protein expression and <i>in vitro</i> binding	34
2.2.8 Acyl-biotin exchange.....	34
2.3 Results.....	35
2.3.1 Binding of TRAPPC2 to Syntaxin 5 is dependent upon the D47 residue in TRAPPC2	35
2.3.2 The yeast mutant <i>trs20D46Y</i> does not prevent processing of carboxypeptidase Y	38

2.3.3 The <i>D46Y</i> mutation in <i>trs20</i> affects its interactions with TRAPP ^{II} and III proteins	39
2.3.4 <i>trs20D46Y</i> phenocopies <i>trs85Δ</i> in both GFP-Snc1p recycling and Calcofluor white hypersensitivity	41
2.3.5 TRAPP ^{III} is destabilized in the <i>trs20D46Y</i> mutant.....	44
2.3.6 Autophagy is defective in the <i>trs20D46Y</i> mutant.....	46
2.3.7 Trs20p and Tca17p have differing functions.....	49
2.3.8 The molecular size of TRAPP ^{III} depends upon membranes and Atg9p	50
2.3.9 Palmitoylated Bet3p is enriched in TRAPP ^{III}	54
2.4 Discussion	55
2.4.1 Complexities in TRAPP ^{III} assembly and function.....	56
2.4.2 Trs20p as an adaptor protein	58
2.4.3 Implications for SEDT	59
Chapter 3: The SMS domain of Trs23p is responsible for the <i>in vitro</i> appearance of the TRAPPI complex in <i>Saccharomyces cerevisiae</i>	60
3.1 Introduction	60
3.2 Materials and methods	63
3.2.1 Strain construction	64
3.2.2 Spotting	65
3.2.3 Preparation of yeast lysates	65
3.2.4 Sucrose gradient fractionation and membrane floatation	66
3.2.5 Membrane extraction.....	66
3.2.6 Size exclusion chromatography	66
3.2.7 Recombinant protein	67
3.2.8 Bacterial lysates	67
3.2.9 Guanine nucleotide exchange factor (GEF) assays.....	67
3.2.10 <i>In vivo</i> and <i>in vitro</i> trafficking assays	68
3.2.11 Yeast two-hybrid assay.....	69
3.2.12 Chemical crosslinking	69
3.3 Results.....	69
3.3.1 Neither the carboxy-terminal 99 residues nor the SMS domain of Trs23p are essential	69
3.3.2 The SMS domain is required for efficient assembly of recombinant TRAPPI.....	72
3.3.3 The SMS domain contributes to Trs23p interactions.....	74
3.3.4 <i>trs23ΔSMS</i> retains Ypt1p GEF activity in yeast lysates.....	75
3.3.5 <i>trs23ΔSMS</i> contain only a single TRAPP peak at physiological salt.....	76
3.3.6 TRAPP ^{II} /III provides Ypt1p GEF activity in <i>trs23ΔSMS</i>	80
3.3.7 <i>trs23ΔSMS</i> does not display defects in membrane traffic.....	81
3.3.8 TRAPPI can form from TRAPP ^{II} /III <i>in vitro</i>	86
3.3.9 TRAPPI appearance is SMS domain-dependent	88
3.4 Discussion	89
Chapter 4: TRAPP ^{II} mediates Ypt6p dynamics at the late Golgi	93
4.1. Introduction:.....	93
4.2 Materials and methods	95
4.2.1 Strain construction	97

4.2.2 Tandem affinity purification (TAP) and mass spectrometry	97
4.2.3 Immunoprecipitations.....	98
4.2.4 Serial dilutions.....	99
4.2.5 Microscopy and Quantification of microscopy.....	99
4.2.6 Yeast two hybrid	99
4.2.7 Subcellular fractionation	99
4.3. Results:.....	100
4.3.1. TRAPP II interacts directly with Gyp6.....	100
4.3.2 <i>YPT6</i> and its GEF interact genetically with TRAPP II subunits.....	103
4.3.3 The integrity of TRAPP II is important for interacting with Gyp6	104
4.3.4 Ypt6p is enriched at the late Golgi in a <i>trs65Δ</i> mutant	106
4.3.5. The localization pattern of GFP-Ypt6p varies between wild type and mutant strains	108
4.4 Discussion:.....	109
Chapter 5: Discussion.....	112
5.1. Distinct TRAPP complexes can be resolved biochemically and functionally	112
5.1.1 Resolution of the yeast TRAPP complexes is dependent upon lysis conditions.	112
5.1.2 TRAPP III mediates the tethering of Atg9p vesicles in non-selective and selective autophagy pathways	114
5.1.3 Bet3p palmitoylation is important for TRAPP III function.....	116
5.1.4 A mutation that causes SEDT in humans prevents the association of Trs85p with the TRAPP core in yeast.....	117
5.2 TRAPP regulates membrane trafficking pathways by interacting with GTPases and their modifying proteins	118
5.3 Conclusions and future directions:	119
Chapter 6: References	120

List of Figures

Figure 1.1 Proteins are transported throughout the cell via multiple membrane trafficking pathway.....	3
Figure 1.2 Selective and non-selective autophagy pathways transport cargo is to the vacuole for degradation.....	6
Figure 1.3 The rab cycle.....	11
Figure 1.4 The structure and composition of yeast and mammalian TRAPP complexes.....	15
Figure 1.5 TRAPPI, II and III act in multiple membrane trafficking pathways...	20
Figure 1.6 TRAPPIII localizes to the PAS and regulates selective and non-selective autophagy through different pathways.....	24
Figure 2.1 TRAPPC2 binds to Syntaxin 5 by yeast two hybrid.....	36
Figure 2.2 TRAPPC2 binds to Syntaxin 5 <i>in vitro</i> and <i>in vivo</i>	37
Figure 2.3 TRAPPC2 binds to SNARE complexes.....	38
Figure 2.4 <i>trs20D46Y</i> does not block trafficking of carboxypeptidase Y.....	39
Figure 2.5 The <i>trs20D46Y</i> mutation disrupts the interaction of Trs20p with TRAPPII and TRAPPIII specific subunits.....	40
Figure 2.6 Genetic interactions affected by <i>trs20D46Y</i>	41
Figure 2.7 <i>trs20D46Y</i> and <i>trs85Δ</i> do not block general secretion.....	42
Figure 2.8 <i>trs20D46Y</i> and <i>trs85Δ</i> strains are sensitive to Calcofluor white.....	43
Figure 2.9 The <i>trs20D46Y</i> mutant phenocopies the GFP-Snc1p recycling defect observed in <i>trs85Δ</i> cells.....	44
Figure 2.10 The levels of Trs85p are reduced in <i>trs20D46Y</i>	45
Figure 2.11 TRAPPIII is destabilized in <i>trs20D46Y</i>	46
Figure 2.12 Both selective and non-selective autophagy are affected in <i>trs20D46Y</i>	47
Figure 2.13 GFP-Ape1 accumulates in <i>trs20D46Y</i> under non-starvation conditions.....	48

Figure 2.14 Tca17p is important for the integrity of TRAPP ^{II} but not TRAPP ^{III}	50
Figure 2.15 The molecular size of TRAPP ^{III} is dependent upon membranes.....	51
Figure 2.16 The molecular size of TRAPP ^{III} is dependent upon Atg9p.....	53
Figure 2.17 Both selective and non-selective autophagy are affected in <i>bet3C80S</i>	54
Figure 2.18 Lipidated Bet3p is enriched in TRAPP ^{III}	55
Figure 2.19 Model for the organization and assembly of TRAPP ^{III}	57
Figure 3.1. Growth properties of <i>trs23</i> mutations.....	71
Figure 3.2 Assembly and function of recombinant TRAPP containing the <i>trs23</i> Δ 99C and <i>trs23</i> Δ SMS proteins.....	73
Figure 3.3 The SMS domain of Trs23p contributes to the strength of Trs23p-TRAPP subunit interactions.....	75
Figure 3.4 GEF activity is unaffected in <i>S. cerevisiae</i> containing <i>trs23</i> Δ SMS.....	76
Figure 3.5 A single TRAPP peak is detected in <i>trs23</i> Δ SMS at physiological salt concentrations.....	78
Figure 3.6 TRAPP ^{II} and TRAPP ^{III} are distinct complexes.....	80
Figure 3.7 Only fractions containing TRAPP ^{II/III} display Ypt1p GEF activity in <i>trs23</i> Δ SMS.....	81
Figure 3.8 CPY trafficking is unaffected in the <i>trs23</i> Δ SMS mutant.....	82
Figure 3.9 Snc1p recycling is unaffected in the <i>trs23</i> Δ SMS mutant.....	83
Figure 3.10 Ypt31p is correctly localized in the <i>trs23</i> Δ SMS mutant.....	84
Figure 3.11 The Cvt pathway is normal in the <i>trs23</i> Δ SMS mutant.....	85
Figure 3.12 Lysates from the <i>trs23</i> Δ SMS mutant are competent for <i>In vitro</i> ER-to-Golgi trafficking.....	86
Figure 3.13 TRAPP ^I can form from TRAPP ^{II/III}	87
Figure 3.14 <i>P. pastoris</i> does not contain a TRAPP ^I peak.....	88
Figure 4.1 Gyp6p interacts with the TRAPP ^{II} complex through Trs130p.....	101
Figure 4.2 TRAPP ^{II} subunits genetically interact with <i>YPT6</i> pathway genes.....	104

Figure 4.3 TRAPP ^{II} co-precipitates with endogenous Gyp6p-HA.....	105
Figure 4.4 GFP-Ypt6p becomes enriched at the late Golgi in a <i>trs65Δ</i> mutant..	107
Figure 4.5 Co-localization of GFP-Ypt6p with the early Golgi is decreased in a <i>trs65Δ</i> and <i>gyp6Δ</i> mutant.....	108
Figure 4.6 Higher frequencies of large punctae are seen in <i>trs65Δ</i> and <i>gyp6Δ</i> mutants.....	109
Figure 5.1 The SMS domain of Trs23p stabilizes the TRAPP core in yeast.....	114
Figure 5.2 Ypt1p recruits effectors specific to non-selective and selective autophagy pathways.....	116

List of Tables

Table 1.1 Yeast and mammalian TRAPP subunits.....	13
Table 3.1 Yeast strains used in Chapter 3.....	63
Table 4.1 Plasmids used in Chapter 4.....	95
Table 4.2 Yeast strains used in Chapter 4.....	95
Table 4.3 Summary of a subset of TRAPP ^{II} interactors by tandem affinity purification and mass spectrometry.....	102

List of abbreviations

3-aminotriazole	3AT
4-(2-hydroxyethyl)-1-piperazineethanesulfonic acid	HEPES
5-fluoroorotic acid	5-FOA
ADP ribosylation factor 1	Arf1
α -mannosidase	Ams
Aminopeptidase I	Ape1
Calcofluor white	CFW
Carboxypeptidase Y	CPY
Class C core vacuole/endosome tethering	CORVET
Cold sensitive	cs
Complex Associated with Tethering Containing Helical Rods	CATCHR
Conserved oligomeric Golgi	COG
Cytosol to vacuole targeting	Cvt
Dimethyl sulfoxide	DMSO
dithiobis[succinimidyl] propionate	DSP
Dithiothreitol	DTT
Early endosome	EE
Electron microscopy	EM
Endoplasmic reticulum	ER
Endoplasmic reticulum exit sites	ERES

ER-Golgi Intermediate Compartment	ERGIC
<i>Escherichia coli</i>	<i>E. coli</i>
Ethylenediaminetetraacetic acid	EDTA
Golgi apparatus	Golgi
Golgi-associated retrograde protein	GARP
Green fluorescent protein	GFP
GTPase accelerating protein	GAP
GTPase dissociation inhibitor	GDI
Guanine nucleotide exchange factor	GEF
Guanosine-5'-diphosphate	GDP
Guanosine-5'-triphosphate	GTP
Hemagglutinin	HA
Homotypic fusion and vacuole protein sorting	HOPS
Late endosome	LE
Multisubunit tethering complex	MTC
Multivesicular body	MVB
<i>N</i> -ethylmaleimide	NEM
Plasma membrane	PM
Polymerase chain reaction	PCR
Pre-autophagosomal structure	PAS
Precursor aminopeptidase 1	prApe1
Pro-collagen II	PCII
Red fluorescent protein	RFP

<i>Saccharomycotina</i> specific domain	SMS
SDS polyacrylamide electrophoresis	SDS-PAGE
Synthetic defined	SD
Small Rab GTPase	Rab
Soluble <i>N</i> -ethylmaleimide-sensitive factor attachment protein receptor	SNARE
Spondyloepiphyseal dysplasia tarda	SED
Standard error of the mean	SEM
Tandem affinity purification	TAP
Temperature sensitive	ts
Transport protein particle	TRAPP
Tre-2, Bub2, Cdc16	TBC
Vesicular stomatitis virus-glycoprotein	VSV-G
Yeast extract. peptone, dextrose	YPD

Chapter 1: Introduction

1.1 Membrane trafficking in yeast

Eukaryotic cells contain organelles, each having a different protein and lipid composition essential for their function. Membrane trafficking describes the movement of proteins and lipids between different cellular compartments to maintain organelle homeostasis. Specificity in membrane trafficking is critical for cell viability to ensure that proteins and lipids are distributed to the correct organelle, allowing each organelle to perform a specialized function. Errors in membrane trafficking have been linked to a large spectrum of diseases, underlying the importance of understanding this process (Aridor and Hannan, 2000, 2002). Many of the genes required for membrane trafficking were identified by mutational studies of the yeast *Saccharomyces cerevisiae* in the lab of Randy Schekman (Novick *et al.*, 1980). There is a high degree of conservation between yeast and human membrane trafficking pathways making yeast a very powerful tool for studying this process. A number of genetic tools are available for studying yeast and the reduced complexity of unicellular yeast permits the elucidation of membrane trafficking mechanisms in higher, multicellular eukaryotic organisms. Proteins are transported along pre-determined pathways that are categorized by the organelles they contain. The two principle membrane trafficking pathways in eukaryotes are the secretory and endocytic pathways.

1.1.1 The secretory pathway

In cells, approximately one third of proteins travel through the secretory pathway which begins at the endoplasmic reticulum (ER) and ends at the plasma membrane (PM) (Figure 1.1) (Barlowe and Miller, 2013). Proteins synthesized at the ER and destined for the secretory pathway are packaged into membrane bound compartments called vesicles, and transported to the Golgi apparatus (Golgi) (Bonifacino and Glick, 2004). In mammals individual Golgi cisternae are stacked into a structure with a cis and trans face, and cargo coming from the ER enters at the cis face and exits the Golgi at the trans face. In *Saccharomyces cerevisiae* (herein referred to as yeast) Golgi cisternae do not form stacks, but they can be categorized into early, medial and late cisternae; cargo from the ER enters

the early Golgi first and exits from the late Golgi (Klumperman, 2011; Suda and Nakano, 2012). The anterograde movement of cargo through the Golgi (cis-to-trans direction) may occur at least in part by a process called cisternal maturation, where early cisternae undergo a gradual transformation into late cisternae (Losev *et al.*, 2006; Matsuura-Tokita *et al.*, 2006). The transformation of early cisternae to late cisternae is mediated by the retrograde (trans-to-cis direction) transport of Golgi resident enzymes from late cisternae to earlier cisternae by vesicular transport (Suda and Nakano, 2012). Cargo exiting the late Golgi are packaged into vesicles and transported to different destinations such as the PM (to be secreted outside the cell or embed within the plasma membrane) and organelles of the endocytic pathway (Suda and Nakano, 2012).

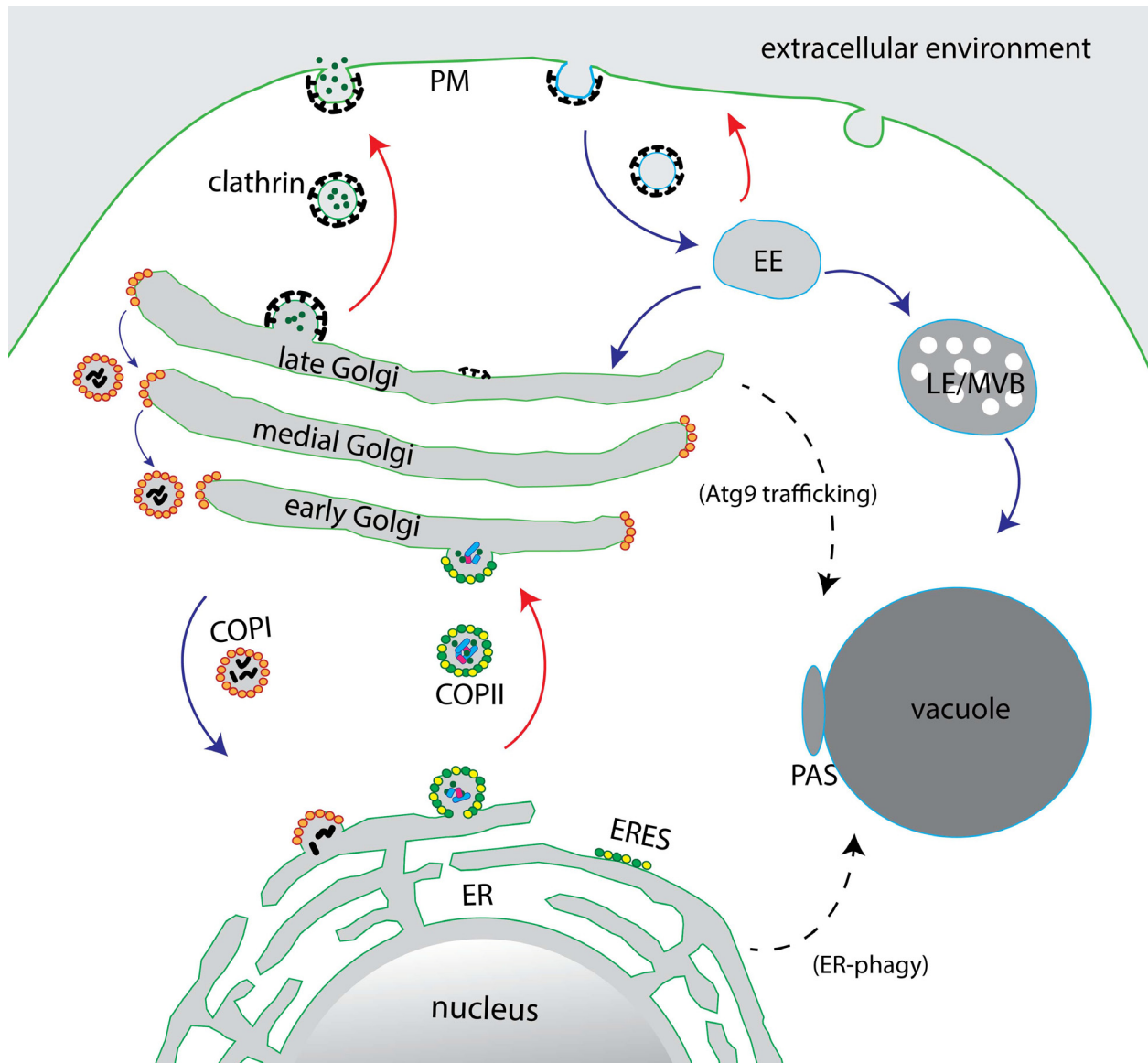


Figure 1.1 Proteins are transported throughout the cell via multiple membrane trafficking pathways. Arrows indicate the direction of movement of vesicles (COPI, COPII and clathrin) between cellular compartments (red indicates anterograde movement, blue indicates retrograde movement and dashed lines indicate autophagy pathways). Membranes of the secretory pathway are outlined in green and endocytic membranes are outlined in blue. (abbreviations: early endosome (EE), late endosome (LE), multivesicular body (MVB), plasma membrane (PM))

1.1.2 The endocytic pathway

The endocytic pathway is responsible for internalization of material from the cell surface and external environment. Vesicles bud from the cytosolic face of the PM and move towards the cell interior where they fuse with endosomes (Figure 1.1) (Baggett and

Wendland, 2001). Endosomes act like sorting stations for cargo and endocytosed material can be sent to various destinations. Cargo can be recycled back to the PM, either directly or through intermediates such as the late Golgi, or travel to the vacuole for degradation via late endosomes/multivesicular bodies (MVBs) (Lemmon and Traub, 2000). The endocytic pathway balances protein input from the secretory pathway through protein internalization, degradation and recycling.

1.1.3 Autophagy

Autophagy is one of the principle pathways in cells for the degradation of proteins and entire organelles. It is conserved among lower and higher eukaryotes but has been extensively studied in yeast. Autophagy pathways can be categorized as macro- and micro-autophagy, and can be further subdivided into selective or non-selective autophagy (Reggiori and Klionsky, 2013). In macroautophagy, material within the cytoplasm is packaged into double membrane vesicles called autophagosomes and subsequently delivered to the interior of the vacuole for degradation by fusion of the autophagosome with the vacuole membrane (Baba *et al.*, 1994). Direct internalization of cargo into the vacuole by membrane invagination, without the need for additional membranes, is called microautophagy (Reggiori and Klionsky, 2013). Genetic screens in yeast have identified a network of over 30 proteins (given the prefix Atg) that are required for autophagy (Tsukada and Ohsumi, 1993; Thumm *et al.*, 1994; Harding *et al.*, 1995). While some Atg proteins are specific to either selective or non-selective autophagy (see below), many function in all autophagy pathways and are considered components of the core autophagy machinery.

Selective macroautophagy is a constitutive process that involves the transport of specific cargo and organelles from the cytosol to the vacuole. The cytosol to vacuole targeting (Cvt) pathway in yeast is a well-studied example of selective autophagy where vacuole resident enzymes synthesized in the cytosol are delivered to the vacuole (Figure 1.2). In this pathway, the vacuolar enzymes, Aminopeptidase I (Ape1) and α -mannosidase,

are selectively packaged into double membrane vesicles called Cvt vesicles that fuse with the vacuole (Scott *et al.*, 1997; Shintani *et al.*, 2002).

Unlike selective macroautophagy, non-selective macroautophagy is described as “self eating” and is induced in response to stress such as nutrient starvation (Mizushima and Klionsky, 2007). When nutrients are unavailable in the environment cytosolic contents are delivered to the vacuole by this process and degraded, to be recycled for essential anabolic processes. Cytosolic components are non-selectively packaged into nascent autophagosomes that fuse with the vacuole once they are fully formed (Figure 1.2). Autophagosomes are much larger than Cvt vesicles, likely due to the non-selective nature of their contents (Baba *et al.*, 1997). While many Atg proteins function specifically in selective autophagy, only a few have been demonstrated to be specific for non-selective autophagy, including the scaffold protein Atg17p (Figure 1.2) (Kamada *et al.*, 2000; Kawamata and Kamada, 2008).

Atg proteins localize to a structure adjacent to the vacuole called the pre-autophagosomal structure (PAS), which is understood to be the site of autophagosome/Cvt vesicle formation (Suzuki *et al.*, 2001; Kawamata and Kamada, 2008). Membranes from the secretory and endocytic pathways are brought to the PAS and incorporated into growing autophagosomes and Cvt vesicles (Figure 1.2) (Dunn, 1990; Reggiori *et al.*, 2004; Ohashi and Munro, 2010; Taylor *et al.*, 2012). A clear link between autophagy and secretory pathways is the transmembrane protein Atg9p, which is delivered to the PAS through the secretory system and is required for PAS formation (Figure 1.2) (Noda *et al.*, 2000; Yamamoto *et al.*, 2012). The movement of Atg9p-containing membranes to the PAS could represent an important mechanism for feeding membranes into macroautophagic pathways (Yamamoto *et al.*, 2012). Like classical membrane trafficking pathways, autophagy involves the transport of cargo and lipids to a target compartment and there is some overlap with the machinery governing these different processes.

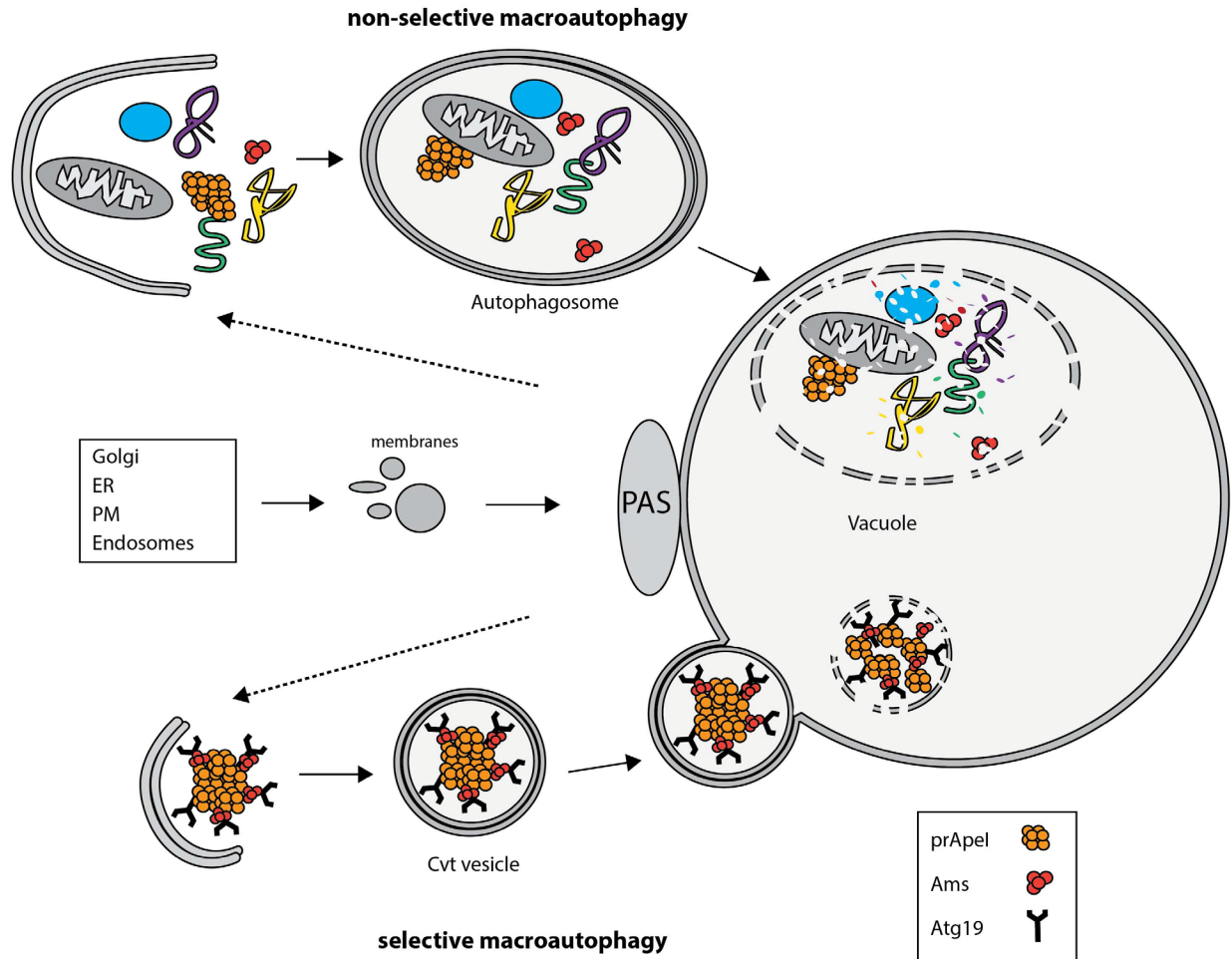


Figure 1.2 Selective and non-selective autophagy pathways transport cargo to the vacuole for degradation. Non-selective and selective (Cvt pathway) macroautophagy pathways are represented schematically. In the selective autophagy pathway oligomers of prApe1 (precursor aminopeptidase 1)/Ams (α -mannosidase) are packaged into Cvt vesicles and transported to the vacuole to be processed. In the non-selective autophagy pathway autophagosomes containing bulk cytosolic components (including Ape1/Ams1) are delivered to the vacuole for processing and degradation. Atg17p is a scaffold protein that is localized to the PAS and is required for non-selective autophagy pathways. Atg9p is a transmembrane protein that is required for PAS formation and is transported to the PAS on membranes from the secretory pathway.

1.2 Several proteins cooperate to regulate membrane trafficking

The vesicle transport hypothesis suggests that cargo is moved within the cell by being packaged into membrane bound vesicles that bud from one compartment and travel to another where they fuse and release their contents (Palade, 1975; Novick *et al.*, 1980;

Balch *et al.*, 1994). Vesicle transport is divided into a series of steps, each regulated by a different class of proteins: vesicle budding, mediated by coat proteins; vesicle tethering/docking, mediated by tethering factors and Rabs; and vesicle fusion, mediated by soluble *N*-ethylmaleimide-sensitive factor attachment protein receptors (SNAREs) (Bonifacino and Glick, 2004). These protein classes each add a layer of specificity to membrane trafficking pathways to ensure the fidelity that is essential for cell viability.

1.2.1 Vesicle coats

In the initial step of vesicle transport, vesicle coat proteins assemble at the site of vesicle budding to overcome the energy required for membrane deformation and vesicle formation (Barlowe *et al.*, 1994; Kirchhausen, 2000; Stachowiak *et al.*, 2013). Different coat protein complexes regulate different membrane trafficking pathways; the COPII coat acts in ER-Golgi trafficking, the COPI coat acts in retrograde trafficking through the Golgi and from the Golgi to the ER, and clathrin coat proteins regulate endocytosis and post Golgi transport (Figure 1.1). Although there are no common subunits shared between these vesicle coats, they do share organizational features as each contains an inner layer that is important for cargo selection and an outer layer that is necessary for coat polymerization and vesicle formation (Faini *et al.*, 2013). Coat proteins interact with molecular motors to transport cargo-containing vesicles along cytoskeletal tracks and downstream elements in vesicle transport such as tethering factors, Rabs and SNAREs to ensure that cargo arrive at the correct destination (Hehnlly and Starnes, 2007; Angers and Merz, 2011).

COPII coated vesicles assemble at ER exit sites (ERES) and the inner layer is formed by the Sec23p/Sec24p heterodimer that is recruited to the site of vesicle budding by the active form of Sar1p, a GTPase (Miller *et al.*, 2002). Sec23p/Sec24p recruits the outer layer proteins, Sec13p/Sec31p, which organize into a tetramer and polymerize around the budding vesicle to promote deformation of the membrane (Barlowe *et al.*, 1994).

Like COPII, COPI components are recruited to the site of vesicle budding by the GTPase protein ADP ribosylation factor 1 (Arf1p), following its activation by a guanine nucleotide exchange factor (GEF) (Serafini *et al.*, 1991). In yeast the proteins Gea1p and its

paralogue Gea2p act as the GEFs for Arf1p to initiate COPI vesicle formation (Peyroche *et al.*, 1996). COPI components are recruited to the membrane as a heptameric complex (also called coatomer) that polymerize and drive vesicle formation (Hara-Kuge *et al.*, 1994). Coatomer structure is well conserved between yeast and mammals with the inner layer consisting of β (Sec26p)-, δ (Ret2p)-, γ (Sec21p)-, and ζ (Ret3p)- COP and the outer layer consisting of α (Cop1p/Sec33p/Ret1p)-, β' (Sec27p)-, ε (Sec28p)- COP (yeast homologues are indicated in brackets) (Barlowe and Miller, 2013).

The inner layer of clathrin-coated vesicles is formed by adaptors that are either multimeric or monomeric and are specific to the site of vesicle budding (McMahon and Mills, 2004). Reminiscent of COPI, active Arf1p is also needed to recruit several of these adaptors complexes to the membrane to initiate vesicle formation (Stamnes and Rothman, 1993; Boehm *et al.*, 2001). Clathrin triskelions, containing three copies of the clathrin light chain and clathrin heavy chain proteins, are brought to specific locations by these adaptors and assemble into an interconnected protein cage to form the vesicle outer layer (Brodsky *et al.*, 2001; Fotin *et al.*, 2004).

While COPI, COPII and clathrin coated vesicles assemble differently, subunits that form the inner layer of coatomer (β , δ , γ and ζ) are homologous to subunits of forming the adaptor complexes of clathrin coated vesicles (Schledzewski *et al.*, 1999). Furthermore, while no sequence homology has been found among proteins forming the vesicle outer layers, structural studies show that proteins forming the vesicle outer layers share a similar organization of protein domains (Faini *et al.*, 2013).

1.2.2 Tethering factors

Tethering factors interact with proteins on the surface of vesicles and/or organelle membranes to help create a physical link between a vesicle and its target compartment. Two categories of tethering factors have been characterized: coiled-coil tethering factors that have an extended rod-like structure and mediate long distance tethering, and multisubunit tethering complexes (MTCs) that span a smaller distance and are implicated

in short distance tethering (Gillingham and Munro, 2003; Yu and Hughson, 2010). Nine MTCs have been identified in yeast and are differentially located throughout the endomembrane system, where they mediate tethering at specific target membranes (Sztul and Lupashin, 2006). MTCs can be grouped together based on the structure of subunit components and the pathways in which they act. The CATCHR (Complex Associated with Tethering Containing Helical Rods) family of MTCs have structurally homologous subunits. This family is composed of the complexes COG (conserved oligomeric Golgi), GARP (Golgi-associated retrograde protein), Dsl1 and the exocyst, which all function in the secretory pathway (Whyte and Munro, 2001, 2002; Yu and Hughson, 2010). CORVET (class C core vacuole/endosome tethering) and HOPS (homotypic fusion and vacuole protein sorting) act in the endocytic pathway and have 4 subunits in common (Peplowska *et al.*, 2007; Solinger and Spang, 2013). The final class of MTCs in yeast is the TRAPP family (transport protein particle), consisting of TRAPPI, TRAPPII and TRAPPIII which share 6 unique core subunits and function in ER-Golgi trafficking, post-Golgi trafficking and autophagy, respectively (Sacher *et al.*, 2001; Barrowman *et al.*, 2010; Lynch-Day *et al.*, 2010) (to be discussed in more detail below, see section 1.3). MTCs act as master coordinators by interacting with many proteins such as guanine nucleotide exchange factors (GEFs), GTPase accelerating proteins (GAPs), Rabs, Rab effectors, soluble *N*-ethylmaleimide-sensitive factor attachment protein receptors (SNAREs), coiled coil tethers and coat proteins, to ensure that vesicles interact with the appropriate target membrane (Cai *et al.*, 2007a; Jackson *et al.*, 2012).

1.2.3 Small Rab GTPases

Small Rab GTPases belong to the Ras superfamily of small GTPases and act as molecular switches that control different membrane trafficking pathways (Zerial and McBride, 2001). In yeast, eleven Rabs (with prefix Ypt) have been identified and over 60 Rabs have been characterized in mammalian cells, reflecting the higher level of complexity in mammalian trafficking pathways (Barr and Lambright, 2010). Rabs associate with membranes through a post-translational prenylation of cysteine residues in their carboxy-terminus and cycle between a membrane associated “active” state that is bound to GTP and an “inactive”, cytosolic state, that is bound to GDP (Figure 1.3) (Calero *et al.*, 2003; Seabra

and Wasmeier, 2004). GEFs activate Rabs by inducing conformational changes in the nucleotide-binding pocket to favor GDP release and allow GTP, which is present in excess over GDP in the cytosol, to bind (Bourne *et al.*, 1990; Bos *et al.*, 2007). GEFs are Rab-specific and promote the association of Rabs to membranes (Pfeffer, 2001). Effector proteins preferentially associate with active Rabs and are recruited to cellular membranes to initiate downstream events required for the docking and fusion of transport vesicles (Grosshans *et al.*, 2006). Coiled coil tethering factors are one class of proteins that act as Rab effectors while MTCs act as both effectors and GEFs for different Rabs (Short *et al.*, 2005; Cai *et al.*, 2007a).

GTPase activating proteins (GAPs) inactivate Rabs and promote membrane dissociation by increasing their intrinsic rate of GTP hydrolysis (Barr and Lambright, 2010). Whereas GEFs activate Rabs by different mechanisms, Rab-GAPs belong to the family of TBC (Tre-2, Bub2, Cdc16)-domain proteins and share the same catalytic domain (Pan *et al.*, 2006). Flanking residues on either side of the TBC domain in each GAP are responsible for substrate recognition but unlike GEFs, some GAPs have shown activity for more than one Rab (Strom *et al.*, 1993; Albert and Gallwitz, 1999). Once Rabs are inactive, they are recognized and extracted from membranes by GDI (GDP dissociation inhibitor), a chaperone that interacts with Rabs and masks the hydrophobic C-terminal prenyl groups (Garrett *et al.*, 1994).

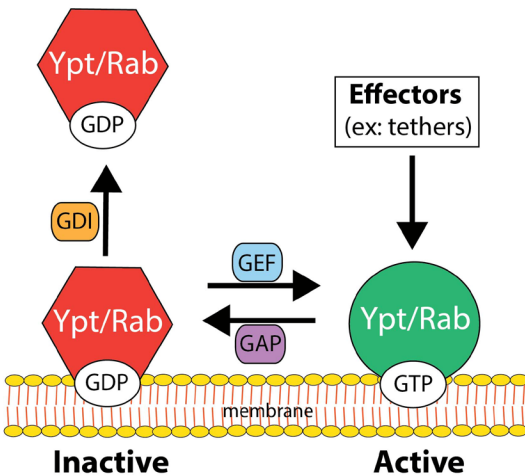


Figure 1.3 The rab cycle. Small Rab GTPases cycle between an active and inactive state through the action of GEFs (guanine nucleotide exchange factors) and GAPs (GTPase accelerating proteins), respectively. Active rabs initiate a pathway by recruiting effectors such as tethering factors that are required for downstream events. Chaperones called GDIs (GTPase dissociation inhibitors) extract inactive rabs from membranes.

1.2.4 SNARES

In the final step of vesicle transport a vesicle must fuse with a target membrane, an energetically unfavorable process that is overcome by a class of membrane-anchored proteins called SNAREs (soluble *N*-ethylmaleimide-sensitive factor attachment protein receptor) (Chen and Scheller, 2001). SNAREs are classified as either R- or Q-SNAREs by virtue of an arginine (R) or glutamine (Q) residue in their coiled-coil SNARE domain. Generally, but not in all cases, R-SNAREs localize to vesicles and Q-SNAREs to target membranes (Fasshauer *et al.*, 1998). When a vesicle and target membrane are in close apposition, 3 Q-SNAREs and 1 R-SNARE (contributed by both membranes), form a trans SNARE complex also known as a SNAREpin (Fasshauer *et al.*, 1998; Weber *et al.*, 1998). According to the “zipper” hypothesis, the SNAREs assemble, or zipper, from N-terminus to the membrane anchored C-terminus to drive the membranes together and overcome the energy barrier required for fusion to occur (Hanson *et al.*, 1997; Lin and Scheller, 1997). Immediately following membrane fusion the assembled SNARE complex is considered a cis-SNARE complex. Like tethering factors and Rabs, different SNAREs are associated with specific organelles and the possible combinations that could occur between Q- and R-

SNAREs contribute to specificity in membrane trafficking (Sollner *et al.*, 1993; Rothman and Warren, 1994).

1.3 TRAPP: a conserved multisubunit tethering complex

1.3.1 The discovery of three TRAPP complexes in yeast

The first transport protein particle (TRAPP) subunit identified in yeast was Bet3p (Blocked Early in Transport 3), a 22kDa protein shown to be essential for ER-Golgi transport (Rossi *et al.*, 1995). When Bet3p was immuno-isolated from a yeast lysate it was found in complex with nine additional subunits: Bet5p, Trs20p, Trs23p, Trs31p, Trs33p, Trs65p, Trs85p, Trs120p, and Trs130p (Table 1.1) (Sacher *et al.*, 1998). Subunits were named by their molecular weights with the exception of Bet5p whose gene had been previously identified as a high copy suppressor of a temperature sensitive *bet3* allele (Jiang *et al.*, 1998).

Initially, all ten subunits were believed to be part of the same complex but further experiments revealed that three TRAPP complexes, all containing Bet3p, were present in yeast and they could be separated by size and function. When yeast lysates were analyzed by size exclusion chromatography on a Superdex200 column, TRAPP was divided between a higher molecular weight peak at the void volume of the column (1MDa) and a lower molecular weight peak at approximately 300kDa (Sacher *et al.*, 2001). When the peaks were analyzed, three subunits, Trs65p, Trs120p and Trs130p, were only found in the higher molecular weight peak indicating that they are part of a separate complex. The larger and smaller complexes, which both contained the core subunits Bet3p, Bet5p, Trs20p, Trs23p, Trs31p and Trs33p, were named TRAPP^{II} and TRAPP^I, respectively (Table 1.1) (Sacher *et al.*, 2001).

Mammalian subunits	Yeast homologue	TRAPP complex
TrappC1	Bet5p	I / II / III
TrappC2	Trs20p	I / II / III
TrappC2L	Tca17p	II
TrappC3/C3L	Bet3p	I / II / III
TrappC4	Trs23p	I / II / III
TrappC5	Trs31p	I / II / III
TrappC6a/C6b	Trs33p	I / II / III
TrappC8	Trs85p	III
TrappC9	Trs120p	II
TrappC10	Trs130p	II
TrappC11	-	III
TrappC12	-	III
TrappC13	Trs65p	II (yeast) / III (mammals)

Table 1.1 Yeast and mammalian TRAPP subunits. Mammalian subunits and the corresponding yeast homologues are listed and their presence in TRAPPI (I), TRAPP II (II) and/or TRAPP III (III) is indicated. TRAPP core subunits are shaded in light blue.

Several years later, the separation of TRAPP complexes by size exclusion was revisited using a Superose 6 column, which has a much higher size exclusion limit. On this column the higher molecular weight peak was resolved into two separate peaks, one appearing at approximately 1000 kDa, containing TRAPP II specific subunits, and an additional peak at the void volume of the column (40MDa), containing Trs85p as well as the core subunits (Choi *et al.*, 2011). This new peak represented a third TRAPP complex and was designated TRAPP III. TRAPPI subunits but not TRAPP II-specific subunits (Trs65p, Trs120p and Trs130p) co-purified with Trs85p from yeast lysates, and vice versa, supporting the notion that TRAPP III was a bona fide complex, that had not been resolved from TRAPP II in earlier experiments (Lynch-Day *et al.*, 2010; Choi *et al.*, 2011).

Following the initial characterization of TRAPP_{II}, the additional TRAPP_{II} subunit, Tca17p, was discovered. Tca17p is a non-essential protein that was identified through its significant homology with the core subunit Trs20p (Montpetit and Conibear, 2009; Scrivens *et al.*, 2009).

In addition to their separation by size, TRAPP_I, II and III also display distinct subcellular localizations and are implicated in different cellular processes (Figure 1.5). TRAPP_{II} is localized to the late Golgi where it functions in both the endocytic and secretory pathway; TRAPP_{III} is essential for constitutive autophagy pathways and accordingly, resides at the PAS; TRAPP_I localizes to the early Golgi and is essential for ER-Golgi trafficking (Barrowman *et al.*, 2010).

1.3.2 Structure and composition of the three yeast TRAPP complexes

1.3.2.1 TRAPP_I core crystal structure

When individual yeast TRAPP subunits are expressed in *E. coli* they are largely insoluble. However, when all or a subset of subunits are co-expressed they assemble to form a soluble complex or sub-complexes (Kim *et al.*, 2006). In this way, the structure of recombinant TRAPP_I was determined by single particle electron microscopy (EM) to a resolution of 30 Å. The complex has a bi-lobed and elongated structure and is 180 Å x 65 Å x 50 Å (length x width x height) (Kim *et al.*, 2006). Whereas yeast subunits assemble into a full complex when co-expressed in *E. coli*, the mammalian TRAPP_I homologues assemble into two half complexes. The crystal structure of these subcomplexes was determined and docked into the yeast EM structure, providing a pseudo-high resolution view of how yeast TRAPP_I is organized. Each heptameric TRAPP_I complex contains two copies of Bet3p and can be divided into two trimeric lobes: Trs20p-Trs31p-Bet3p and Bet5p-Bet3p-Trs33p that are connected by the subunit, Trs23p (Figure 1.4A) (Kim *et al.*, 2006).

A more detailed view of yeast TRAPP_I was obtained when TRAPP_I, without the flanking subunits, Trs20p and Trs33p, was crystallized in complex with the small Rab GTPase Ypt1p (Figure 1.4A) (Cai *et al.*, 2008). This structure in combination with the mammalian structure, revealed that TRAPP_I subunits can be divided into two families

based on their structural similarities; the Bet3 family includes Bet3p, Trs33p and Trs31p and the Sedlin family includes Trs20p, Trs23p and Bet5p (Kim *et al.*, 2006; Cai *et al.*, 2008).

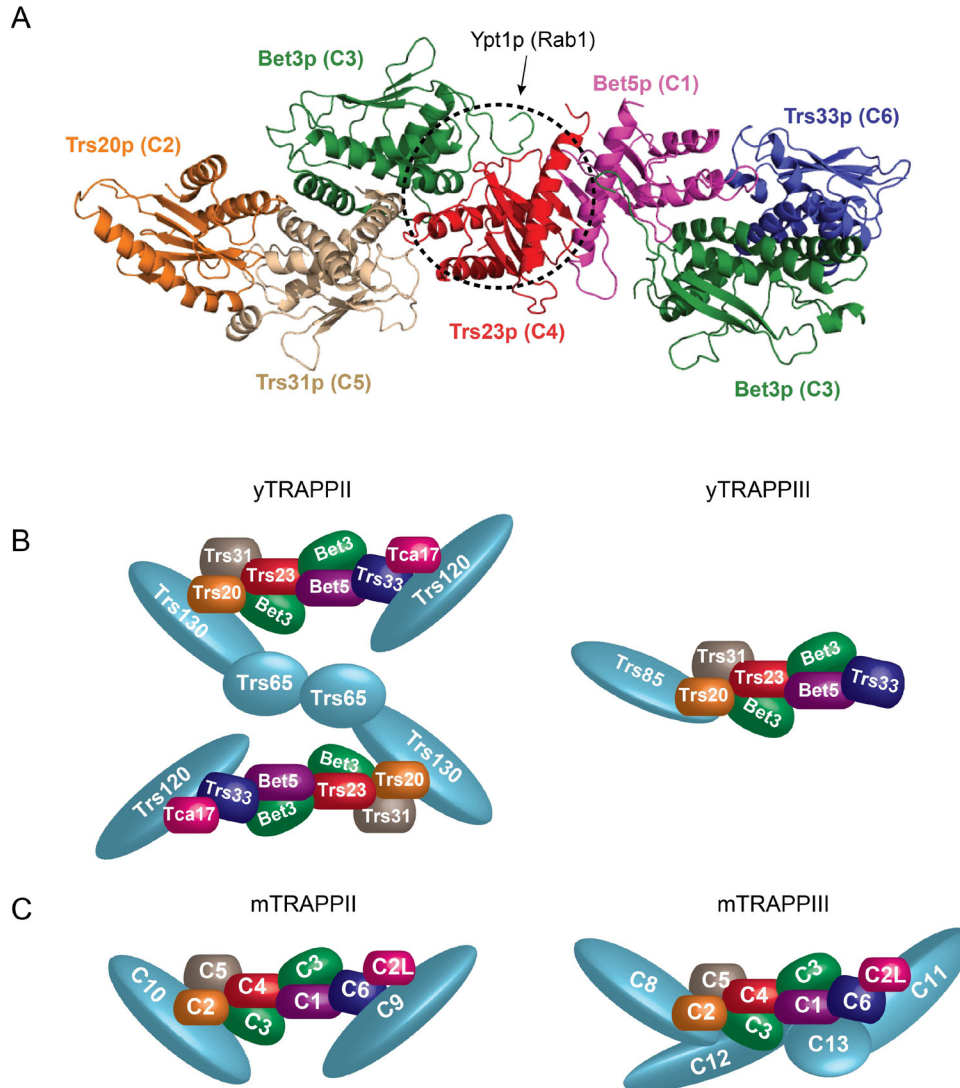


Figure 1.4 The structure and composition of yeast and mammalian TRAPP complexes. (A) The TRAPP core crystal structure is represented with the Rab1/Ypt1p binding interface indicated by a black dashed circle. The inner subunits Trs31p-Trs23p-Bet5p-Bet3p are modified from the crystal structure of yeast TRAPPIn complex with Ypt1p (PDB ID: 3CUE). The crystal structures of TrappC6a and TrappC2 were docked onto the structure to represent Trs33p and Trs20p, respectively (PDB ID: 2J3T and 2J3W). Mammalian homologues (without the TRAPP prefix) are indicated in brackets next to the yeast subunit name. (B) Yeast TRAPP II and III are represented schematically based on EM structures of the native complexes (Yip *et al.*, 2010; Tan *et al.*, 2013). (C) Mammalian TRAPP II and III are modeled after the yeast structures with additional subunits added.

1.3.2.2 TRAPP^{II} EM structure

The structure of native TRAPP^{II} purified from yeast lysates was determined by EM, and revealed the complex to be a dimer (Yip *et al.*, 2010). Each TRAPP^{II} monomer consists of a TRAPP^I core, capped on either end by Trs120p or Trs130p and a copy of Trs65p, all together forming a triangular shape, so that two triangular monomers form a diamond (Figure 1.4B). In the TRAPP^{II} structure, both copies of Trs65p appear to link two monomers together and the importance of Trs65p in stabilizing these dimers is evidenced by the absence of dimer formation when TRAPP^{II} was purified from a *trs65Δ* strain (Yip *et al.*, 2010). Consistent with this result, on a size exclusion column, TRAPP^{II} from wild type lysates fractionates at ~ 1MDa whereas TRAPP^{II} from *trs65Δ* lysates, appears at ~700kDa (Choi *et al.*, 2011). The dimer has two-fold symmetry so that the same surface is exposed on either end of the complex.

Although Tca17p co-fractionates with and interacts genetically with TRAPP^{II}, it co-purifies with the complex in substoichiometric amounts leading to speculation that Tca17p may only transiently associate with TRAPP^{II} (Yip *et al.*, 2010). However size exclusion experiments show that in the absence of Tca17p the interaction between the core and TRAPP^{II} specific subunits is de-stabilized (Choi *et al.*, 2011). Furthermore, Tca17p co-localizes with the TRAPP^{II} subunit, Trs130p, by fluorescence microscopy (Montpetit and Conibear, 2009). The exact location of Tca17p within TRAPP^{II} is not known, but binding experiments between its mammalian homologue, TRAPPC2L, and the mammalian TRAPP core indicate that it may be positioned on the opposite side of the complex from Trs20p/TRAPPC2 (Scrivens *et al.*, 2009).

1.3.2.3 TRAPP^{III} EM structure

The last TRAPP complex to be characterized in yeast was TRAPP^{III}, which consists of the core and the TRAPP^{III} specific subunit Trs85p (Lynch-Day *et al.*, 2010). Paradoxically, on a size exclusion column, TRAPP^{III} appears to be the largest of the complexes, at a massive 40MDa or larger, but does not form oligomers or contain

additional subunits aside from the core (~200kDa) and a single copy of Trs85p (~85kDa) (Choi *et al.*, 2011).

The EM structures of native and recombinant TRAPPIII were recently determined, and shown to be similar. The complex appears “banana-shaped” with Trs85p occupying the top ¼ of the structure and connecting with the core, which occupies the bottom ¾ of the structure, at the Trs20p end (Figure 1.4B) (Tan *et al.*, 2013). No significant structural changes are observed in the core when it is part of TRAPPIII, in comparison to TRAPPI (which consists of just the core), suggesting that many TRAPPI binding surfaces would remain exposed (Tan *et al.*, 2013).

1.3.3 TRAPP as a GEF

1.3.3.1 TRAPPIs a GEF for Ypt1p:

All three yeast complexes act as GEFs for the small Rab GTPase Ypt1p. TRAPPIs unique among GEFs in that four subunits contribute towards and are required for its GEF activity. The minimal assembly required for TRAPP GEF activity *in vitro* is Bet3p (2 copies)-Trs23p-Bet5p-Trs31p, representing the TRAPP core without 2 subunits, Trs20p and Trs33p (Kim *et al.*, 2006). These four subunits were crystallized in complex with Ypt1p elucidating the mechanism of how TRAPP facilitates the exchange of GDP for GTP on Ypt1p. Ypt1p makes contact with the acidic surface of TRAPP, primarily through interactions with Trs23p, and to a lesser extent Bet5p and one copy of Bet3p, while Trs31p and the second copy of Bet3p provide structural support (Figure 1.4A) (Cai *et al.*, 2008). This interaction induces structural changes in Ypt1p, most prominently in the nucleotide-binding pocket of Ypt1p. In the crystal structure the carboxy-terminus of one copy of Bet3p is inserted into this pocket, providing steric hindrance that would facilitate the loss of GDP and the uptake of GTP (Cai *et al.*, 2008). Interestingly, many of the very highly conserved residues of the TRAPP core are positioned at the surface and are involved in GEF activity, suggesting that the GEF activity of TRAPPIs also conserved (Kim *et al.*, 2006).

All three yeast TRAPP complexes exhibit GEF activity towards Ypt1p. TRAPPI and TRAPPIII activity has been demonstrated with complexes purified from yeast lysates as

well as with recombinant complexes produced in *E. coli* (Jones *et al.*, 2000; Wang *et al.*, 2000; Kim *et al.*, 2006; Lynch-Day *et al.*, 2010; Tan *et al.*, 2013). TRAPP^{II} GEF activity has only been demonstrated for the complex purified from yeast lysates, as TRAPP^{II} has not yet been successfully produced *in vitro* (Lynch-Day *et al.*, 2010). The additional subunits in TRAPP^{II}/III do not alter or mask the Ypt1p binding site but instead they have been proposed to direct the GEF activity of the TRAPPI core to a specific destination within the cell.

1.3.3.2 TRAPP^{II} may be a GEF for Ypt32

TRAPP^{II} subunits interact genetically with the Rabs encoded by *YPT31* and *YPT32* that act in the late secretory pathway and mutations in TRAPP^{II}-specific subunits perturb Ypt31p localization indicating that TRAPP^{II} and Ypt31/32p function in common pathways (Morozova *et al.*, 2006; Liang and Morozova, 2007; Montpetit and Conibear, 2009; Tokarev *et al.*, 2009; Choi *et al.*, 2011). Consistent with this, the TRAPP^{II} complex has been reported to be a GEF for Ypt31/32p. In several studies TRAPP^{II} displayed GEF activity towards Ypt31/32p and not Ypt1p, leading to an elegant model that the addition of TRAPP^{II}-specific subunits convert TRAPPI, a complex acting in the early secretory pathway, into a Ypt32p GEF, that acts further downstream (Jones *et al.*, 2000; Morozova *et al.*, 2006). However, this result has not been repeated by other groups and pull down experiments as well as EM structure analysis demonstrated that TRAPP^{II} purified from yeast lysates binds Ypt1p but not Ypt31/32p (Yip *et al.*, 2010). A possible explanation for the discrepancy between researchers could be different experimental designs. Recombinant TRAPP^{II} has not yet been produced and when the complex is purified from lysates, other proteins may be co-precipitating with the complex, such as the true Ypt31/32p GEF. Alternatively, the integrity of TRAPP^{II} may be altered in certain conditions compromising its Ypt31/32p GEF activity.

1.3.4 TRAPPI, II, and III act in different membrane trafficking pathways

1.3.4.1 TRAPPI is essential for ER-Golgi trafficking

TRAPPI acts early in the secretory pathway in ER-Golgi trafficking where it is required for ER-derived COPII vesicles to tether to the early Golgi (Figure 1.5). Certain mutations in TRAPPI core subunits block the maturation of the vacuolar protease

carboxypeptidase Y (CPY) beyond its ER form (p1), causing vesicle accumulation between the Golgi and ER and dilation of the ER (Rossi *et al.*, 1995; Jiang *et al.*, 1998; Sacher *et al.*, 2001). These phenotypes are consistent with TRAPPI acting downstream of COPII vesicle budding and upstream of vesicle fusion with the early Golgi. In an *in vitro* transport assay, Golgi that was depleted of Bet3p, and consequently of TRAPPI, was not competent for transport supporting a role for Bet3p at the early Golgi (Sacher *et al.*, 1998). Later experiments demonstrated that TRAPPI, but not TRAPP II, binds COPII vesicles and that Bet3p-depleted Golgi loses its ability to bind COPII vesicles, strongly suggesting that TRAPPI acts as a vesicle tethering factor and not as a factor regulating vesicle fusion (Barrowman *et al.*, 2000; Sacher *et al.*, 2001).

The physical link between TRAPPI and COPII is provided by the direct interaction between Bet3p and the COPII inner coat subunit Sec23p, an interaction also observed between the respective human homologues (Cai *et al.*, 2007b). According to a recent model of TRAPPI-based tethering (Lord *et al.*, 2011), TRAPPI via its interaction with Sec23p binds COPII vesicles that have budded from the ER. The complex then activates Ypt1p making the vesicle competent for docking at the Golgi through the interaction of Ypt1p with its effectors, such as the coiled coil tether Uso1p. Once tethered at the Golgi, the kinase Hrr25p releases TRAPPI from the vesicle by competitively binding to Sec23p which it phosphorylates to initiate downstream fusion events. The sequential binding of TRAPPI and Hrr25p to COPII vesicles via Sec23p would provide directionality to the movement of COPII vesicles travelling from the ER to the Golgi. Other players in this mechanism such as specific phosphatases that would dephosphorylate Sec23p remain to be discovered (Conibear, 2011).

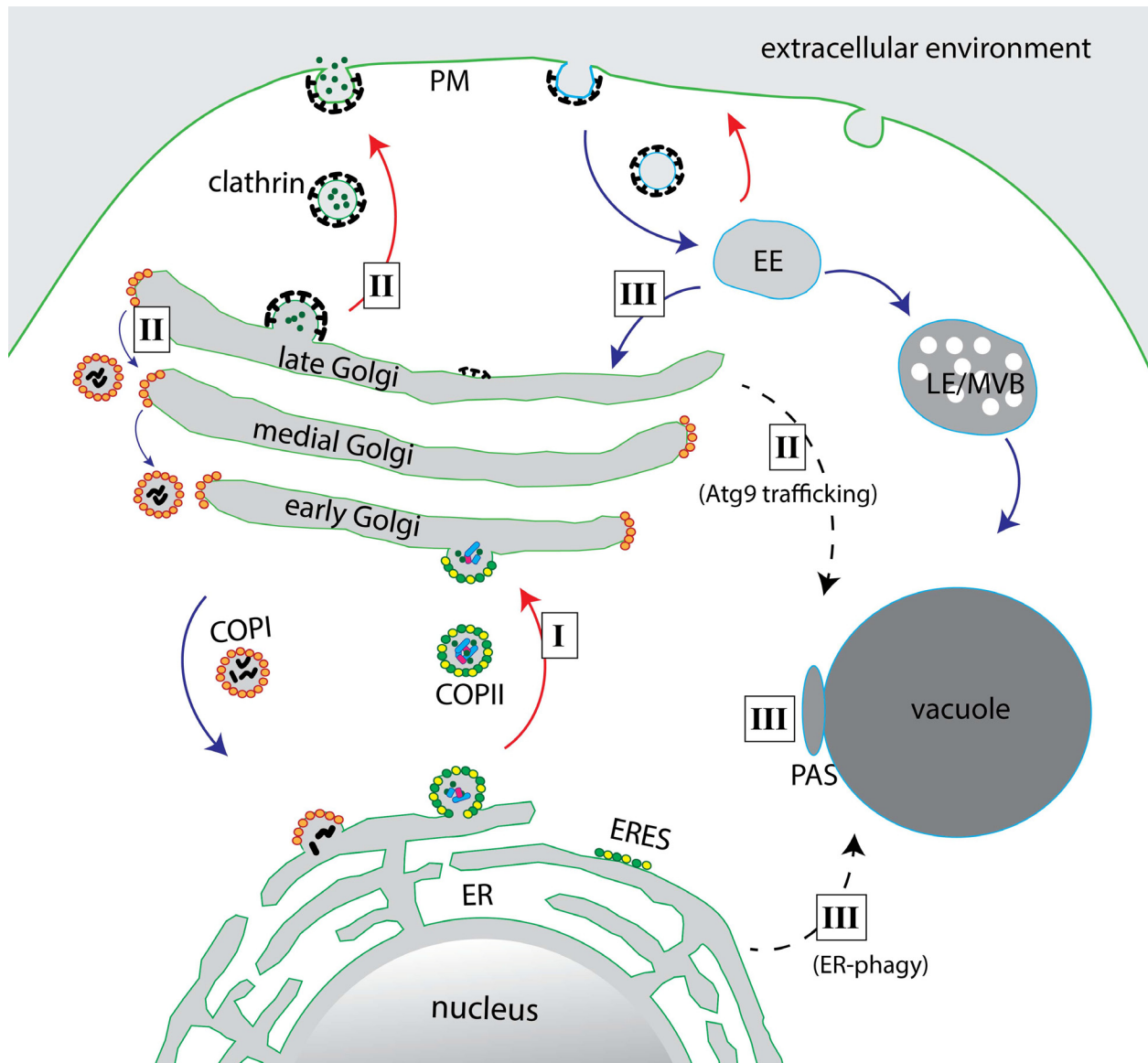


Figure 1.5 TRAPPI, II and III act in multiple membrane trafficking pathways. TRAPPI, TRAPPII and TRAPPIII are indicated by I, II and III, respectively. Arrows indicate the direction of movement of vesicles (COPI, COPII and clathrin) between cellular compartments (red indicates anterograde movement, blue indicates retrograde movement and dashed lines indicate autophagy pathways). Membranes of the secretory pathway are outlined in green and endocytic membranes are outlined in blue. (abbreviations: early endosome (EE), late endosome (LE), multivesicular body (MVB), plasma membrane (PM))

1.3.4.2 TRAPPII carries out functions at the late Golgi

Whereas TRAPPI acts at the early Golgi, the TRAPPII complex localizes to the late Golgi and carries out functions associated with this organelle, such as endocytosis and post-

Golgi trafficking (Figure 1.5). Mutations in TRAPP II-specific subunits disrupt the recycling of the plasma membrane SNARE Snc1p which, when endocytosed, is recycled back to the plasma membrane (PM) via the late Golgi. GFP-Snc1p is normally concentrated at the PM but in TRAPP II mutants it accumulates in the cell interior, indicating that its transport back to the plasma membrane is blocked (Cai *et al.*, 2005; Montpetit and Conibear, 2009). Specific mutations in *ypt1* also impair Snc1p recycling through the early Golgi, raising the possibility that just as Ypt1p must be activated by TRAPP I in ER-Golgi trafficking, Ypt1p must be activated by TRAPP II to mediate the entry and exit of cargo at the late Golgi (Lafourcade *et al.*, 2004; Sclafani *et al.*, 2010).

TRAPP II mutants also affect the secretory system at the level of the late Golgi. In these mutants, cargo such as CPY and invertase travelling through the secretory system, accumulate in their Golgi modified form, indicating that exit from the Golgi is blocked (Sacher *et al.*, 2001; Cai *et al.*, 2005). Furthermore, EM analysis of a *trs130* mutant revealed the accumulation of toroid-shaped Golgi membranes, a phenotype seen when proteins acting at the level of the Golgi are mutated (Sacher *et al.*, 2001).

Similar to the interaction of TRAPP I with COPII, TRAPP II interacts with the COPI vesicle coat. COPI subunits co-purify with TRAPP II from yeast lysates and TRAPP II mutants cause COPI subunits to improperly localize. Taken together, these results have led to the suggestion that TRAPP II acts to tether COPI vesicles at the Golgi (Cai *et al.*, 2005; Chen *et al.*, 2011). This appears to be conserved in mammals as the mammalian homologues of Trs120p and Trs130p interact with γ -COP, a mammalian COPI subunit (Yamasaki *et al.*, 2009).

In addition to binding COPI vesicles, TRAPP II may also act in their formation. Trs65p interacts directly with the carboxy-terminus of Gea2p, a GEF for the GTPase Arf1p, which, upon activation, recruits COPI subunits to the site of vesicle budding (Chen *et al.*, 2011). These investigators proposed that the Trs65p-Gea2p interaction does not contribute to COPI recruitment but instead strengthens the link between TRAPP II and COPI vesicles.

TRAPP-II-controlled trafficking from the late Golgi is also involved in autophagy pathways. Mutations in TRAPP-II-specific subunits cause defects in non-selective and selective autophagy and this defect is linked to the trafficking of Atg9p from the late Golgi to the PAS (Figure 1.5) (Zou *et al.*, 2013). Whereas TRAPP-III has a direct role in PAS assembly (as will be discussed in the next section), TRAPP-II appears to affect autophagy pathways indirectly by mediating the anterograde transport of autophagy proteins to the PAS.

1.3.4.3 TRAPP-III regulates endocytosis and autophagy

Several studies have focused on the TRAPP-III complex as it was recently characterized as a completely separate complex from TRAPP-I and II. The only TRAPP-III specific subunit, Trs85p, is non-essential, and most of the work aimed at determining the function of TRAPP-III has focused on this subunit. Like TRAPP-II mutants, the *trs85Δ* mutant is defective in Snc1p recycling and accumulates GFP-Snc1p internally, suggesting that TRAPP-III also functions in an endocytic recycling pathway that travels through the late Golgi (Figure 1.5) (Montpetit and Conibear, 2009). Whereas GFP-Snc1p in TRAPP-II mutants show various punctate and diffuse patterns of localization, GFP-Snc1p in *trs85Δ* has a very dramatic phenotype, as it aggregates into very few intense, large punctae in the cell interior, and a negligible percentage of cells show PM localization (Cai *et al.*, 2005; Montpetit and Conibear, 2009; Brunet *et al.*, 2013). Although TRAPP-III and TRAPP-II are both involved in Snc1p recycling, they likely act at different points in the pathway. Chs3p is another cargo that follows a similar route as Snc1p, and defects in its trafficking affect the resistance of cells to the drug Calcofluor white (CFW). Mutations that block its trafficking to the plasma membrane make cells resistant to CFW while mutations that block its retrieval from the PM make cells sensitive to CFW (Valdivia *et al.*, 2002). Interestingly, a *trs85Δ* mutation sensitizes cells to CFW, whereas a mutation in the TRAPP-II specific subunit *trs130* confers resistance, supporting the notion that these complexes are affecting the early endosome to late Golgi recycling pathway differently (Yamamoto and Jigami, 2002; Brunet *et al.*, 2013).

The most extensively studied function of TRAPP^{III} is in autophagy as it is essential for the yeast Cvt pathway and contributes to, but is not required for, starvation induced macroautophagy (Meiling-Wesse *et al.*, 2005; Nazarko *et al.*, 2005). Trs85p and Ypt1p co-localize and interact with each other at the PAS and Atg9p-containing membranes, and this interaction is essential for PAS formation (Figure 1.6) (Lynch-Day *et al.*, 2010; Lipatova *et al.*, 2012). The autophagy protein Atg11p was identified as an effector of Ypt1p that failed to localize to the PAS in *trs85Δ* (Lipatova *et al.*, 2013). These investigators presented a model whereby TRAPP^{III} activates Ypt1p on Atg9p containing membranes, initiating the recruitment of Atg11p and potentially other effectors that are required for PAS formation (Figure 1.6). Atg11p is required for the Cvt pathway but not macroautophagy, consistent with macroautophagy still occurring in the absence of TRAPP^{III}. In support of this model, Trs85p and Ypt1p were identified as components of immunisolated Atg9p vesicles (Kakuta *et al.*, 2012). The GEF-Rab-effector module of TRAPP^{III}-Ypt1p-Atg11p was also shown to function in ER-phagy, another autophagy pathway that occurs in nutrient rich conditions and degrades portions of the ER (Figure 1.5) (Lipatova *et al.*, 2013).

Under starvation conditions, TRAPP^{III} functions via a different pathway to regulate PAS formation, by recruitment of a different set of effectors (Figure 1.6). It was reported that in starved cells, TRAPP^{III} is recruited to the PAS by Atg17p, where it activates Ypt1p (Wang *et al.*, 2013). Activated Ypt1p then recruits the kinase Atg1p as an effector that will activate and recruit other proteins required for autophagy. It is possible that Trs85p resides on Atg9p vesicles and the recruitment of TRAPP^{III} to the PAS by Atg17p serves to tether these vesicles at the PAS and promote autophagosome formation. In Chapter 2 evidence is presented that Atg9p, but not Atg17p, is required for the association of TRAPP^{III} with membranes in starvation conditions, which is compatible with this proposed model.

The association of Ypt1p with Atg1p is conserved in mammals, as the Ypt1p homologue Rab1 associates with the Atg1p homologue Ulk1 in HeLa lysates (Wang *et al.*, 2013). Additionally, depletion of several mammalian TRAPP^{III} subunits by siRNA (small

interfering RNA), cause an increase or decrease in autophagosome formation (Behrends *et al.*, 2010). The Cvt pathway is not conserved in higher eukaryotes such as mammals, but mammalian TRAPPIII may function in autophagy in a similar manner as it does in yeast macroautophagy.

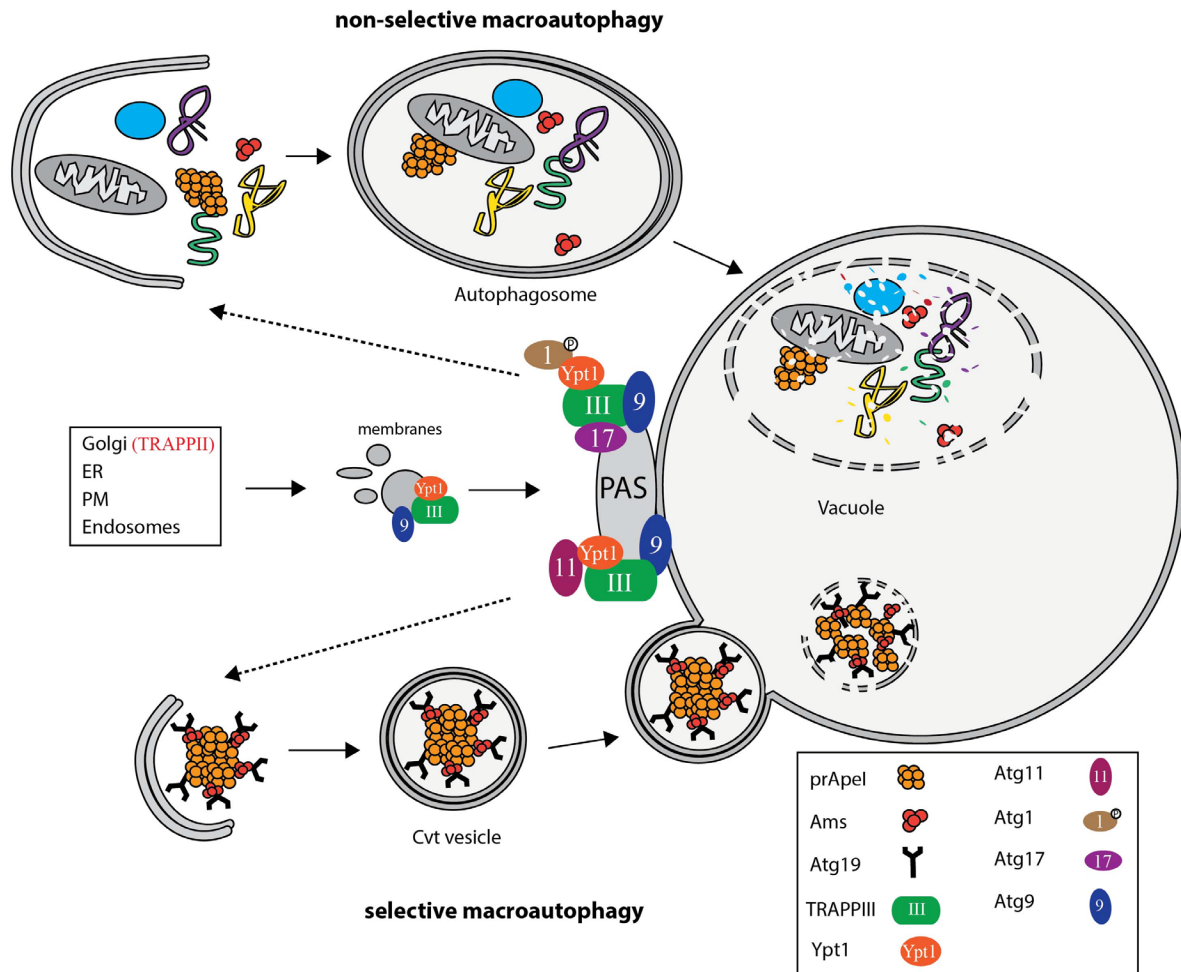


Figure 1.6 TRAPPIII localizes to the PAS and regulates selective and non-selective autophagy through different pathways. Non-selective and selective (Cvt pathway) macroautophagy pathways are represented schematically. Cvt vesicles (selective), containing oligomers of prApe1 (precursor aminopeptidase 1)/Ams (α -mannosidase), and autophagosomes (non-selective) are delivered to the vacuole for processing and degradation. In non-selective autophagy Atg9p is required for the association of TRAPPIII with membranes, and Atg17p recruits TRAPPIII to the PAS where it activates Ypt1p. The kinase Atg1p binds to Ypt1p as an effector that activates and recruits other proteins required for autophagy. In selective autophagy, TRAPPIII activates Ypt1p at the PAS and Atg11p, a protein specific to and required for the Cvt pathway, is recruited as a Ypt1p effector (Shintani *et al.*, 2002). TRAPPII mediates the trafficking of Atg9p-containing membranes to the PAS.

1.3.5 Mammalian TRAPP complexes

TRAPP was initially described in yeast (yTRAPP) but TRAPP has also been characterized in mammalian cells (mTRAPP) and every yeast subunit has a mammalian homologue (Table 1.1). When HeLa cell lysates are separated on a size exclusion column they yield two high molecular weight peaks which represent mammalian TRAPP_{II} and TRAPP_{III} (Figure 1.4C), but no peak is observed for the equivalent of a TRAPP_I core complex (Scrivens *et al.*, 2011; Bassik *et al.*, 2013). This difference may be caused by structural differences between the yeast Trs23p core subunit and its mammalian homologue TrappC4 as discussed in Chapter 3.

Two additional mammalian TRAPP subunits that have no identifiable yeast homologues were characterized, and they were both found in the mTRAPP_{III} complex (Figure 1.4C). The nomenclature adopted for mammalian TRAPP subunits is TrappC# where “#” is 1-13; novel subunits were named TrappC11 and TrappC12 accordingly (Table 1.1) (Gavin *et al.*, 2002; Choi *et al.*, 2011; Scrivens *et al.*, 2011; Bassik *et al.*, 2013). Mammalian TRAPP_Is also differ from yeast in that several mammalian subunits have more than one isoform. The mammalian homologue of Trs33p, TrappC6, has two isoforms, TrappC6a and TrappC6b, and two Bet3p homologues exist, TrappC3 and TrappC3L (Kümmel *et al.*, 2008; Scrivens *et al.*, 2011).

Consistent with the subunits being largely conserved between yeast and mammals, the function of TRAPP_Is also, at least partially, conserved. Purified mTRAPP_{II} from HeLa lysates exhibits GEF activity for the Ypt1p homologue Rab1 and depleting several TRAPP subunits causes a Golgi fragmentation phenotype, indicating that the complex is required for membrane trafficking which is important for Golgi homeostasis (Yu *et al.*, 2006; Scrivens *et al.*, 2009, 2011; Yamasaki *et al.*, 2009). TrappC3, like its yeast homologue Bet3p, interacts with Sec23 and mTRAPP_{III} co-precipitates with COPII coat proteins while mTRAPP_{II} associates with COPI coat proteins (Yu *et al.*, 2006; Yamasaki *et al.*, 2009; Bassik *et al.*, 2013).

In yeast, COPII vesicles that have emerged from the ER fuse directly with the Golgi in a process called heterotypic fusion. In mammalian cells, COPII vesicles undergo homotypic fusion to coalesce into the ER-Golgi Intermediate Compartment (ERGIC) (Xu and Hay, 2004). TrappC3 has been localized to the transitional ER and is required for formation of the ERGIC by mediating homotypic COPII fusion, but whether it performs this function within the context of mTRAPPIII is not known (Yu *et al.*, 2006). Additionally, in an *in vitro* transport assay, the immunodepletion of TrappC3 prevents VSV-G from reaching the Golgi, consistent with this subunit acting in the early secretory pathway (Loh *et al.*, 2005). Similarly, and analogous to the requirement for yTRAPPI in ER-Golgi trafficking, depletion of the mTRAPPIII subunits TrappC11 and TrappC12 arrest the reporter protein ts045VSV-G-GFP at ERES or at peripheral ERGIC apposed to ERES (Scrivens *et al.*, 2011). Mutations in both mTRAPPII and mTRAPPIII specific subunits have been linked to several different human diseases (Brunet and Sacher, 2014).

1.3.6 Mutations in the human Trs20 homologue TRAPPC2 cause SEDT

Mutations in the mammalian *TRS20* homologue, *TRAPPC2*, cause the skeletal disease X-linked spondyloepiphyseal dysplasia tarda (SEDT). SEDT occurs in males between the ages of 3 and 12 and causes individuals to have a disproportionately short stature and trunk and a barrel-shaped chest (Gedeon *et al.*, 1999; Fan and Tang, 2013). Approximately 50 mutations occurring along the length of the protein have been reported with the majority causing premature truncation of TrappC2, and four resulting in missense mutations (Shaw *et al.*, 2003; Fan and Tang, 2013).

SEDT is caused by a defect in the secretion of extracellular matrix proteins such as pro-collagen from chondrocytes and the role of TrappC2 in this specific process was not immediately evident, especially given its ubiquitous expression in all tissues (Gedeon *et al.*, 2001). Further complicating this problem is an incomplete understanding of how cells overcome the challenge of secreting 300nm pro-collagen fibrils in COPII vesicles that are normally ~60-70nm in size (Barlowe *et al.*, 1994; Fromme and Schekman, 2005)

The mechanism for the involvement of TrappC2 in collagen secretion was elucidated by TrappC2-depletion experiments in fibroblasts and chondrocytes. Depletion of TrappC2 by siRNA blocked the secretion of pro-collagen II (PCII), which accumulated in the ER, but not smaller cargo such as VSV-G-GFP (Venditti *et al.*, 2012). TrappC3 depletion caused a similar phenotype suggesting that TrappC2 is acting as part of a complex. Venditti *et al.* further showed that TrappC2 is recruited to ERES through an interaction with the pro-collagen receptor TANGO1, where TrappC2 interacts with the activated form of the COPII GTPase Sar1-GTP. Activated Sar1 facilitates constriction of the growing COPII vesicle, but TrappC2 promotes Sar1 inactivation and membrane dissociation, permitting the vesicle to reach an adequate size to package a 300nm PCII fibril (Venditti *et al.*, 2012). Interestingly, the PCII-specific defect is dependent on the degree of TrappC2 depletion. In the same cells, a more severe knockdown of TrappC2 caused a more general secretion defect, and the same Golgi fragmentation phenotype previously reported was observed (Scrivens *et al.*, 2009; Venditti *et al.*, 2012).

1.4 The purpose of this thesis

For my thesis work I have used yeast as a model system to understand how specific subunits contribute to the integrity of the TRAPP complexes and how these complexes regulate membrane trafficking pathways. Specifically, I addressed the following questions: (1) How do Trs20p and Trs23p, two essential core subunits, contribute to the integrity and function of the yeast TRAPP complexes and what are the implications of these findings for the equivalent mammalian complexes? (2) What are the functional consequences of an interaction between the yeast TRAPP_{II} complex and the Ytp6 GAP Gyp6p and within what cellular context does this interaction occur?

Several mutations in *TRAPPC2*, an essential TRAPP core subunit, have been linked to the skeletal disorder SEDT. In an attempt to understand how TRAPP-controlled processes may contribute to the etiology of SEDT, I examined how specific mutations in the well-conserved *TRAPPC2* homologue, *TRS20*, affect TRAPP controlled processes in yeast. I found that mutations in *TRS20* negatively affect TRAPP_{II} and TRAPP_{III} but a missense mutation that is analogous to a SEDT-causing mutation in humans specifically blocks TRAPP_{III}-

mediated trafficking pathways and TRAPPIII assembly. These results are presented in Chapter 2 and were published in 2013 in *Traffic* (Brunet *et al.*, 2013)

Trs23p is an essential TRAPP core subunit that links the two ends of yeast TRAPPI together (Figure 1.4A) and is required for Ypt1p directed GEF activity. In Chapter 3 of this dissertation I examined how mutations in Trs23p affect the structural integrity and the function of TRAPPI, II and III. I showed that the deletion of a *Saccharomyces cerevisiae* specific domain (SMS) from Trs23p prevents the TRAPP core from assembling, both *in vitro* and *in vivo* but, surprisingly, functions attributed to the TRAPPI complex were not compromised. Based on these results, I speculate that the TRAPPI complex is a fragment of the two larger TRAPP complexes and is released upon cell lysis. Furthermore, the failure to identify a mammalian TRAPPI complex may be explained by the absence of the SMS domain in the Trs23p homologue, TRAPPC4. The results of Chapter 3 were published in *Cellular Logistics* in 2012 (Brunet *et al.*, 2012).

The organization and structure of TRAPPII has been well characterized in recent years but its mechanism for regulating various membrane trafficking pathways is largely unknown. In the aim of identifying TRAPPII binding partners I analyzed the affinity purified complex by mass spectrometry and identified the Ypt6p GAP, Gyp6p, as a positive interactor. By yeast two hybrid and co-immunoprecipitation I showed that the interaction of Gyp6p with TRAPPII is direct and occurs via the Trs130p subunit. I further present evidence that this interaction is important for the dynamics of Ypt6 at the late Golgi, which could represent a novel mechanism for how TRAPPII controls specific trafficking pathways. These results are presented in Chapter 4 and are not yet published.

Chapter 2: A *trs20* mutation that mimics an SEDT-causing mutation blocks selective and non-selective autophagy: a model for TRAPPIII organization

This Chapter was published as a manuscript in the journal *Traffic* (Brunet *et al.*, 2013). I shared first authorship of this paper with Nassim Shahrzad and I am responsible for the following figures: Figure 2.4, 2.6(A &B), 2.7, 2.8, 2.10, 2.11, 2.12, 2.14(B), 2.15, 2.16, 2.17 and 2.18.

2.1 Introduction

The ability of a cell to properly localize its protein complement is critical for the cell to function correctly. Referred to as membrane transport, the process is mediated by vesicle carriers that move between various compartments. There are many factors involved in ensuring the fidelity of this process and defects in this trafficking process lead to numerous disorders (Aridor and Hannan, 2000, 2002). Although strong defects in membrane traffic would be expected to result in embryonic lethality, more subtle mutations may lead to tissue-specific disorders.

The overall process involves tethering factors, small GTP-binding proteins of the rab family, coat proteins that encompass the transport vesicles and SNARE proteins that are involved in vesicle fusion with the target membrane (Cai *et al.*, 2007a). Intimate connections between each of these factors have been identified in various transport steps. In transport between the endoplasmic reticulum (ER) and Golgi in yeast, the tethering factor TRAPPI binds to the coat protein Sec23p, thus acting to bridge the vesicle and the target membrane (Cai *et al.*, 2007b; Lord *et al.*, 2011). In addition, as a guanine nucleotide exchange factor (GEF), TRAPPI activates the GTPase Ypt1p (Jones *et al.*, 2000; Wang *et al.*, 2000). Although a direct link between TRAPPI and SNAREs has yet to be demonstrated, SNARE complex assembly is impaired in a *bet3* mutant, a gene that encodes an essential TRAPPI subunit (Rossi *et al.*, 1995). Thus, as a tethering factor, TRAPPI serves to link all of these processes to ensure proper targeting of ER-derived transport vesicles.

TRAPPI is composed of six distinct polypeptides (Bet5p, Bet3p, Trs20p, Trs23p, Trs31p, Trs33p) although the levels of Trs20p appear to be sub-stoichiometric in this complex (Sacher *et al.*, 2001). Two related complexes called TRAPP^{II} and III have also been described (Sacher *et al.*, 2001; Lynch-Day *et al.*, 2010). Each complex contains the TRAPPI core along with unique polypeptides: Trs65p, Tca17p, Trs120p and Trs130p for TRAPP^{II}, and Trs85p for TRAPP^{III} (Sacher *et al.*, 2001; Montpetit and Conibear, 2009; Lynch-Day *et al.*, 2010; Choi *et al.*, 2011). TRAPP^{II} has been implicated in traffic at the late Golgi, endocytosis and non-selective autophagy (Sacher *et al.*, 2001; Cai *et al.*, 2005; Zou *et al.*, 2013) and TRAPP^{III} has been shown to function in selective autophagy (Meiling-Wesse *et al.*, 2005; Lynch-Day *et al.*, 2010; Lipatova *et al.*, 2012). Interestingly, Trs85p, the TRAPP^{III}-specific subunit, has been implicated in ER-to-Golgi transport as well (Sacher *et al.*, 2001; Zou *et al.*, 2012b). Since the TRAPPI core possesses Ypt1p GEF activity, both TRAPP^{II} and III have also been shown to be capable of activating Ypt1p (Sacher *et al.*, 2001; Lynch-Day *et al.*, 2010). Indeed, Ypt1p has been implicated in the same membrane trafficking processes as TRAPPI, II and III (Segev *et al.*, 1988; Bacon *et al.*, 1989; Jedd *et al.*, 1995; Lynch-Day *et al.*, 2010; Sclafani *et al.*, 2010; Lipatova *et al.*, 2012).

In humans, mutations in TRAPPC2 (C2), the homolog of the yeast TRAPPI core protein Trs20p, have been linked to the skeletal disorder spondyloepiphyseal dysplasia tarda (SED^T) (Shaw *et al.*, 2003). This X-linked disorder affects bone growth in the spine and the ends of long bones in the arms and legs. Patients are of short stature and develop dysplasia of joints in the shoulders, hips and knees. The disorder appears to result from an inability of chondrocytes to secrete collagen (Tiller *et al.*, 2001). Indeed, given the size of pro-collagen (~300nm) and the diameter of an ER-derived carrier (~60nm) it has been an unanswered question as to how pro-collagen is transported between the ER and Golgi. Furthermore, understanding how a ubiquitously expressed protein such as C2 could lead to the phenotype seen in SED^T patients has been a major focus of researchers studying TRAPP. A recent report suggested that recruitment of C2 to ER exit sites by the pro-collagen receptor Tango1 regulates the cycle of the GTPase Sar1, thus allowing carriers to achieve a size sufficient to accommodate the large pro-collagen molecule (Venditti *et al.*, 2012).

While elegant, we speculated that the model put forth regarding the role of C2 in pro-collagen secretion may not explain the etiology of all SEDT mutations since yeast do not secrete collagen nor do they possess a readily identifiable homolog of the collagen receptor. Furthermore, C2-dependent Golgi fragmentation and collagen secretion are separable functions (Scrivens *et al.*, 2009; Venditti *et al.*, 2012) suggesting C2 may have several roles in the cell. Interestingly, an SEDT-causing missense mutation at D47 in C2 (C2D47Y) cannot suppress the lethality of a yeast *trs20* Δ mutation although wild type C2 can (Gecz *et al.*, 2003). Since yeast do not produce collagen, this suggests that the D47 residue is involved in some other process. We therefore set out to characterize the interactions and function of the C2D47Y protein and its yeast homolog *trs20D46Yp*. Here we demonstrate an interaction between C2 and the SNARE protein Syntaxin 5 and show that this interaction is sensitive to the D47Y mutation. In yeast, *trs20D46Yp* is not involved in anterograde transport but is defective in endocytosis and both selective and non-selective autophagy, correlating with a destabilization of TRAPPIII. We also show that the appearance of TRAPPIII is dependent upon Atg9p and that the function of TRAPPIII is influenced by palmitoylation of Bet3p, suggesting unexpected complexities in TRAPPIII assembly and localization.

2.2 Materials and methods

2.2.1 Yeast strains and molecular biological techniques

All yeast strains were constructed using standard genetic techniques. *TRS20* mutations were introduced by site-directed mutagenesis using High-Fidelity Polymerase (Roche) and expressed in yeast under the endogenous *TRS20* promoter from a single-copy plasmid (pRS315 or pRS316). The C2D47Y mutation was constructed as above and cloned into the pRK5-myc plasmid facilitating detection of the mutant protein with anti-myc antibody. For yeast two-hybrid analysis, open reading frames were inserted into pGBKT7 or pGADT7 using either restriction enzyme cloning or Gateway cloning into modified, Gateway-compatible vectors (Scrivens *et al.*, 2011).

2.2.2 Yeast two-hybrid analysis

Yeast cells (AH109 and Y187) were transformed with either pGBKT7 or pGADT7 constructs. The cells were mated overnight on YPD plates and then replicated to selective medium (-leucine/-tryptophan, -leucine/-tryptophan/-histidine \pm 2mM 3-aminotriazole, -leucine/-tryptophan/-histidine/-adenine) to ensure that both plasmids were present and to test for an interaction. Growth was monitored daily for up to 8 days.

2.2.3 Cell culture and immunoprecipitation

HeLa and 293T cells were maintained in a humidified environment with 5% CO₂ at 37°C. Transfections were performed using the Ca₂PO₄ method and 10µg of plasmid DNA per 10cm dish. In certain cases cells were treated with 10µM *N*-ethylmaleimide (NEM) during the time course indicated in Figure 2.3. For immunoprecipitations, 500µg of lysate prepared in lysis buffer (150mM NaCl, 50mM Tris pH 7.2, 1mM DTT, 1% Triton X-100, 0.5mM EDTA, 1 mini-tablet of protease inhibitor cocktail (Roche) per 10mL) was incubated with 0.4µg of anti-Syntaxin 5 antibody (Santa Cruz) overnight on ice. The sample was then incubated with a 10µl bed volume of protein A-agarose beads for 60 minutes in the cold. The beads were washed 3 times with lysis buffer and eluted by boiling with 25µl SDS-PAGE sample buffer.

2.2.4 Yeast trafficking assays

The assay for carboxypeptidase Y (CPY) transport and GFP-Snc1p localization were performed as previously described (Brunet *et al.*, 2012). For the CPY assay the cells were shifted to 37°C for 60 minutes.

For the general secretion assay, 2 OD₆₀₀ units of cells were pre-shifted to 37°C for 30 minutes. The cells were then pulse-labeled with 100µCi ³⁵S-methionine/cysteine for 15 minutes and chased with 10mM unlabeled methionine and cysteine for 15 minutes. Before pelleting the cells NaN₃/NaF was added to the culture to a final concentration of 0.5mM. The cells were pelleted and the growth medium was precipitated with 10% trichloroacetic

acid on ice. The pellet was dissolved in SDS-PAGE sample buffer and fractionated by SDS-PAGE.

Calcofluor white (CFW) growth was monitored by spotting serial dilutions of cells on YPD \pm 10 μ g/ml CFW and incubating the plates at 30°C. Growth was monitored daily for up to 5 days.

Processing of pre-Ape1p was performed by monitoring the forms of the protein using Western analysis (Klionsky *et al.*, 1992). Cells were grown overnight to an OD₆₀₀ \leq 1 in YPD and resuspended in pre-warmed YPD medium at 37.5°C (for heat sensitive mutants) or 30°C for 1 hour. For selective autophagy cells were immediately processed for lysis (see below). For non-selective autophagy cells were pelleted, washed in water and re-suspended in pre-warmed synthetic medium lacking nitrogen, incubated for 2-4h at 37.5°C (for heat sensitive mutants) or 30°C, and then processed for lysis. Localization of GFP-Ape1p was performed on fixed cells according to the GFP-Snc1p protocol above.

2.2.5 Preparation of yeast cell lysates

Lysates for size exclusion chromatography were prepared as previously described (Brunet *et al.*, 2012) and 2-5mg of total protein was fractionated on a Superose 6 column. In some cases 1% Triton X-100 was added to the lysis buffer and was included in the size exclusion column buffer. For pre-Ape1p processing, lysates were prepared by converting the cells to spheroplasts in medium containing 1.4M sorbitol, 50mM KP_i pH 7.5, 36mM β -mercaptoethanol, 33 μ g/ml zymolyase 100T for 30 minutes at 37.5°C. Spheroplasts were lysed in 1% SDS, boiled and cleared by centrifugation.

2.2.6 Optiprep gradient assay

A yeast lysate from *TRS85*-HA cells was prepared in the absence of detergent and fractionated on a Superose 6 column as described (Brunet *et al.*, 2012). Fractions containing TRAPP_{III} were pooled and a portion was supplemented with 1% Triton X-100 before incubating on ice for 30 minutes. A sample (100 μ l) was combined with size

exclusion column buffer to a final volume of 300 μ l and then loaded on top of a step Optiprep gradient composed of 1 ml 15%, 1 ml 30%, 1 ml 40%, 0.8 ml 45% and 1.2 ml 54% Optiprep. The sample was centrifuged in an SW55 rotor at 36,000 rpm for 16 hours. Fractions were collected from the top of the tube and probed for Trs85p-HA with anti-HA antibody.

2.2.7 Recombinant protein expression and *in vitro* binding

Syntaxin 5 (amino acids 1-333) was recombined into pDEST15 (GST fusion vector) from a Gateway entry clone. C2 and C2D47Y were recombined into pDEST17 (His fusion vector) from Gateway entry clones. Protein was expressed by inducing with 1mM IPTG in BL21(DE3) cells overnight at 25°C. The protein was purified on glutathione-agarose resin or Ni²⁺-NTA resin as per manufacturer's instructions.

In vitro binding assays contained 0.5 μ M of GST-Syntaxin 5 with increasing amounts (0, 0.1, 0.2, 0.5 μ M) of His-tagged C2 wild type or D47Y. Samples were made up to a total volume of 250 μ l with 1x binding buffer (10mM HEPES pH 7.4, 25mM NaCl, 115mM KCl, 2mM MgCl₂, 0.1% Triton X-100) and left on ice at 4°C for 1 hour to allow binding. Pulldown employed 10 μ l glutathione agarose resin (GE Healthcare) in the cold for 1 hour. Samples were washed 3x with binding buffer and eluted by boiling with SDS-PAGE sample buffer. Western blotting was performed using HRP-conjugated anti-His antibody (Qiagen).

2.2.8 Acyl-biotin exchange

Biotinylation of acylated proteins was performed essentially as described (Hou *et al.*, 2005; Wan *et al.*, 2007) with minor modifications. A wild type yeast lysate was prepared in the absence of detergent and fractionated on a Superose 6 column as described (Brunet *et al.*, 2012). Fractions containing TRAPPI, II and III were separately pooled and incubated at 4°C for 30 minutes in 1% Triton X-100 with 25mM *N*-ethylmaleimide. The proteins were precipitated two times using methanol/chloroform and resuspended in buffer A (2% SDS, 8M urea, 100mM NaCl, 50mM TrisHCl, pH 7.4). Six volumes of a solution containing 1M hydroxylamine and 300 μ M biotin-BMCC (Pierce) was added and incubated for 2 hours at

4°C. The proteins were precipitated one time using methanol/chloroform, resuspended in PBS containing 0.1% Triton X-100 and incubated with 15µl of streptavidin-agarose beads (Sigma) for 1 hour at room temperature. The beads were washed in PBS containing 0.5M NaCl and 0.1% Triton X-100 after which the proteins were eluted by boiling in a 3:1 mix of buffer A: 4xSDS-PAGE sample buffer. Bet3p was detected by Western analysis using anti-Bet3p IgG.

2.3 Results

2.3.1 Binding of TRAPPC2 to Syntaxin 5 is dependent upon the D47 residue in TRAPPC2

A recent study suggested that C2 participates in the export of pro-collagen by regulating the Sar1p GTPase cycle (Venditti *et al.*, 2012). C2 is recruited to ER exit sites through an interaction with the collagen receptor Tango1. We reasoned that C2 has additional functions for the following reasons: (i) the yeast *Saccharomyces cerevisiae* does not have a recognizable Tango1 homolog nor a collagen-like molecule yet the yeast homolog of C2 (Trs20p) is encoded by an essential gene, and (ii) the role of C2 in collagen export and Golgi morphology can be separated based on the extent of C2 knockdown (Scrivens *et al.*, 2009; Venditti *et al.*, 2012). Since C2 is structurally related to longin-domain-containing SNARE proteins (Gonzalez Jr. *et al.*, 2001; Tochio *et al.*, 2001; Jang *et al.*, 2002) we speculated that it may interact with SNAREs involved in the early secretory pathway of mammalian cells. Using a yeast two-hybrid assay, we screened for interactions between C2 and the early secretory pathway SNAREs Syntaxin 5, membrin, Sec22b, Ykt6, Bet1 and GS28. As shown in Figure 2.1A, we detected an interaction between C2 and Syntaxin 5. The interaction was mediated through the SNARE domain of Syntaxin 5 (Figure 2.1B). This interaction was not due to the fact that C2 is a longin-domain-containing protein since TRAPPC1 and TRAPPC4, two other TRAPP components with longin domains, did not interact with Syntaxin 5 (Figure 2.1C). In an attempt to define the region of C2 that participates in the interaction with Syntaxin 5 we found that the pathogenic missense mutation D47Y in C2 found in patients with SEDT significantly weakened the interaction (Figure 2.1D). Mutations near D47, however, had no effect (Figure 2.1D).

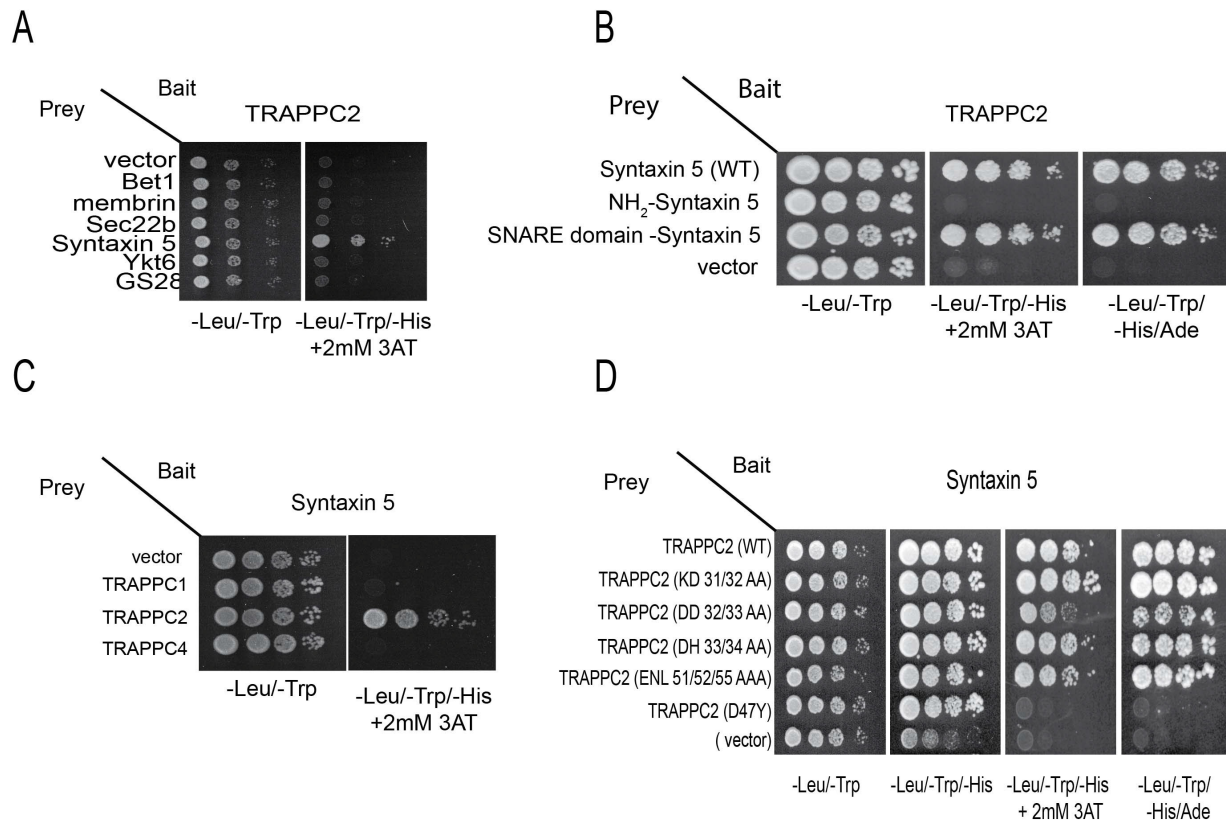


Figure 2.1 TRAPPC2 binds to Syntaxin 5 by yeast two hybrid. (A) TRAPPC2 was cloned into the yeast two hybrid vector pGBKT7 and the SNAREs indicated were cloned into pGADT7. The plasmids were transformed into AH109 and Y187 cells, mated and spotted as serial dilutions onto SD-leu/-trp and SD-leu/-trp/-his/-ade and grown at 30°C for ~3 days. (B) Full length Syntaxin 5, the SNARE domain (amino acids 263-333) or the amino-terminal domain (amino acids 1-262) of Syntaxin 5 were cloned into pGADT7 and tested for an interaction by yeast two hybrid with TRAPPC2 (or an empty pGADT7 vector control) as described in (A). (C) TRAPPC2 in pGBKT7 was tested for its ability to interact with the indicated TRAPP proteins expressed in pGADT7 by yeast two hybrid. (D) TRAPPC2 or the indicated mutants were inserted into pGBKT7 and tested for their ability to interact with Syntaxin 5 cloned into pGADT7 by yeast two hybrid.

In order to confirm the interaction between C2 and Syntaxin 5, we performed *in vitro* binding studies with GST-tagged Syntaxin 5 and His-tagged C2. As shown in Figure 2.2A, an interaction between the two proteins was detected *in vitro*. Consistent with the yeast two-hybrid assay above (Figure 2.1C), the D47Y mutation in C2 weakened this interaction *in vitro* (Figure 2.2A). As a third confirmation of this interaction we expressed myc-tagged C2 or C2D47Y in HeLa cells, immunoprecipitated Syntaxin 5 from the lysates prepared from the transfected cells and probed the immunoprecipitates for the presence of

myc-C2. Consistent with the first two assays, we noted an interaction between Syntaxin 5 and C2 that was weakened by the D47Y mutation in C2 (Figure 2.2B).

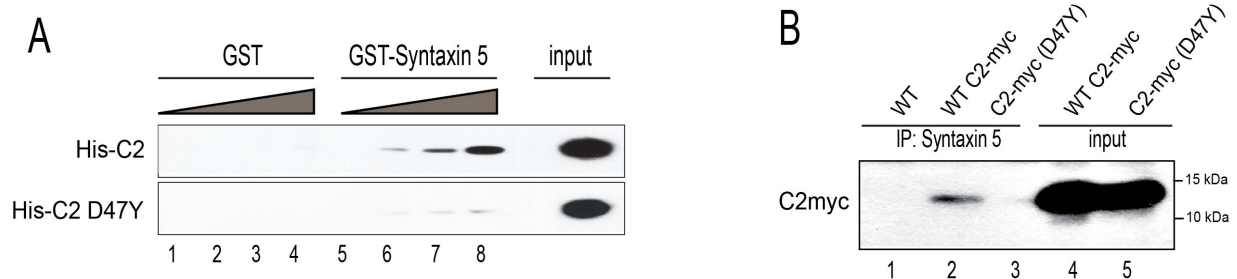


Figure 2.2 TRAPPC2 binds to Syntaxin 5 *in vitro* and *in vivo*. (A) Increasing amounts of His-tagged TRAPPC2 or TRAPPC2D47Y (0, 0.05, 0.1, 0.25 μ M) were incubated with 0.5 μ M GST-tagged Syntaxin 5 as indicated in materials and methods. The bound TRAPPC2 was detected by Western analysis using anti-His IgG. An input representing 10% is shown. The lower panel shows a coomassie-stained gel of the bait proteins GST and GST-Syntaxin 5. (B) Lysates from HeLa cells transfected with myc-tagged TRAPPC2 or TRAPPC2D47Y were treated with anti-Syntaxin 5 IgG and the immunoprecipitates were probed for the presence of myc-TRAPPC2 and Syntaxin 5 by Western analysis using anti-myc or anti-Syntaxin 5 IgG. A portion (10%) of the input is also shown.

Syntaxin 5 can be found as a component of a larger SNARE complex or free from other SNAREs (Williams *et al.*, 2004). SNARE complex formation is increased by treatment of intact cells with *N*-ethylmaleimide (NEM) (Williams *et al.*, 2004). In order to investigate whether C2 binds to Syntaxin 5 in a SNARE complex, HeLa cells were transfected with C2-myc and cells were either untreated or treated with 10 μ M NEM, a concentration sufficient to lead to SNARE complex accumulation (N.S. and M.S., unpublished observation), for increasing times. Lysates prepared from the cells were immunoprecipitated with Syntaxin 5 antibody and probed for C2-myc. Untreated cells showed a small amount of C2 co-precipitating with Syntaxin 5 (Figure 2.3A). The amount of co-precipitating C2 increased with increasing times of NEM treatment, suggesting that C2 binds to Syntaxin 5-containing SNARE complexes. Endogenous C2 was also shown to co-precipitate with Syntaxin 5 in HeLa cells in an NEM-dependent manner (Figure 2.3B).



Figure 2.3 TRAPPC2 binds to SNARE complexes. (A) HeLa cells were transfected with myc-tagged TRAPPC2 or TRAPPC2D47Y and then treated for increasing times (indicated) with 10 μ M NEM. Lysates were prepared and Syntaxin 5 was immunoprecipitated as in Figure 2.2 B (lanes 2-5). Lysate in lane 1 was from a non-transfected culture. The bound, tagged TRAPPC2 was detected using anti-mycIgG and Syntaxin 5 was detected using anti-Syntaxin 5 IgG. A portion (10%) of the input is shown. (B) Non-transfected HeLa cells were treated for increasing times (indicated) with 10 μ M NEM. Lysates were prepared and processed as in (A). Lysate in lane 1 was not incubated with IgG during the precipitation and only received protein A-agarose beads. Endogenous TRAPPC2 was detected using anti-TRAPPC2 IgG. A portion (10%) of the input is shown.

2.3.2 The yeast mutant *trs20D46Y* does not prevent processing of carboxypeptidase Y

The human C2 D47 residue is conserved in the yeast Trs20 protein at D46. Since yeast do not secrete collagen, and since we failed to detect a similar interaction between Trs20p and the yeast Syntaxin 5 homolog Sed5p (not shown), this conserved residue must be involved in some other cellular process. To address this we studied the consequences of the equivalent mutation in *TRS20* (*trs20D46Y*) in yeast. Although this mutant was slightly heat sensitive, it was not as severely-compromised as *trs20ts*, a mutant that was constructed by random mutagenesis (see Figure 2.6A). In order to investigate whether *trs20D46Y* blocked early secretory protein traffic we performed a pulse-chase experiment using the vacuolar hydrolase carboxypeptidase Y (CPY). This commonly used secretory marker protein is translated and inserted into the ER as a “p1” form. It then traffics to the Golgi where it migrates as a slower “p2” form before it is delivered to the vacuole as a faster-migrating “m” form (Stevens *et al.*, 1982). As shown in Figure 2.4, neither *trs20D46Y* nor *trs20ts* displayed a defect in the processing of CPY. In addition, *trs85 Δ* , a gene whose product has previously been reported to function in ER-to-Golgi transport but has more recently been implicated in selective autophagy, also processed CPY similar to wild type.

These results suggest that *trs20D46Y* does not function in ER-to-Golgi traffic but may affect some aspect of TRAPP II and/or III activity.



Figure 2.4 *trs20D46Y* does not block trafficking of carboxypeptidase Y. Yeast strains indicated were pulsed with ^{35}S -methionine for 4 minutes and chased with unlabeled methionine for the times indicated as described in materials and methods. Carboxypeptidase Y (CPY) was immunoprecipitated using anti-CPY IgG, and the forms of CPY were visualized by radioautography.

2.3.3 The *D46Y* mutation in *trs20* affects its interactions with TRAPP II and III proteins

To begin to understand where the D46 residue in Trs20p functions, we compared the interactions of Trs20p and *trs20D46Yp* with all known components of the TRAPP complex using the yeast two-hybrid assay. As shown in Figure 2.5, Trs20p interacted with Trs31p, Bet3p, Trs85p, Trs120p and Trs130p (all other TRAPP subunit interactions tested were negative). The first two proteins are components of the TRAPP core and these interactions were seen in the crystal structure of both the yeast and mammalian complexes (Kim *et al.*, 2006; Cai *et al.*, 2008). Trs85p is a component of TRAPP III while Trs120p and Trs130p are found in the TRAPP II complex. These results are consistent with a recent report suggesting that the mammalian Trs20p homolog C2 interacts with both the Trs120p (TRAPPC9) and Trs85p (TRAPPC8) homologs (Zong *et al.*, 2011). Interestingly, while the *D46Y* mutation in Trs20p did not affect the interaction with neither Bet3p nor Trs31p, it did weaken the interaction between Trs20p and the TRAPP II/III-specific components Trs85p, Trs120p and Trs130p (Figure 2.5).

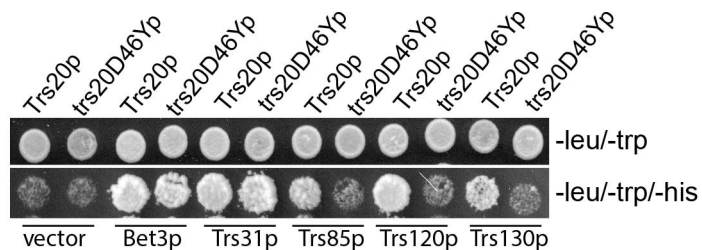


Figure 2.5 The *trs20D46Y* mutation disrupts the interaction of Trs20p with TRAPP II and TRAPP III specific subunits. The open reading frames encoding *TRS20* and *trs20D46Y* were cloned into pGBKT7, transformed into AH109 yeast cells, and mated to Y187 yeast that harbored pGADT7 containing the indicated TRAPP open reading frames. The resulting diploids were spotted onto SD-leu/-trp (top panel) or SD-leu/-trp/-his (bottom panel).

We also used yeast genetic interactions to investigate the connection between *TRS20* and the TRAPP II and III complexes. Although *trs20D46Y* is mildly heat sensitive, the phenotype was more pronounced in the presence of HA-tagged Trs130p but not with HA-tagged Trs85p (Figure 2.6A). Neither *trs20D46Y* nor *trs20ts* displayed genetic interactions with *trs85Δ*, although *trs20ts* was synthetically lethal with *trs65Δ* (a gene encoding a TRAPP II subunit) (Figure 2.6B). Finally, using the more heat-sensitive *trs20D46Y* mutation in the *TRS130-HA* background, we found that, in addition to the expected suppression conferred by *TRS20* and *TRS130*, *TRS120* was capable of suppressing the temperature-sensitive growth phenotype (Figure 2.6C). These results suggest that, while *trs20D46Y* does not have a strong growth phenotype, it does display interactions with genes encoding TRAPP II and III subunits.

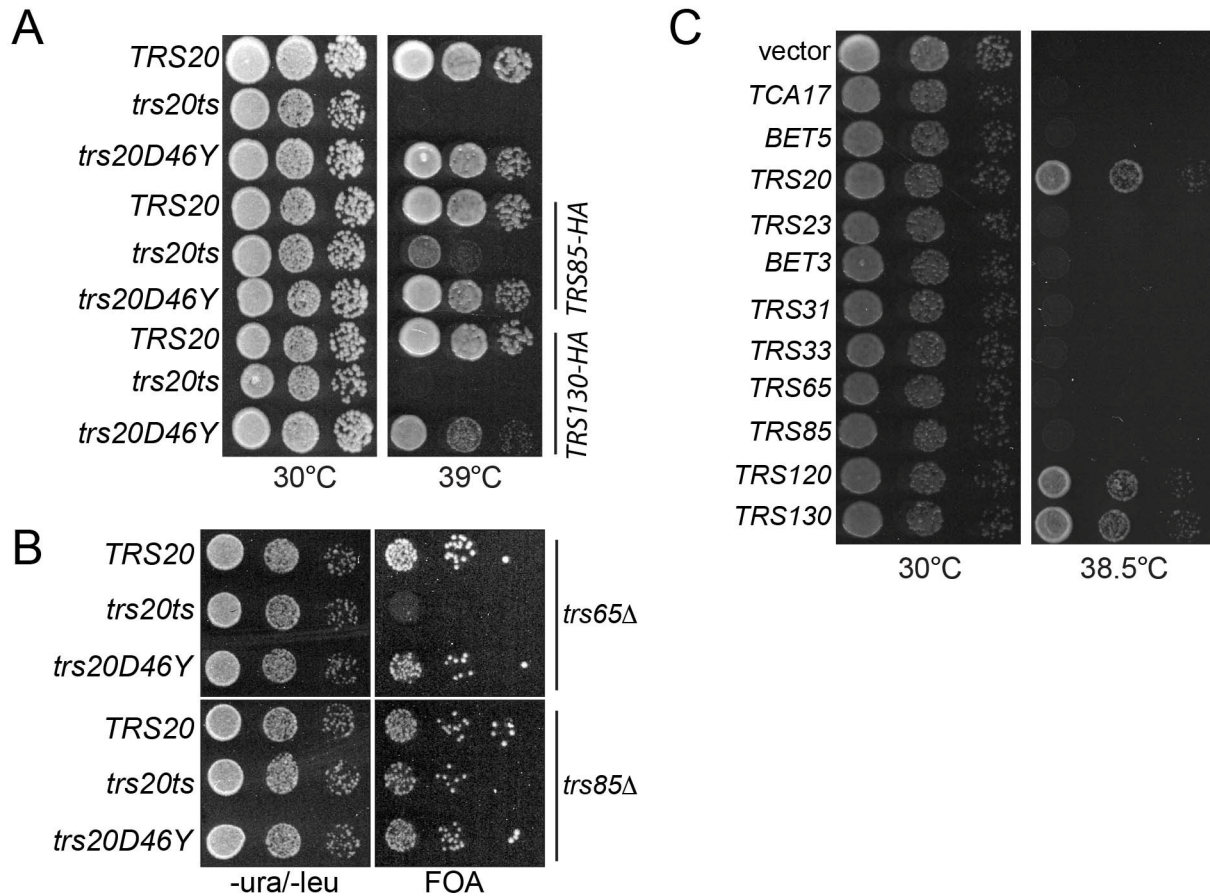


Figure 2.6 Genetic interactions affected by *trs20D46Y*. (A) A yeast strain with *trs20D46Y* as the sole copy of *TRS20* was spotted as a serial dilution on YPD plates and grown at either 30°C or 39°C. A *trs20ts* strain (Ben-Aroya *et al.*, 2008)(56) was also included. The same *trs20* mutations were introduced into a yeast strain with the sole copy of *TRS130* tagged with the HA epitope. (B) The *trs20D46Y* mutation was introduced into a yeast strain in which the chromosomal copy of *TRS65* (*trs65Δ*) or *TRS85* (*trs85Δ*) was deleted and a copy of wild type *TRS65* or *TRS85* was maintained on a *URA3*-based plasmid. The plasmid was counter-selected on 5-fluoroorotic acid-containing plates. (C) A yeast strain (*TRS130*-HA *trs20D46Y*; see A) was transformed with a plasmid containing the indicated TRAPP gene and grown on YPD plates at either 30°C or 38.5°C.

2.3.4 *trs20D46Y* phenocopies *trs85Δ* in both GFP-Snc1p recycling and Calcofluor white hypersensitivity

Since early secretory protein traffic was unaffected in *trs20D46Y* cells, we examined the cells for a general secretion defect. Included in these studies was the *trs85Δ* mutant since Trs20p showed a D46-dependent interaction with Trs85p (see above). Cells were pulsed with ³⁵S-methionine and then chased with cold methionine and the culture

supernatant was assayed for secreted proteins. As expected, *sec18*, a gene involved in virtually all membrane trafficking steps, potently blocked the appearance of secreted proteins compared to wild type (Figure 2.7). In contrast, *trs20D46Y* appeared similar to wild type, suggesting that secretion is not defective in this mutant. A similar result was seen for *trs85Δ* (Figure 2.7) whereas *trs130ts* showed a partial block in secretion (not shown; see (Cai *et al.*, 2005)). A partial block in secretion was also seen in *trs20ts* (Figure 2.7).

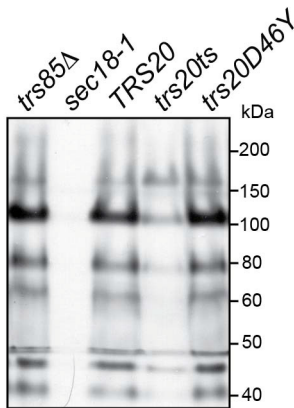


Figure 2.7 *trs20D46Y* and *trs85Δ* do not block general secretion. Yeast strains indicated were pulsed with ^{35}S -methionine for 15 minutes and chased with unlabeled methionine for 15 minutes. The yeast were separated from the growth medium during a brief centrifugation and proteins in the growth medium were precipitated with trichloroacetic acid. The precipitates were visualized by radioautography.

Calcofluor white (CFW) sensitivity is often used as a measure of activity of the endocytic pathway (Valdivia *et al.*, 2002). This compound binds to chitin in the yeast cell wall, enters the cell and ultimately results in cell death. A defect in endocytosis leads to elevated chitin levels in the cell wall and a hypersensitivity of the cells to CFW while a defect in anterograde traffic results in CFW resistance. In the case of *trs20D46Y* the cells were hypersensitive to CFW (Figure 2.8). This was also the case for *trs20ts* and *trs85Δ*.

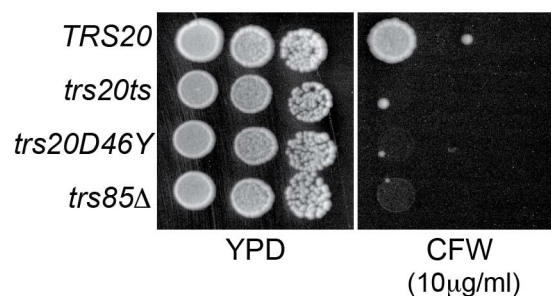


Figure 2.8 *trs20D46Y* and *trs85Δ* strains are sensitive to Calcofluor white. The indicated yeast strains were spotted as serial dilutions on YPD plates either with or without 10µg/ml Calcofluor white and grown at 30°C.

We next examined GFP-Snc1p localization in these cells. Snc1p is a SNARE protein that cycles between the Golgi and plasma membrane via the endocytic pathway. When fused to GFP, the protein localizes to the plasma membrane and to small buds in dividing cells (Figure 2.9). Previous studies have shown an accumulation of internal structures in *trs85Δ* cells (Montpetit and Conibear, 2009; Brunet *et al.*, 2012) (Figure 2.9). Similarly, we found internal, GFP-Snc1p-positive structures in *trs20D46Y* and *trs20ts*. Collectively, our results suggest that *trs20D46Y* affects post-Golgi/endosome trafficking. The similar phenotype seen in *trs85Δ* and the interaction between Trs20p and the TRAPP III-specific component Trs85p suggest Trs20p may act in autophagy.

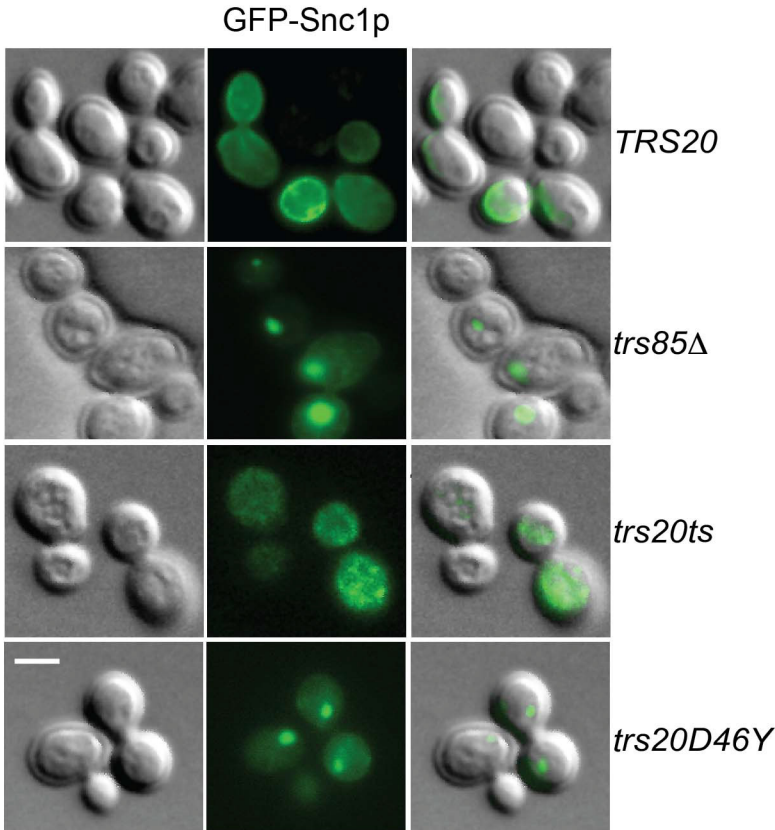


Figure 2.9 The *trs20D46Y* mutant phenocopies the GFP-Snc1p recycling defect observed in *trs85Δ* cells. Yeast strains were transformed with a plasmid containing GFP-Snc1p. The cells were fixed with paraformaldehyde and the localization of GFP-Snc1p was assessed by fluorescence microscopy. Accumulation of GFP-Snc1p on internal structures is seen in $24\pm 1\%$, $62\pm 2\%$, $77\pm 1\%$ and $89\pm 3\%$ of wild type, *trs20ts*, *trs20D46Y* and *trs85Δ* cells, respectively (N=150 for each strain, performed in triplicate). The scale bar is $5\mu\text{m}$.

2.3.5 TRAPPIII is destabilized in the *trs20D46Y* mutant

To better understand the trafficking step(s) affected in *trs20D46Y*, we examined the assembly state of the TRAPP complexes. First, yeast lysates from wild type or *trs20* mutants were probed for Trs20p, Trs23p (TRAPPI core protein), Trs130p-HA (TRAPPII subunit) and Trs85p-HA (TRAPPIII subunit). As seen in Figure 2.10, Trs130p-HA levels were unaffected in *trs20D46Y* but were greatly reduced in *trs20ts* cells, suggesting destabilization of TRAPPII in the latter mutant. In addition, both mutants showed greatly reduced levels of Trs85p-HA. Only *trs20ts*, but not *trs20D46Y*, showed reduced Trs20p levels. Neither mutant displayed significant changes in the levels of Trs23p. These results suggest that the integrity of TRAPPIII, but not TRAPPII, may be affected in *trs20D46Y*.

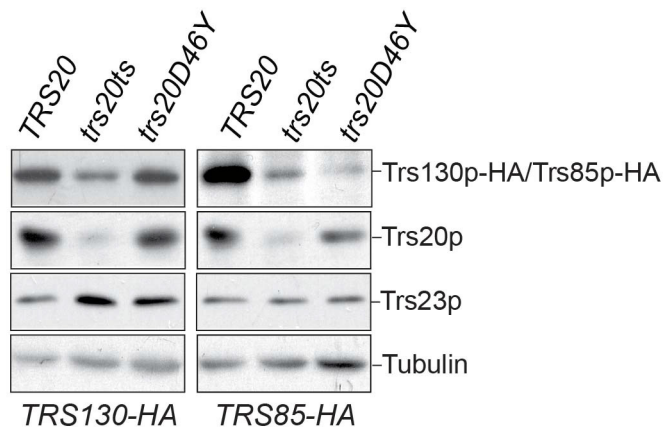


Figure 2.10 The levels of Trs85p are reduced in *trs20D46Y*. *TRS85* or *TRS130* was tagged with a 3XHA epitope in either wild type, *trs20D46Y* and *trs20ts*. Lysates prepared from these strains were probed with anti-HA IgG, anti-Trs20p, anti-Trs23p and anti-tubulin (as a loading control).

To examine this, we fractionated lysates on a Superose 6 column that we and others previously showed efficiently separates TRAPPI, II and III (Choi *et al.*, 2011; Brunet *et al.*, 2012). The fractions from the column were probed with anti-Trs23p antibody. This protein is an integral component of the TRAPPI core and, thus, is found in all three TRAPP complexes. As previously reported for wild type cells, Trs23p was detected in the fractions corresponding to TRAPPI, II and III (Figure 2.11A). In the *trs20D46Y* mutant there was a striking loss in the Trs23p signal in only the TRAPPIII fractions. In contrast to *trs20D46Y*, the Trs23p signal in both TRAPPII and III was reduced in *trs20ts* (Figure 2.11A). Upon examination of Trs85p-HA, there was a decrease in this protein from the TRAPPIII peak in both *trs20D46Y* and *trs20ts*, consistent with the decrease in protein levels from whole cell lysates (Figure 2.11B). The results from the Superose 6 column suggest that TRAPPIII is selectively destabilized in the *trs20D46Y* mutant. This destabilization may be due to a weakened interaction between Trs20p and Trs85p in this mutant (see Figure 2.5).

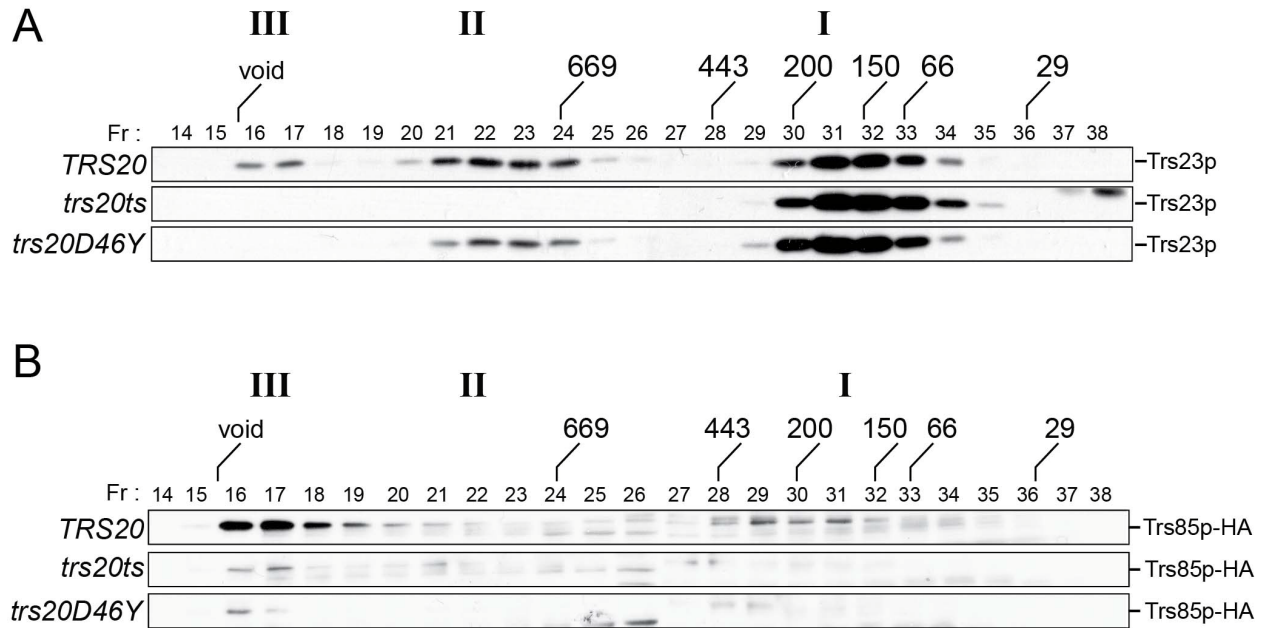


Figure 2.11 TRAPPIII is destabilized in *trs20D46Y*. Lysates from the Trs85p-HA-tagged strains in Figure 2.10 were fractionated on a Superose 6 size exclusion column in 300mM NaCl and fractions were probed with (A) anti-Trs23p or (B) anti-HA (to detect Trs85p-HA) IgG. The location of the TRAPPI, II and III fractions are indicated as are the fractionation of molecular size standards.

2.3.6 Autophagy is defective in the *trs20D46Y* mutant

Based on the destabilization of TRAPPIII, a complex involved in autophagy, we tested whether *trs20D46Y* affected autophagy. Growing cells in the presence or absence of a nitrogen source allows one to distinguish between the selective cytosol-to-vacuole (Cvt) autophagic pathway (+nitrogen) and the non-selective pathway (-nitrogen). We first probed for the marker protein Ape1p which uses the selective pathway in the presence of nitrogen but is transported to the vacuole in a non-selective manner in the absence of nitrogen (Scott *et al.*, 1996). The processing of Ape1p is detected by examining the levels of the precursor form of the protein and the processed form that appears as a faster-migrating species by SDS-PAGE using an Ape1p antibody. Consistent with the destabilization of TRAPPIII in *trs20D46Y*, Ape1p processing in the presence of nitrogen was completely blocked when compared to wild type (Figure 2.12, +N panel). In accordance with previous studies, *trs85Δ* and *atg1Δ* (a gene that is critical for autophagy) also showed blocks in the selective pathway (Meiling-Wesse *et al.*, 2005; Lynch-Day *et al.*, 2010) as did

trs20ts (Figure 2.12). In the absence of nitrogen, when Ape1p is processed by non-selective autophagy, a significant amount of mature Ape1p was detected in *trs20D46Y*, *trs20ts* and *trs85Δ* with small amounts of the precursor form also present, suggesting a defect in non-selective autophagy (Figure 2.12, -N panel).

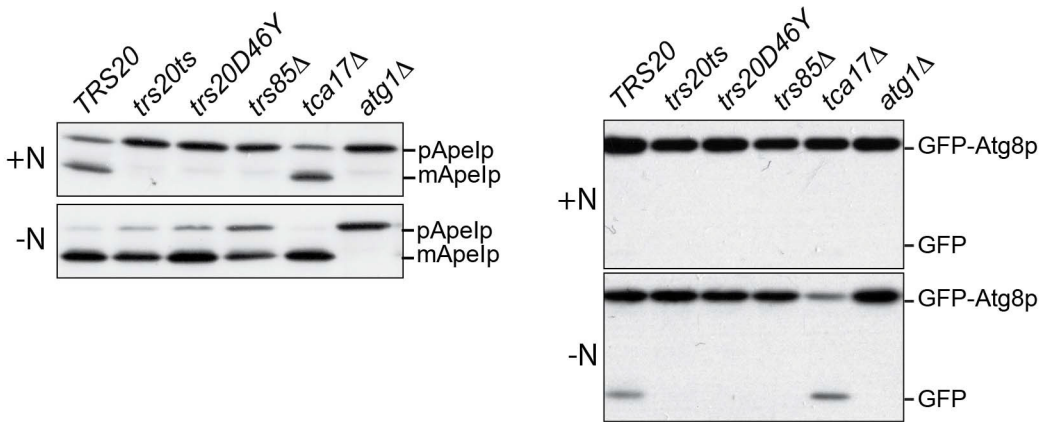


Figure 2.12 Both selective and non-selective autophagy are affected in *trs20D46Y*.

The indicated yeast strains were grown in rich (+N; upper panel) or nitrogen starvation (-N; lower panel) medium as described in materials and methods. Equal amounts of protein were fractionated by SDS-PAGE and analyzed by Western analysis using anti-Ape1p IgG or anti-GFP (to monitor GFP-Atg8p processing) as indicated.

To further confirm autophagic defects in *trs20D46Y*, we examined the localization of Ape1p-GFP. In wild type cells, a single punctum of fluorescence is often detected that represents Ape1p in the preautophagosomal structure (PAS) (Shintani *et al.*, 2002) (Figure 2.13). Interestingly, *trs20D46Y* showed a single but much larger punctum of Ape1p-GFP fluorescence suggesting the protein accumulates in the PAS. This is consistent with the autophagic defect seen by Western analysis above. Furthermore, *trs85Δ* and *trs20ts* also displayed a similar phenotype of a single, but much larger, punctum of fluorescence (Figure 2.13). A single, large punctum such as that seen in *trs20D46Y* and *trs85Δ* has been reported in other mutants that block the Cvt pathway (Shintani *et al.*, 2002).

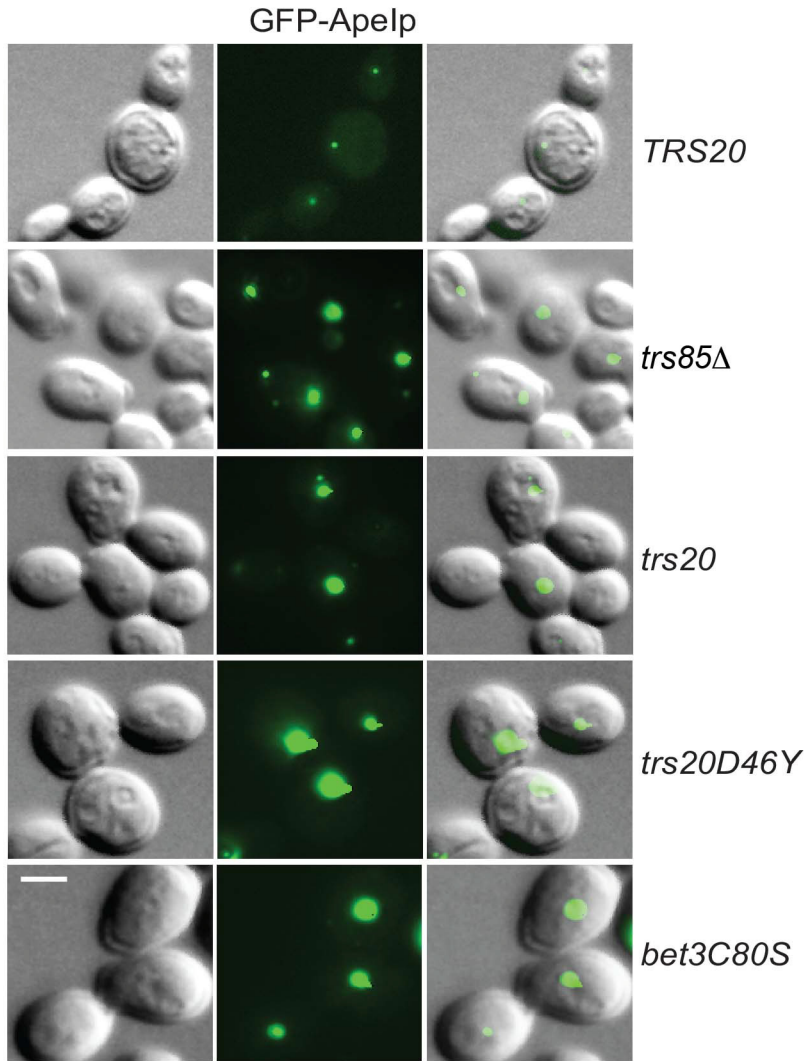


Figure 2.13 GFP-Ape1 accumulates in *trs20D46Y* under non-starvation conditions. The strains indicated were transformed with GFP-Ape1p, fixed and visualized by fluorescence microscopy. The scale bar is 2 μ m. Note the larger size of the GFP-Ape1p punctum in the mutants compared to wild type.

To more carefully assess whether *trs20D46Y* affects non-selective autophagy, we examined the processing of GFP-Atg8p. Upon uptake into the vacuole under nitrogen starvation conditions, this fusion protein is cleaved, liberating GFP. This processing can be detected by Western analysis. As seen in Figure 2.12, *trs20D46Y* as well as *trs20ts* displayed a defect in GFP-Atg8p processing in nitrogen starved medium (-N). A similar defect was also seen for *trs85Δ*, consistent with previous studies (Meiling-Wesse *et al.*, 2005; Zou *et al.*,

2012a). Collectively, our results demonstrate that *trs20D46Y* affects both the selective (Cvt) and non-selective autophagic pathways without affecting anterograde transport.

2.3.7 Trs20p and Tca17p have differing functions

Trs20p and its mammalian homolog C2 are phylogenetically and structurally related to a newly-identified TRAPP-interacting protein called Tca17p in yeast (TRAPPC2L in higher eukaryotes) (Jang *et al.*, 2002; Kim *et al.*, 2006; Cai *et al.*, 2008; Scrivens *et al.*, 2009) (Protein Data Bank ID 3PR6). We therefore examined the interaction profile of Tca17p and the biochemical consequences in yeast of *tca17Δ* to that seen for Trs20p and *trs20D46Y*. By yeast two hybrid analysis, and in accordance with our previously reported genetic interaction (Scrivens *et al.*, 2009), when compared to the three TRAPP subunits whose interactions were affected by *trs20D46Yp* (i.e. Trs85p, Trs120p and Trs130p), we found that Tca17p only interacted with Trs130p (Figure 2.14A). In addition, size exclusion chromatography showed that *tca17Δ* altered the integrity of the TRAPP^{II} peak but did not alter the integrity of the TRAPP^{III} peak (Figure 2.14B) (Choi *et al.*, 2011). Finally, in contrast to *trs20D46Y*, *tca17Δ* did not block the processing of Ape1p in rich medium nor of GFP-Atg8p in starvation medium (Figure 2.12). While this latter result is in contradiction to that recently reported for *tca17ts* (Zou *et al.*, 2013), it is noteworthy that our mutant is a simple *tca17* deletion as compared to *tca17ts* which also includes modifications to *TRS120* and *TRS130*. In combination with our previous results showing that human C2, but not human C2L, could suppress *trs20Δ* (Scrivens *et al.*, 2009), we suggest that Tca17p and Trs20p, although evolutionarily and structurally related, are functionally distinct.

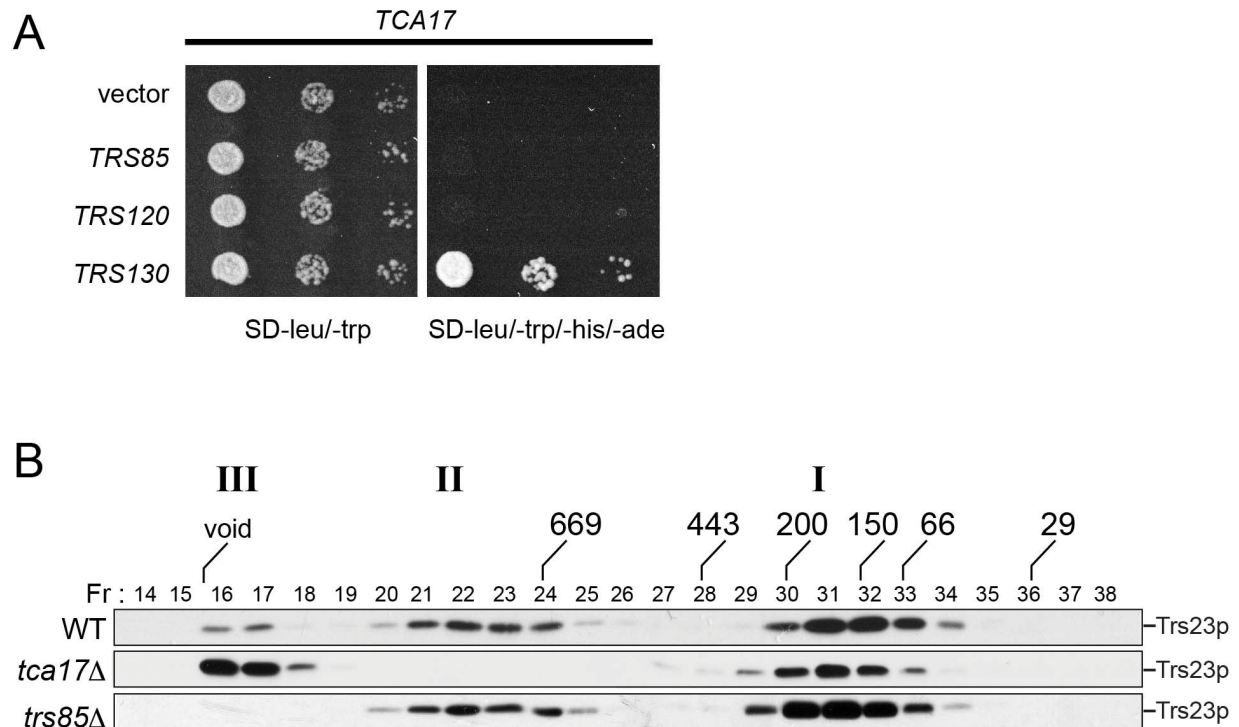


Figure 2.14 Tca17p is important for the integrity of TRAPP II but not TRAPP III. (A) The open reading frame encoding *TCA17* was cloned into pGBKT7, transformed into AH109 yeast cells, and mated to Y187 yeast that harbored pGADT7 containing the open reading frame for either *TRS130*, *TRS120* or *TRS85*. Growth on SD-leu/-trp/-his/-ade indicates that Tca17p binds to only Trs130p. This Figure is related to Figure 2.5. (B) Lysate prepared from *tca17Δ* or *trs85Δ* was fractionated on a Superose 6 size exclusion column in 300mM NaCl. The peaks for TRAPP I, II and III are indicated. Also shown is the same wild type blot shown in Figure 2.11A for comparison. The Trs23p signal in the TRAPP II fractions is missing but remains in the TRAPP III fractions.

2.3.8 The molecular size of TRAPP III depends upon membranes and Atg9p

The composition of TRAPP III differs from that of TRAPP I by the addition of a single subunit, Trs85p. However, the molecular size of TRAPP III (>1MDa) is much greater than that of TRAPP I (~200kDa), and this difference cannot be accounted for by this single 85kDa protein. A previous study did not identify any other polypeptides in this complex and oligomerization was also ruled out (Choi *et al.*, 2011) (S.B. and M.S., unpublished observation). Suspecting that the large molecular size of TRAPP III was due to association with membranes, we examined the fractionation of Trs23p and Trs85p-HA in lysates prepared using Triton X-100. While Trs85p-HA shifted to a fraction with a smaller molecular size near TRAPP I, Trs23p spread out between the fractions spanning TRAPP III

to II (Figure 2.15A). This spreading of the Trs23p peak in Triton X-100 was independent of Trs85p since a similar pattern was seen in *trs85Δ* treated with the detergent (Figure 2.15A). Such an effect was previously noted for Trs130p in a *tca17Δ* strain (Choi *et al.*, 2011). Since Trs23p is absent from the TRAPP^{III} fractions in *trs85Δ* prepared without detergent (Figure 2.14B), this result suggests that the fractionation of Trs23p seen in the presence of Triton X-100 is likely due to changes to TRAPP^{II}. Our results indicate that, in the absence of detergent, TRAPP^{III} is associated with Triton X-100-soluble membranes. Consistent with this notion, TRAPP^{III} penetrated an Optiprep gradient further in the absence, as compared to the presence, of Triton X-100 (Figure 2.15B).

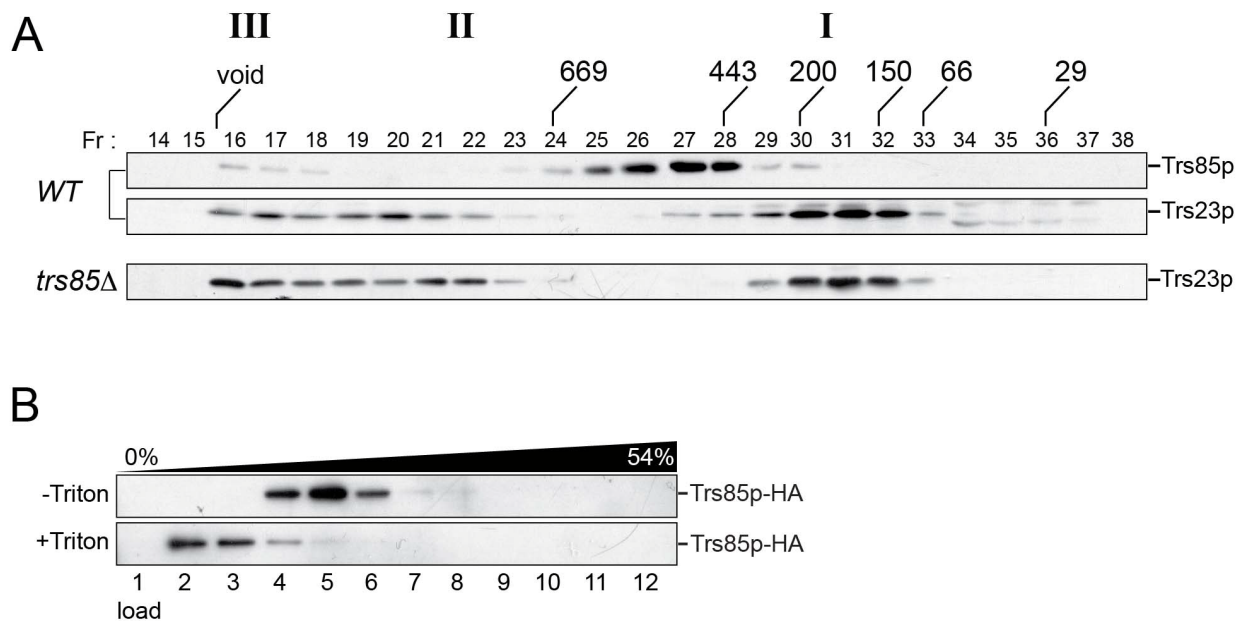


Figure 2.15 The molecular size of TRAPP^{III} is dependent upon membranes. Lysate was prepared from (A) *TRS85*-HA or *trs85Δ* strains with 300mM NaCl/1% Triton X-100. The lysates were fractionated on a Superose 6 size exclusion column. The fractions were probed for Trs23p and Trs85p-HA as indicated. (B) Pooled fractions from a Superose 6 column enriched in TRAPP^{III} derived from a *TRS85*-HA strain that was not treated with Triton X-100 were loaded on top of an Optiprep step gradient prepared as described in materials and methods. The top-loaded sample was either left untreated or incubated with 1% Triton X-100 before centrifugation on the gradient. Fractions were collected from the top of the gradient and probed for Trs85p-HA.

We next set out to identify a putative TRAPP^{III} receptor on autophagic membranes by screening *atgΔ* mutants for changes in the fractionation pattern of TRAPP^{III} on a size

exclusion column. Our studies led us to focus on *atg9* Δ . In whole cell lysates, the levels of Trs85p-HA, but not Trs23p, were dramatically reduced upon nitrogen starvation in *atg9* Δ compared to wild type (Figure 2.16A, compare +/- nitrogen). Correspondingly, there was a decrease in the appearance of Trs85p-HA in the TRAPP^{III} peak in nitrogen-starved *atg9* Δ cells relative to non-starved cells (Figure 2.16B). Remarkably, Trs23p was also reduced in the TRAPP^{III} fractions (Figure 2.16B). This result is similar to that seen for *trs20D46Y* (see Figure 2.10 and 2.11) in which the cellular levels of Trs85p-HA, but not Trs23p, are reduced yet the amounts of both proteins in the TRAPP^{III} fraction are greatly diminished. We next examined Atg17p since this protein has been reported to recruit Atg9p to autophagic membranes (Sekito *et al.*, 2009). In a nitrogen-starved *atg17* Δ strain, we did not detect a significant decrease in the levels of neither Trs85p-HA nor of Trs23p relative to wild type (Figure 2.16A) and there were no differences in the fractionation of these proteins in the TRAPP^{III} peak (Figure 2.16B) compared to non-starved cells. Collectively, our results suggest that the recruitment of TRAPP^{III} during non-selective, but not during selective, autophagy requires Atg9p, and that an assembled TRAPP^{III} complex is required for both selective and non-selective autophagy.

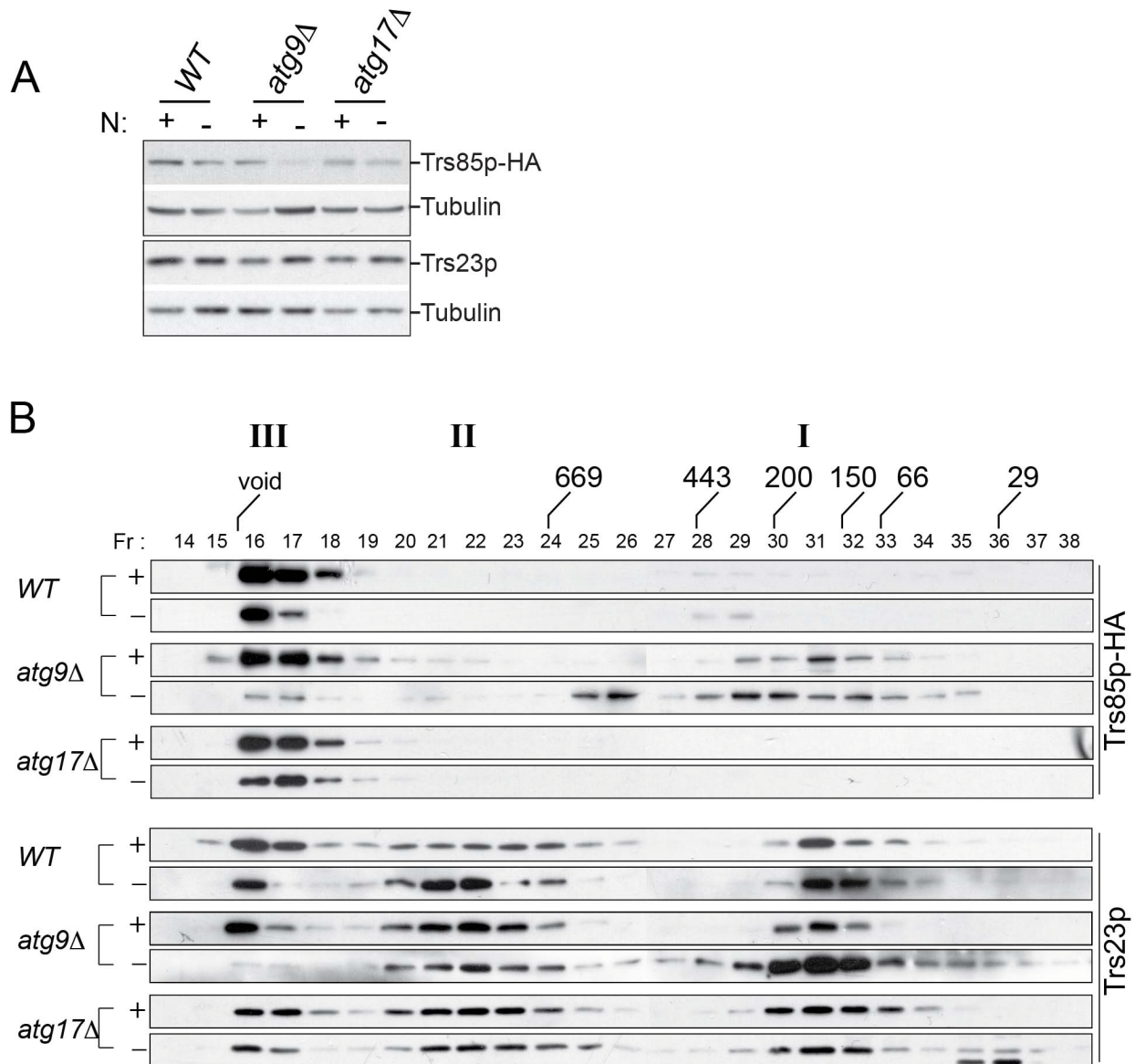


Figure 2.16 The molecular size of TRAPPIII is dependent upon Atg9p (A) Lysate in 300mM NaCl was prepared from wild type, *atg9Δ*, *atg17Δ*, *atg9Δ/TRS85-HA* or *atg17Δ/TRS85-HA* grown in YPD (+) or nitrogen starvation medium (-). Lysates were probed for either Trs23p, Trs85p-HA or tubulin (as a loading control). (B) A total of 2mg of lysate from the cells in (A) was fractionated on a Superose 6 column and probed for Trs23p or Trs85p-HA as indicated.

2.3.9 Palmitoylated Bet3p is enriched in TRAPPIII

TRAPPIII appears to be membrane associated while TRAPPI is more easily separated from membranes since fractionation of the latter on a size exclusion column is not affected by detergent. What can account for this difference? The TRAPPI core subunit Bet3p was shown to be lipid-modified by either palmitoylation or myristoylation (Kim *et al.*, 2005; Turnbull *et al.*, 2005). The modified cysteine residue at position 80 in the yeast protein is highly conserved yet, surprisingly, mutation of this residue does not lead to any observable growth phenotype. We speculated that lipid-modified Bet3p may partially account for the association of the TRAPPIII complex with PAS membranes. If this is the case, *bet3C80S*, a mutant that prevents Bet3p palmitoylation (Kim *et al.*, 2005; Turnbull *et al.*, 2005; Kummel *et al.*, 2006), may block autophagy. Indeed, compared to wild type, *bet3C80S* displayed both a defect in Ape1p processing in the presence, but not the absence, of nitrogen and a starvation-induced reduction in GFP-Atg8p processing (Figure 2.17). In addition, *bet3C80S* also displayed an enlarged Ape1p-GFP punctum similar to that seen for *trs85Δ* and *trs20D46Y* (Figure 2.13). This suggests that palmitoylation of Bet3p is involved in the efficient functioning of TRAPPIII in both selective and non-selective autophagy.

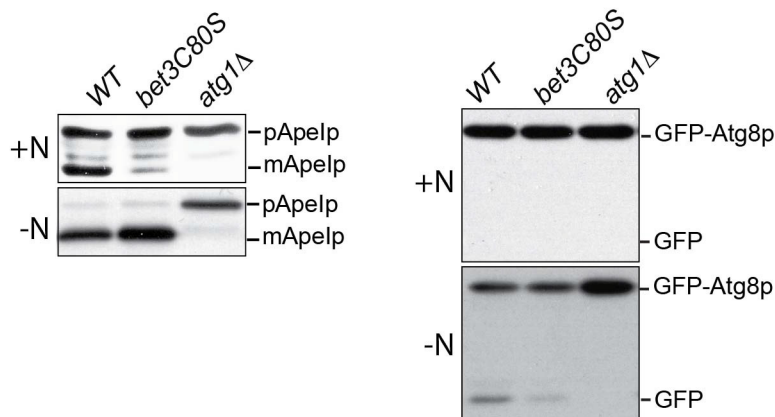


Figure 2.17 Both selective and non-selective autophagy are affected in *bet3C80S*. Lysates from wild type, *bet3C80S* and *atg1Δ* were prepared from cultures grown in YPD (+N) or nitrogen starvation (-N) medium as described in materials and methods and analyzed by Western analysis with anti-Ape1p IgG or anti-GFP (to monitor GFP-Atg8p processing) as indicated.

Given the results above we speculated that palmitoylated Bet3p would be enriched in TRAPPIII. To test this notion, a wild type lysate was fractionated by size exclusion chromatography and the fractions containing TRAPPI, II and III were pooled separately and subjected to acyl-biotin exchange. In this assay, acyl chains on proteins are exchanged for a biotin moiety which can then bind to streptavidin-agarose beads. Precipitation of proteins onto the beads indicates that the proteins were initially acylated. As shown in Figure 2.18, after normalization to Bet3p levels in the input, acylated Bet3p was greatly enriched in TRAPPIII. Our results suggest that acylated Bet3p is important for the function and/or localization of the TRAPPIII complex.

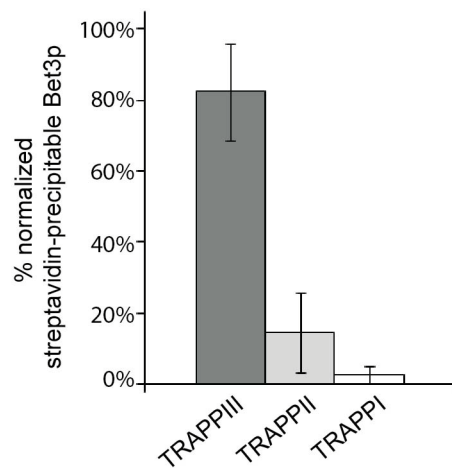


Figure 2.18 Lipidated Bet3p is enriched in TRAPPIII. A wild type lysate was fractionated on a Superose 6 column and the peak of TRAPPI, II and III were pooled individually and subjected to acyl-biotin exchange as described in materials and methods. A portion of each input fraction, to enable normalization to Bet3p, along with the entire precipitate from the streptavidin-agarose beads was subjected to Western analysis using anti-Bet3p serum and quantitated using Image J. Error bars indicate standard deviation.

2.4 Discussion

Here we demonstrate that the mammalian TRAPP protein C2 binds to the SNARE protein Syntaxin 5. This interaction is weakened by the pathogenic D47Y mutation in C2 and led us to speculate that a yeast mutation patterned after this mutation in the C2 homolog Trs20p would affect early secretory pathway traffic. Instead this yeast mutant (*trs20D46Y*) did not display anterograde trafficking defects but was defective in the selective (Cvt) and non-selective autophagy pathways. In addition, *trs20D46Y*, *atg9 Δ* and *bet3C80S* mutants revealed complexities in the organization and function of the TRAPPIII

complex that is involved in these pathways. It should be stressed that, although the *trs20* mutants examined in this study did not display trafficking defects in the early secretory pathway, other residues in this protein may in fact impinge on this process.

2.4.1 Complexities in TRAPPIII assembly and function

The subunit composition of TRAPPIII differs from TRAPPI by just a single additional protein (Trs85p in TRAPPIII), yet the molecular size of TRAPPIII is much greater than that of TRAPPI (see Figures 2.10, 2.11, 2.15, and 2.16) (Choi *et al.*, 2011; Brunet *et al.*, 2012) and this is not due to oligomerization of Trs85p/TRAPPIII (Choi *et al.*, 2011) (S.B. and M.S., unpublished observation). We found that the cellular levels of the TRAPPIII-specific protein Trs85p-HA, but not the TRAPPI core protein Trs23p, were greatly diminished in *trs20D46Y* as well as in *atg9Δ*, but unaffected in *atg17Δ* relative to wild type. The former two mutants showed reduced levels of both Trs85p-HA and Trs23p in the TRAPPIII fractions. Our results imply that, during non-selective autophagy, the recruitment of TRAPPIII to autophagic membranes is dependent upon Atg9p (Figure 2.19A). Our data do not address which, if any, subunit of TRAPPIII interacts directly with Atg9p. However, a recent report suggested that Trs85p, but not other TRAPPI core subunits, binds directly to Atg9p and its localization is affected in *atg9Δ* cells (Kakuta *et al.*, 2012). If this is the case, our results with *trs20D46Y* suggest that recruitment of the TRAPPI core to the Atg9p-Trs85p unit is mediated in part by Trs20p and particularly by its conserved D46 residue. Our data leave open the possibility that the TRAPPI core may be recruited to membranes distinct from those containing Trs85p in which case their interaction to form TRAPPIII may contribute to tethering (Figure 2.19B). This would be similar to the mechanism of exocyst complex-mediated tethering in which vesicles are tethered to the plasma membrane via interactions between exocyst components on separate membranes (Boyd *et al.*, 2004). Since the cellular levels of Trs85p-HA and the appearance of Trs85p-HA and Trs23p in TRAPPIII were not affected under rich growth conditions in *atg9Δ*, recruitment of TRAPPIII to autophagic membranes during selective autophagy must be dependent on an as yet unidentified factor (Figure 2.19C).

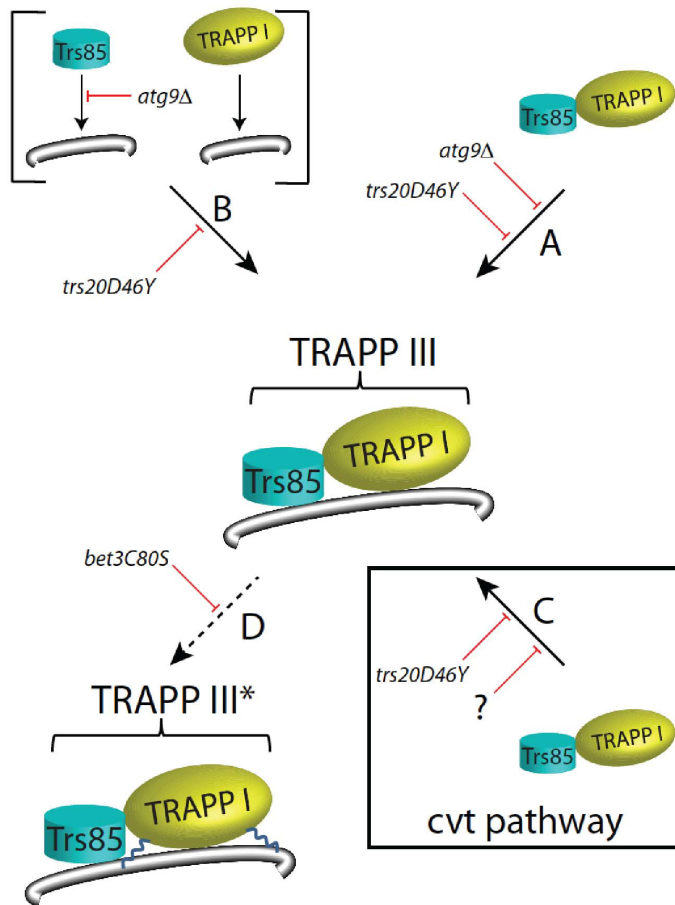


Figure 2.19 Model for the organization and assembly of TRAPPIII. Assembly of TRAPPIII is dependent upon an interaction between Trs20p and Trs85p and is mediated by the conserved D46 residue in Trs20p. Assembled TRAPPIII is then recruited to autophagic membranes in an Atg9p-dependent manner (A). This may be mediated by a direct interaction between Trs85p and Atg9p as recently suggested (Kakuta *et al.*, 2012). Alternatively, Trs85p and Trs23p may be recruited to separate membranes, and their interaction to form TRAPPIII is mediated by the same Trs20p-Trs85p interaction described above (B). Note that the involvement of Atg9p in this scenario is based on a recent study (Kakuta *et al.*, 2012). Although TRAPPIII assembly in the selective (Cvt) pathway is also mediated by a Trs20p-Trs85p interaction, recruitment to autophagic membranes does not appear to require Atg9p and some as yet unknown factor (denoted as ?) may be involved (C). In both cases (selective and non-selective autophagy) lipitation of Bet3p in TRAPPIII increases the functional efficiency of the TRAPPIII complex (denoted by TRAPPIII*). The steps that are blocked by the various mutants used in this study are indicated by red lines.

Our results provide a clue as to the role of *trs20D46Y* in autophagy. Based on Ape1p processing in rich medium, this mutant affects the Cvt pathway. While there was only a minor defect in Ape1p processing under nitrogen-starved conditions, examination of GFP-Atg8p under these conditions indicated that non-selective autophagy was also strongly

affected. A similar phenotype consisting of a mild defect of Ape1p processing but a strong defect in GFP-Atg8p processing in starvation conditions has been reported for the TRAPP mutant *trs85Δ* as well as for *vac8Δ* (Cheong *et al.*, 2005; Meiling-Wesse *et al.*, 2005; Zou *et al.*, 2013). In the latter mutant, autophagic bodies were reduced in both number and size. Our results, therefore, suggest that in *trs20D46Y* Cvt vesicles fail to form. However, in nitrogen-starved conditions, while some autophagosomes may form, their size is likely to be abnormally small.

What is the role of Bet3p lipidation in TRAPPIII function? The enrichment of lipidated Bet3p in TRAPPIII and the fact that TRAPPIII remains membrane-associated in *bet3C80S* (S.B. and M.S., unpublished observation), suggests that lipidation alone cannot account for TRAPPIII membrane attachment. It is tempting to speculate that lipidated Bet3p may localize the complex to a membrane sub-domain of autophagic vesicles. It is noteworthy that acylation of proteins is one mechanism that directs their intracellular localization (Roskoski Jr., 2003; Munro, 2005). Alternatively, lipidation of Bet3p/TRAPPC3 has been postulated to alter its structure (Turnbull *et al.*, 2005; Kummel *et al.*, 2006, 2010), which may promote binding to these specialized membrane regions or increase the efficiency of TRAPPIII function (Figure 2.19D).

2.4.2 Trs20p as an adaptor protein

When compared to *tca17Δ*, our results with *trs20D46Y* suggest that Trs20p can act as an adaptor protein for the TRAPP II-specific subunit Trs120p and the TRAPPIII-specific subunit Trs85p. This adaptor function of Trs20p is similar to that reported for the mammalian homolog C2 (Zong *et al.*, 2011). Since Trs85p and Trs120p do not reside in the same complex, their interaction with Trs20p is not mutually exclusive. The fact that the D46Y mutation in Trs20p weakens both interactions suggests that these two TRAPP subunits interact with Trs20p in a similar fashion. The suggestion that Trs120p binds directly to Trs20p is in disagreement with the recently published electron microscopic structure of the TRAPP II complex, which suggested that Trs20p was in direct contact with Trs130p while Trs120p was on a side of the complex opposite to that of Trs20p (Yip *et al.*,

2010). While our results leave this possibility open, we do not believe this to be the case for the following reasons. The interaction between Trs20p and Trs130p is much weaker than that between Trs20p and Trs120p (M.S., unpublished observation). In addition, the similarity in structure between Trs20p and Tca17p leaves open the possibility that some Trs20p interactions occur due to the similar structure between these two proteins and do not take place *in vivo*. Indeed, Tca17p was found to bind only to Trs130p which is consistent with a previous study showing that Tca17p binds to the amino-terminus of Trs130p (Choi *et al.*, 2011) and our earlier result showing a strong genetic interaction between *TCA17* and *TRS130* (Scrivens *et al.*, 2009). We suggest that Tca17p may be the TRAPP subunit that interacts with Trs130p while Trs20p acts as an adaptor to allow either Trs85p or Trs120p to interact with the TRAPPI core complex. It remains unclear how Tca17p interacts with the TRAPPI core and how it is excluded from TRAPPIII.

2.4.3 Implications for SEDT

The C2D47Y mutation was identified in a patient with spondyloepiphyseal dysplasia tarda (SEDT) (Shaw *et al.*, 2003). A recent study suggested that C2 (called sedlin) regulates the Sar1 GTPase cycle at ER exit sites to allow ER-derived carriers to grow to a size that can accommodate large cargo such as collagen (Venditti *et al.*, 2012). It is the transport of pro-collagen that is believed to be defective in SEDT patients. Although we could not detect an interaction between Trs20p and the yeast Syntaxin 5 homolog Sed5p, it is possible that the mammalian Trs20p homolog C2 evolved the ability to interact with Syntaxin 5. In this case, pro-collagen release from the Golgi in patients with the C2D47Y mutation may not be affected but fusion of the megacarriers with the Golgi would be defective. Alternatively, Syntaxin 5 has been implicated in membrane traffic steps beyond the ER-to-Golgi portion of the secretory pathway including the endocytic pathway (Xu *et al.*, 2002; Tai *et al.*, 2004) and pro-collagen transport in patients with the C2D47Y mutation may be blocked at these later stages. It is noteworthy that defects in endocytosis could indirectly block anterograde transport, suggesting that the C2D47Y mutation may have an indirect effect on pro-collagen transport. At present, it is difficult to envision how a defect in autophagy could affect pro-collagen transport. Studies on the role of mammalian C2 in both endocytosis and autophagy will help address these possibilities.

Chapter 3: The SMS domain of Trs23p is responsible for the *in vitro* appearance of the TRAPPI complex in *Saccharomyces cerevisiae*

This Chapter was published as a manuscript in the journal *Cellular Logistics* (Brunet *et al.*, 2012). I am responsible for all figures in this manuscript with the exception of Figure 3.1 (C & D) and Figure 3.12 (A).

3.1 Introduction

Newly synthesized proteins destined for secretion are packaged into COP II-coated transport vesicles at the endoplasmic reticulum (ER) (Lee and Miller, 2007). These vesicles are then recognized by and fuse with the earliest (*cis*) Golgi compartment. Similar budding, recognition and fusion events take place from nearly every endomembrane compartment within the cell, and understanding how each vesicle is specifically recognized has represented a major focus of efforts in the field of vesicle transport. Many factors participate in the overall process including SNAREs, Ypt/Rab GTPases, vesicle coat proteins and vesicle tethers (Cai *et al.*, 2007a; Sztul and Lupashin, 2009). While SNAREs were originally postulated to impart specificity in vesicle transport (Sollner *et al.*, 1993), it is now accepted that all of the other aforementioned factors can function upstream of the SNAREs and thus participate in specificity.

Upon arrival at a target membrane, the vesicle is recognized by any one of a number of possible tethering factors. These tethering factors have been classified as either coiled-coil proteins or large multisubunit tethering complexes (MTC) (Gillingham and Munro, 2003; Yu and Hughson, 2010). The tethering event leaves open many questions such as which tethering factor acts first or if they act simultaneously, and whether the mechanism of tethering is conserved at the various compartments. Nonetheless, it has been suggested that the tethering factors are among the first contacts between the vesicle and the target membrane and, as such, may contribute to the exquisite specificity in vesicle transport (Yu and Hughson, 2010).

One of the earliest MTCs identified was the TRAPP complex (Sacher *et al.*, 2001, 2008). Although this complex has not been demonstrated to tether two distinct membranes together, it is believed to accomplish this either directly or by leading to recruitment of the factor(s) that does this. In the yeast *S. cerevisiae* there are three forms of the complex called TRAPPI, II and III (Sacher *et al.*, 1998, 2001; Cai *et al.*, 2005; Lynch-Day *et al.*, 2010). As such, TRAPP poses a unique set of problems with respect to the role of these complexes in determining specificity in this organism. All three complexes contain the same "core" of six polypeptides (Bet3p, Bet5p, Trs20p, Trs23p, Trs31p, Trs33p) with TRAPPII containing four additional subunits (Tca17p, Trs65p, Trs120p, Trs130p) and TRAPPIII containing one additional subunit (Trs85p). While TRAPPI has been implicated in ER-to-Golgi transport (Sacher *et al.*, 1998, 2001), TRAPPII has been shown to function at a later Golgi compartment (Sacher *et al.*, 2001; Cai *et al.*, 2005) and TRAPPIII was suggested to function in autophagy (Meiling-Wesse *et al.*, 2005; Nazarko *et al.*, 2005; Lynch-Day *et al.*, 2010). Confounding the problem of TRAPP-mediated specificity is the fact that Bet3p, a common subunit found in two copies within the core (Sacher *et al.*, 2000; Kim *et al.*, 2006; Cai *et al.*, 2008), was shown to bind to Sec23p, a component of the ER-derived COP II coat (Cai *et al.*, 2007b), suggesting that the Sec23p-binding site on all copies of Bet3p must be blocked in both TRAPPII and III. In addition, this core of the complex was shown to be sufficient for Ypt1-directed guanine nucleotide exchange factor (GEF) activity (Kim *et al.*, 2006) and indeed all three complexes have been reported to be capable of such activity (Sacher *et al.*, 1998, 2001; Jones *et al.*, 2000; Wang *et al.*, 2000; Lynch-Day *et al.*, 2010). Finally, to date only one complex has been reported in mammalian cells and it was recently shown that this complex contains homologs of the *S. cerevisiae* TRAPPII- and III-specific proteins (Yamasaki *et al.*, 2009; Choi *et al.*, 2011; Scrivens *et al.*, 2011).

In an effort to better understand the relationship between the TRAPP complexes, we focused on Trs23p that links two Bet3p-containing subcomplexes to form the TRAPP holocomplex (Kim *et al.*, 2006; Cai *et al.*, 2008), thus providing GEF activity. In addition, Trs23p interacts with the GTPase Ypt1p (Cai *et al.*, 2008). Also unique to this subunit is a PDZ-like domain in higher eukaryotes and a *Saccharomycotina*-specific domain seen in the *S. cerevisiae* protein (Kim *et al.*, 2006; Cai *et al.*, 2008; Fan *et al.*, 2009a, 2009b).

Furthermore, co-expression of the core proteins leads to assembly of a functional complex when using the *S. cerevisiae* proteins but the mammalian proteins fail to assemble (Kim *et al.*, 2006), suggesting differences in the assembly and/or stability of the core between both organisms.

Using random and targeted mutagenesis we have constructed a series of mutations in Trs23p. We show that neither the carboxy-terminal 99 amino acids (*trs23Δ99C*) nor the *Saccharomycotina*-specific domain (*trs23ΔSMS*) of Trs23p are essential for viability. A more extensive characterization of *trs23ΔSMS* showed no growth defect and that TRAPPI subunits are shifted to a much smaller molecular size suggesting that this domain is responsible for the appearance of TRAPPI *in vitro*. The absence of TRAPPI did not affect ER-to-Golgi traffic either *in vivo* or *in vitro*, nor later Golgi traffic or autophagy. We demonstrate that under physiological conditions TRAPP II co-fractionates with TRAPP III, and this is the only source of TRAPP seen in *trs23ΔSMS*. Importantly, we demonstrate that the fraction containing a mixture of TRAPP II and III can be induced to produce TRAPPI and dimeric TRAPP II by incubation in high salt. Finally, we show that in contrast to *S. cerevisiae*, the closely-related yeast *Pichia pastoris*, which lacks the SMS domain in Trs23p, does not contain a TRAPPI peak. Our data suggest that the SMS domain stabilizes the TRAPPI core complex and that this complex may be an *in vitro* anomaly. The implications of these findings on membrane trafficking are discussed.

3.2 Materials and methods

Table 3.1 Yeast strains used in Chapter 3.

MSY20	<i>MATa can100 leu2-3112 his3-11 trp1Δ ura3-1 ade2-1</i>
MSY62	<i>MATαhis3Δ1 leu2Δ0 ura3Δ0 MET15trs23Δ::KanMX pRS316-TRS23</i>
MSY107	<i>MATαhis3Δ1 leu2Δ0 ura3Δ0MET15 trs23Δ::KanMX pRS316-TRS23 pRS315-trs23Δ202C</i>
MSY109	<i>MATαhis3Δ1 leu2Δ0 ura3Δ0 MET15trs23Δ::KanMX pRS316-TRS23 pRS315-trs23Δ167C</i>
MSY118	<i>MATαhis3Δ1 leu2Δ0 ura3Δ0 MET15trs23Δ::KanMX pRS315-trs23Δ99C</i>
MSY119	<i>MATαhis3Δ1 leu2Δ0 ura3Δ0 MET15 trs23Δ::KanMX pRS315-TRS23</i>
MSY243a	<i>MATαhis3Δ1leu2Δ0 ura3Δ0 MET15 trs23Δ::KanMX pRS316- trs23Δ99C</i>
MSY245	<i>MATαhis3Δ1 leu2Δ0 ura3Δ0 MET15 trs23Δ::Neurseothricin pRS316-TRS23</i>
MSY251	<i>MATαhis3Δ1 leu2Δ0 ura3Δ0 MET15 trs23Δ::KanMX pRS316-TRS23 pRS315-trs23^{MPR/AWS}</i>
MSY297	<i>MATαhis3Δ1 leu2Δ0 ura3Δ0 MET15 trs23Δ::KanMX pRS316-TRS23 pRS315-trs23ΔSMS</i>
MSY366	<i>MATa trp1-901 leu2-3 112 ura3-52 his3-200 gal4Δ gal80Δ LYS2::GAL1_{UAS}-GAL1_{TATA}-HIS3 GAL2_{UAS}-GAL2_{TATA}-ADE2 URA3::MEL1_{UAS}-MEL1_{TATA}-lacZ pGADT7-BET5</i>
MSY367	<i>MATa trp1-901 leu2-3 112 ura3-52 his3-200 gal4Δ gal80Δ LYS2::GAL1_{UAS}-GAL1_{TATA}-HIS3 GAL2_{UAS}-GAL2_{TATA}-ADE2 URA3::MEL1_{UAS}-MEL1_{TATA}-lacZ pGADT7-TRS20</i>
MSY370	<i>MATa trp1-901 leu2-3 112 ura3-52 his3-200 gal4Δ gal80Δ LYS2::GAL1_{UAS}-GAL1_{TATA}-HIS3 GAL2_{UAS}-GAL2_{TATA}-ADE2 URA3::MEL1_{UAS}-MEL1_{TATA}-lacZ pGADT7-TRS31</i>
MSY449	<i>MATα ura3-52 his3-200 ade2-101 trp1-901 leu2-3 112 met- gal4Δ gal80Δ URA3::GAL1_{UAS}-GAL1_{TATA}-lacZ pGBKT7_{GTWY}-TRS23</i>
MSY450	<i>MATα ura3-52 his3-200 ade2-101 trp1-901 leu2-3 112 met- gal4Δ gal80Δ URA3::GAL1_{UAS}-GAL1_{TATA}-lacZ pGBKT7_{GTWY}- trs23ΔSMS</i>
MSY453	<i>MATa trp1-901 leu2-3 112 ura3-52 his3-200 gal4Δ gal80Δ LYS2::GAL1_{UAS}-GAL1_{TATA}-HIS3 GAL2_{UAS}-GAL2_{TATA}-ADE2 URA3::MEL1_{UAS}-MEL1_{TATA}-lacZ pGADT7</i>
MSY458	<i>MATα his3Δ1 leu2Δ0ura3Δ0MET15trs23Δ::KanMX pRS315-trs23Δ99C pRS416-GFP-SNC1</i>
MSY459	<i>MATα his3Δ1 leu2Δ0 ura3Δ0 MET15 trs23Δ::KanMX pRS315-TRS23 pRS416-GFP-SNC1</i>
MSY460	<i>MATαhis3Δ1 leu2Δ0 ura3Δ0 MET15 trs23Δ::KanMX pRS315- trs23^{MPR/AWS}</i>
MSY471	<i>MATαhis3Δ1 leu2Δ0 ura3Δ0 MET15 trs23Δ::KanMX pRS315- trs23ΔSMS</i>

MSY474	<i>MAT</i> α <i>his3</i> Δ 1 <i>leu2</i> Δ 0 <i>ura3</i> Δ 0 <i>MET15 trs23</i> Δ :: <i>KanMX TRS130-3xHA::HIS3 pRS315-trs23</i> Δ 99C
MSY475	<i>MAT</i> α <i>his3</i> Δ 1 <i>leu2</i> Δ 0 <i>ura3</i> Δ 0 <i>MET15 trs23</i> Δ :: <i>KanMX TRS130-3xHA::HIS3 pRS315-TRS23</i>
MSY478	<i>MAT</i> α <i>can100 leu2-3112 his3-11 trp1</i> Δ <i>ura3-1 ade2-1 trs85</i> Δ :: <i>HIS3 pRS416-GFP-SNC1</i>
MSY485	<i>MAT</i> α <i>his3</i> Δ 1 <i>leu2</i> Δ 0 <i>ura3</i> Δ 0 <i>MET15 trs23</i> Δ :: <i>KanMX pRS316- trs23</i> Δ 99C <i>pRS315 GFP-YPT31</i>
MSY486	<i>MAT</i> α <i>his3</i> Δ 1 <i>leu2</i> Δ 0 <i>ura3</i> Δ 0 <i>MET15 trs23</i> Δ :: <i>KanMX pRS316-TRS23 pRS315 -GFP-YPT31</i>
MSY531	<i>MAT</i> α <i>his3</i> Δ 1 <i>leu2</i> Δ 0 <i>ura3</i> Δ 0 <i>MET15 trs23</i> Δ :: <i>KanMX TRS130-3xHA::HIS3 pRS315-trs23</i> ^{MPR/AWS}
MSY532	<i>MAT</i> α <i>his3</i> Δ 1 <i>leu2</i> Δ 0 <i>ura3</i> Δ 0 <i>MET15 trs23</i> Δ :: <i>KanMX TRS130-3xHA::HIS3 pRS315-trs23</i> Δ SMS
MSY545	<i>MAT</i> α <i>his3</i> Δ 1 <i>leu2</i> Δ 0 <i>ura3</i> Δ 0 <i>MET15 trs23</i> Δ :: <i>KanMX pRS316-TRS23 pRS315-trs23</i> Δ 15N
MSY546	<i>MAT</i> α <i>his3</i> Δ 1 <i>leu2</i> Δ 0 <i>ura3</i> Δ 0 <i>MET15 trs23</i> Δ :: <i>KanMX pRS316-TRS23 pRS315-trs23</i> Δ 109C
MSY560	<i>MAT</i> α <i>his3</i> Δ 1 <i>leu2</i> Δ 0 <i>ura3</i> Δ 0 <i>MET15 trs23</i> Δ :: <i>KanMX pRS315-trs23</i> Δ SMS <i>pRS416-GFP-SNC1</i>
MSY561	<i>MAT</i> α <i>his3</i> Δ 1 <i>leu2</i> Δ 0 <i>ura3</i> Δ 0 <i>MET15 trs23</i> Δ :: <i>KanMX pRS315-trs23</i> Δ SMS <i>TRS85-3xHA::HIS3</i>
MSY563	<i>MAT</i> α <i>his3</i> Δ 1 <i>leu2</i> Δ 0 <i>ura3</i> Δ 0 <i>MET15 trs23</i> Δ :: <i>KanMX pRS315-TRS23 TRS85-3xHA::HIS3</i>
MSY570	<i>MAT</i> α <i>his3</i> Δ 1 <i>leu2</i> Δ 0 <i>ura3</i> Δ 0 <i>MET15 trs23</i> Δ :: <i>KanMX pRS315-TRS23 pRS416-APE1-GFP</i>
MSY572	<i>MAT</i> α <i>his3</i> Δ 1 <i>leu2</i> Δ 0 <i>ura3</i> Δ 0 <i>MET15 trs23</i> Δ :: <i>KanMX pRS315-trs23</i> Δ SMS <i>pRS416-APE1-GFP</i>
MSY573	<i>MAT</i> α <i>his3</i> Δ 1 <i>leu2</i> Δ 0 <i>lys2</i> Δ 0 <i>ura3</i> Δ 0 <i>YDR108w(trs85</i> Δ):: <i>KanMX pRS416- APE1-GFP</i>
MSY580	<i>MAT</i> α <i>his3</i> Δ 1 <i>leu2</i> Δ 0 <i>ura3</i> Δ 0 <i>MET15 trs23</i> Δ :: <i>KanMX pRS316-trs23</i> Δ SMS <i>pRS315-GFP-YPT31</i>
MSY582	<i>MAT</i> α / <i>his3</i> Δ 1/ <i>his3</i> Δ 200 <i>leu2</i> Δ 0/ <i>leu2-3,112ura3</i> Δ 0/ <i>ura3-52 LYS2/lys2-801 MET15/met15</i> Δ 0 <i>SUC2/suc2</i> Δ 9 <i>CAN1/can1::hisG</i> <i>TRS130/TRS130-13xmyc::HIS3 TRS85/TRS85-TAP::HIS3</i> <i>MX6</i>

3.2.1 Strain construction

A list of all strains used in this study is shown in Table 3.1. All *trs23* mutations were constructed using the same parental strain (MSY62). The *trs23* mutations were generated

using the splicing by overlap extension PCR method or random mutagenesis. Mutant strains were created by plasmid shuffling using 5-fluoroorotic acid (5-FOA) counterselection. Endogenous *TRS130* and *TRS85* were tagged at the carboxy-terminus with a hemagglutinin (HA) epitope by genomic insertion of a cassette amplified from pFA6a-3HA-HIS3MX6 (Longtine *et al.*, 1998). Insertion at the correct location was verified by PCR and Western blot analysis.

3.2.2 Spotting

Yeast strains were inoculated into 3 ml of minimal medium and grown in a shaker incubator overnight at 30°C. The OD₆₀₀ was normalized to the lowest value and 10-fold serial dilutions were spotted onto minimal medium with 5-FOA or YPD (1% yeast extract, 2% peptone, 2% glucose). Yeast were placed at the permissive temperature of 30°C to serve as a growth control and at the restrictive temperatures of 16°C and 38°C.

3.2.3 Preparation of yeast lysates

For fractionation of yeast cytosols, cells were grown to mid log phase (OD₆₀₀ of 1-1.5) overnight at 25°C. Cells were converted to spheroplasts as previously described (Kim *et al.*, 1999). Spheroplasts were lysed in lysis buffer (20mM HEPES pH 7.3, 2mM EDTA, 50-300mM NaCl, 1mM DTT, and 1X protease inhibitor cocktail (PIC)), Dounce homogenized and centrifuged at 21,000g (high speed spin) in an SW55Ti rotor for 15 minutes at 4°C.

For GEF assays, membrane extraction and subcellular fractionation and examining levels of TRAPP proteins, cells were grown to early log phase (OD₆₀₀ of 1-1.5) overnight at 25°C. Cells were converted to spheroplasts as above, lysed in lysis buffer (20mM HEPES pH 7.3, 1mM DTT, 1x PIC), Dounce homogenized and centrifuged at 500g for 5 minutes to remove unbroken cells and debris. The supernatant was centrifuged at 16,000g (low speed spin) in a table-top microcentrifuge for 10 minutes at 4°C.

3.2.4 Sucrose gradient fractionation and membrane floatation

For equilibrium fractionation, the 16,000g pellet from 400 OD₆₀₀ units of starting material was resuspended in 500 µl of 5% sucrose, Dounce homogenized and layered on top of a discontinuous sucrose gradient (1 ml each of 10%, 15%, 20%, 25%, 30%, 35%, 40%, 45%, 50%, 55% and 500 µl of 60% sucrose). Gradients were centrifuged for 17 hours at 178,000g in an SW41Ti rotor at 4°C. Fractions of 500 µl were collected from top to bottom with a peristaltic pump.

For membrane floatation the 16,000g pellet from 400 OD₆₀₀ units of starting material was resuspended in 500 µl of 60% sucrose and placed on the bottom of a centrifuge tube. A discontinuous step sucrose gradient was layered on top (1 ml each of 50%, 40%, 30%, 20% and 10% sucrose) and gradients were centrifuged for 4 hours at 178,000g in an SW55Ti rotor. Fractions of 500 µl were collected from top to bottom with a peristaltic pump. Sucrose solutions (w/w) were dissolved in 20mM HEPES pH 7.3.

3.2.5 Membrane extraction

The 16,000g pellet from approximately 70 OD₆₀₀ units of starting material was resuspended to a final volume of 200 µl in lysis buffer (see above) or lysis buffer with either 1% Triton X-100, 0.5M NaCl, 0.1M Na₂CO₃ pH 11.0 or 5M urea, Dounce homogenized and incubated on ice for 30 minutes. Samples were centrifuged at 16,000g in a microcentrifuge for 10 minutes at 4°C. A volume of 100 µl of supernatant was added to 100 µl of 2X Laemmli sample buffer and the pellet was resuspended in 200 µl of 1X sample buffer.

3.2.6 Size exclusion chromatography

For comparison between wild type and *trs23ΔSMS*, 5mg of total protein from a 21,000g supernatant was fractionated in the following gel filtration buffer: 20mM HEPES pH 7.3, 50-300mM NaCl, 1mM DTT (this component was excluded in crosslinking experiments). In Figure 3.12B buffer B88 was used (Barlowe, 1997).

Concentrated AKTA fractions for guanine nucleotide exchange factor assays (see below) were prepared by fractionating 20mg of total protein from a 21,000g supernatant (10mg at a time) and fractions were concentrated using a Millipore Amicon centrifugal filter to a final volume of 200 μ l. Gel filtration buffer contained 150mM NaCl.

Samples were injected onto either a Superose 6 or a Superdex 200 column (GE Healthcare) connected to an AKTA liquid chromatography system. Fractions of 0.5 ml were collected and re-suspended in Laemmli sample buffer, fractionated by SDS-PAGE and analyzed by Western blotting. Endogenous Trs33p, Bet3p and Trs23p were detected using polyclonal antibodies raised in rabbits, the HA epitope was detected using a commercially available monoclonal antibody (HA.7, Sigma), the *myc* epitope was detected using the monoclonal antibody 9E10 and the TAP tag was detected with anti-TAP antibody (OpenBiosystems).

3.2.7 Recombinant protein

Yeast TRAPP subunits were expressed and purified from *E. coli* BL21(DE3) cells as previously described (Kim *et al.*, 2006). Bet3p and Trs33p subunits were 6xHis-tagged and complexes were purified using Ni²⁺-NTA (Qiagen) followed by size-exclusion chromatography on a Superdex 200 column.

3.4.8 Bacterial lysates

Yeast TRAPP subunits were expressed in *E. coli* BL21 (DE3) cells as for recombinant protein (see above). Cells were sonicated in lysis buffer (20mM HEPES pH 7.3, 1mM DTT) and the lysates were clarified by centrifugation at 30,000g in a JA25.50 rotor (Beckman) prior to their use in guanine nucleotide exchange factor assays.

3.2.9 Guanine nucleotide exchange factor (GEF) assays

GEF assays were performed as previously described (Wang *et al.*, 2000). Each reaction was started in a volume of 80 μ l with yeast or bacterial lysates added to a final concentration of 4mg/ml. For Ypt1p alone, bovine serum albumin (BSA) or *E. coli* BL21

(DE3) lysate was added to a final concentration of 4mg/ml. The zero minute time point for each sample was taken immediately after the pre-loaded Rab was added and 18 μ l was removed for each subsequent time point. Percent ^3H -GDP remaining was based on the individual zero for each sample.

3.2.10 *In vivo* and *in vitro* trafficking assays

The CPY pulse chase experiment was performed as previously described with some modifications (Rossi *et al.*, 1995). Five OD₆₀₀ units of cells in early log phase (OD₆₀₀ 1-1.5) were temperature shifted in a shaking 38.5°C water bath for 30 minutes. Cells were labeled with 250 μ Ci of ^{35}S -methionine/cysteine (Promix, Perkin-Elmer) (pulsed) for 4 minutes followed by the addition of cold methionine/cysteine (chased) at a final concentration of 10mM. The zero time point was taken immediately after the cold methionine/cysteine was added. Cells were chased for a total of 30 minutes with an equal volume of cells being removed every 10 minutes. Cells from each time point were converted to spheroplasts, lysed and CPY was immunoprecipitated overnight using a rabbit polyclonal anti-CPY antibody (Abcam). Immunoprecipitated CPY was fractionated by SDS-PAGE and the amounts loaded were normalized to the counts per minute measured from whole cell lysates. The gel was Coomassie-stained, dried and labeled CPY was detected by autoradiography.

Microscopy-based assays (GFP-Snc1p, GFP-Ypt31p) were performed by transforming yeast with the appropriate plasmid. Cells were grown to early log phase overnight at 25°C and 5 OD₆₀₀ units of cells were resuspended in 1 ml of 3.7% paraformaldehyde (PFA), incubated at room temperature for 15 minutes, pelleted and resuspended in ice cold methanol for 5 minutes. Cells were then washed with wash buffer (1.4M sorbitol, 50mM KPi, pH 7.5) and resuspended in 100 μ l of the same buffer. Cells were visualized using a Zeiss axioplan microscope fitted with an X-cite series 120Q light source (EXFO Life Sciences) and a Lumenera Infinity 3-1C 1.4 megapixel cooled CCD camera.

The *in vitro* reconstituted ER-to-Golgi assay using purified proteins was performed as described (Barlowe, 1997).

Maturation of Ape1p-GFP was performed by first transforming the plasmid into yeast. The cells were then grown overnight to early log phase in minimal medium lacking uracil at which point they were converted to spheroplasts and lysed in 20mM HEPES, pH 7.3, 100mM NaCl, 0.1mM DTT, 2mM EDTA with protease inhibitors. Equal amounts of protein were fractionated by SDS-PAGE, transferred to PVDF membrane and probed with mouse anti-GFP (Roche). Quantitation was performed using Image J freeware.

3.2.11 Yeast two-hybrid assay

TRS23 and variants of this protein were cloned into a Gateway®-modified pGBKT7 vector (pGBKT7_{GTWY}) (Scrivens *et al.*, 2011). All other TRAPP subunits were cloned into the pGADT7 vector by restriction enzyme cloning. Mating and analysis were as described by Scrivens *et al.* (2011).

3.2.12 Chemical crosslinking

Fractionated samples in gel filtration buffer (50mM NaCl) were treated with 2mM dithiobis[succinimidyl] propionate (DSP) for 3 hours on ice. The reaction was quenched by adding Tris pH 7.5 to a final concentration of 20mM and incubating at room temperature for 15 minutes. For immunoprecipitation, the sample was diluted with gel filtration buffer (100mM NaCl) containing 1% Triton X-100 and incubated with 2µg IgG overnight on ice. The next day, immune complexes were collected on protein A beads, washed with lysis buffer and processed for Western analysis. In some experiments the crosslinked samples were re-fractionated on a Superose 6 column as described above.

3.3 Results

3.3.1 Neither the carboxy-terminal 99 residues nor the SMS domain of Trs23p are essential

In an effort to examine the role of the Trs23p subunit in TRAPP function, we conducted a random mutagenesis screen using hydroxylamine to identify conditional

mutations in *TRS23*. This screen identified a mildly temperature (heat)-sensitive (*ts*) and cold sensitive (*cs*) mutant. Upon sequencing of the mutation, *TRS23* was found to contain a C361T mutation that introduced a nonsense mutation following the 120th amino acid (herein referred to as *trs23Δ99C*), indicating that the carboxy-terminal 99 amino acids of Trs23p are not essential for vegetative growth of the yeast (Figure 3.1A,B,C). Further carboxy-terminal truncations generated by either random (*trs23Δ167C*, *trs23Δ202C*) or site-directed (*trs23Δ109C*) mutagenesis were found to be lethal (Figure 3.1A,C). Alignment of *S. cerevisiae* Trs23p with its human counterpart (TRAPPC4) indicates that residues 56-115 comprise a domain not found in higher eukaryotes (Figure 3.1D; also see Kim *et al*, 2006). This domain is only present in species within the *Saccharomycotina* phylum and, hence, we will refer to it as the *Saccharomycotina*-specific (SMS) domain. Since truncation of Trs23p that removed even a small portion of this domain (*trs23Δ109C*) resulted in lethality, we tested whether the SMS domain itself was essential for function by deleting this domain (herein referred to as *trs23ΔSMS*). This mutant did not display a discernible growth phenotype at either extreme temperature tested (Figure 3.1B,C) suggesting it is not essential for function. Furthermore, truncations of Trs23p from the amino-terminus (removal of the first 15 amino acids) resulted in lethality (Figure 3.1A,C). Collectively, our data suggest that the carboxy-terminus of Trs23p does not provide an essential function to the protein and that the SMS domain is required for some aspect of Trs23p function that can be compensated by the carboxy-terminus of the protein.

An earlier report suggested that Trs23 containing the triple point mutation M200A/P201W/R203S (herein referred to as *trs23^{MPR/AWS}*) was lethal (Cai *et al.*, 2008). Since we have just demonstrated that the carboxy-terminus of Trs23p, which contains the aforementioned residues, is not essential for growth, we re-examined the growth characteristics of this triple point mutant. Consistent with our *trs23Δ99C* mutant, we found that *trs23^{MPR/AWS}* was not lethal but did in fact display a severe *cs* phenotype (Figure 3.1B,C). We further found that *trs23^{MPR/AWS}* is not dominant since neither a heterozygous diploid strain nor a haploid strain containing *trs23^{MPR/AWS}* and wild type *TRS23* displayed any growth defects. Although the reason for the discrepancy in the lethality of *trs23^{MPR/AWS}*

is not clear, the phenotype we now show is consistent with the non-essential nature of the carboxy-terminus of *TRS23*.

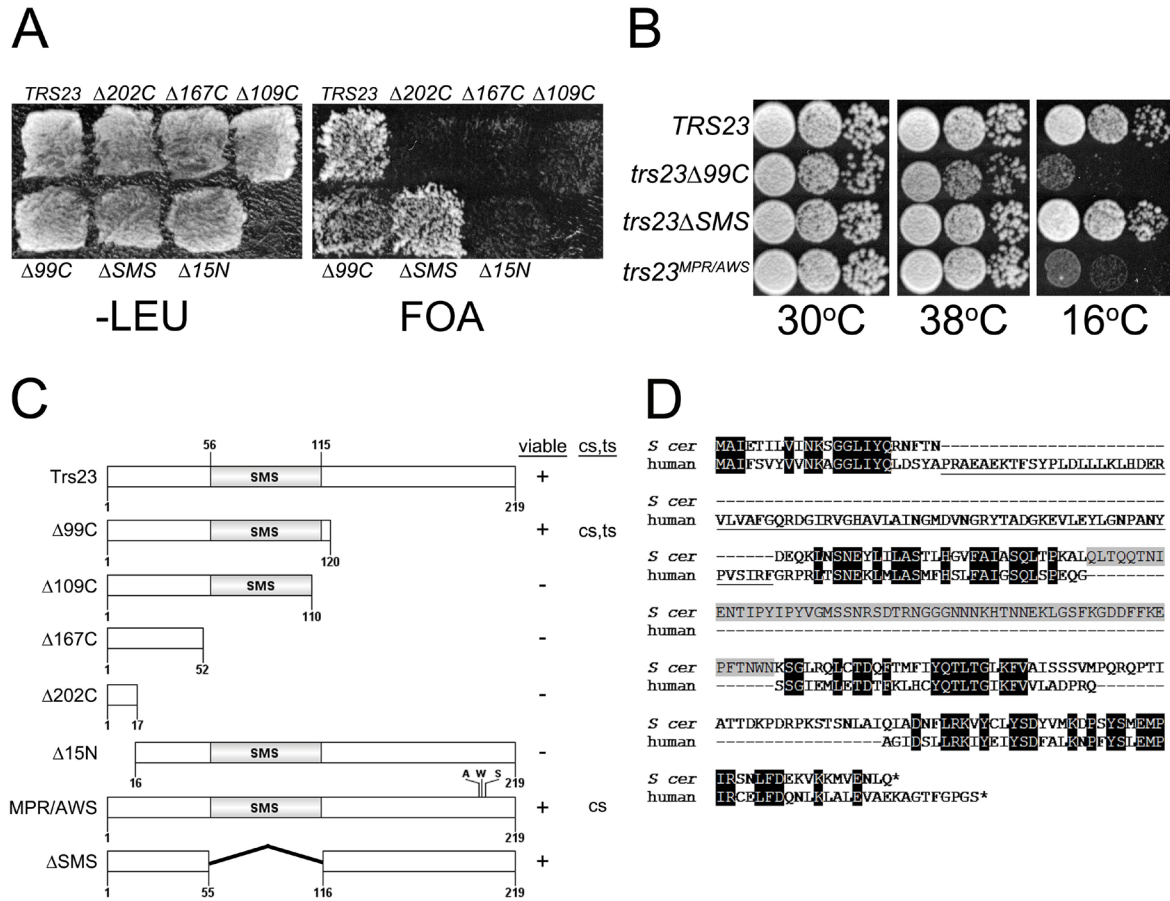


Figure 3.1 Growth properties of *trs23* mutations. (A) MSY62 was transformed with a plasmid (pRS315) containing *TRS23* that was subjected to either random mutagenesis yielding nonsense mutations after the 17th, 52nd and 120th amino acids (*trs23* $\Delta 202C$, *trs23* $\Delta 167C$ and *trs23* $\Delta 99C$, respectively); or site-directed mutagenesis to generate a nonsense mutation after amino acid 110 (*trs23* $\Delta 109C$) or deletion of either the first 15 amino acids (*trs23* $\Delta 15N$) or the SMS domain (*trs23* ΔSMS). Cells were plated on either SD-leucine or on 5-FOA to counterselect against wild type *TRS23* in the *URA3*-containing plasmid pRS316 and incubated at 30°C. (B) Serial 10-fold dilutions of wild type or yeast strains with the mutations indicated were plated on YPD and incubated at either permissive temperature (30°C) or the restrictive temperatures of 16°C or 38°C. (C) A schematic showing all of the *TRS23* mutations used in this study with their viability and growth phenotypes indicated (cs, cold sensitive; ts, heat sensitive). (D) Human TRAPPC4 (accession number NP_057230.1) and *S. cerevisiae* Trs23p (accession number NP_101532.1) were aligned using Clustal W and the gaps were inserted manually in accordance with Kim et al, 2006. Identities are shaded in black, the PDZ-like domain of human TRAPPC4 is underlined and the SMS domain of Trs23p is shaded in gray.

3.3.2 The SMS domain is required for efficient assembly of recombinant TRAPPI

To begin to address the consequences of the removal of either the carboxy-terminus or the SMS domain of Trs23p, we expressed these proteins in our recombinant bacterial system that generates a functional TRAPPI complex (rTRAPPI) that can be detected using size exclusion chromatography (Kim *et al.*, 2006). As shown in Figure 3.2A, although the truncated trs23 Δ 99C protein was produced and could be detected by anti-Trs23p antibody in the cell lysate, it was largely insoluble and did not co-purify with His-tagged Bet3p. In contrast to the cells expressing wild type Trs23p where rTRAPPI is found in a high molecular size fraction, rTRAPPI was absent in lysates expressing either the trs23 Δ 99C or the trs23 Δ SMS proteins (Figure 3.2B). Instead, cells expressing trs23 Δ 99C contained a Bet3p-Trs33p-Bet5p subcomplex while those expressing trs23 Δ SMS contained a Bet3p-Trs33p-Bet5p-trs23 Δ SMS subcomplex.

Since small amounts of rTRAPPI may be present in the lysates generated from the two mutants, we assayed the lysate for guanine nucleotide exchange factor (GEF) activity for the GTPase Ypt1p since this activity is robust with rTRAPPI (Kim *et al.*, 2006; Cai *et al.*, 2008). Compared to lysates with wild type Trs23p and consistent with no detectable rTRAPPI, lysate with trs23 Δ 99C displayed near background levels of GEF activity (Figure 3.2C). In contrast, lysate prepared from cells expressing the trs23 Δ SMS protein displayed GEF activity intermediate to that of wild type and Ypt1p alone (Figure 3.2C) suggesting that small, but undetectable, amounts of rTRAPPI do indeed form in these cells. Our results suggest that, *in vitro*, rTRAPPI cannot assemble with the trs23 Δ 99C protein. They further suggest that the SMS domain of Trs23p is not essential for GEF activity of rTRAPPI but is required for its efficient assembly.

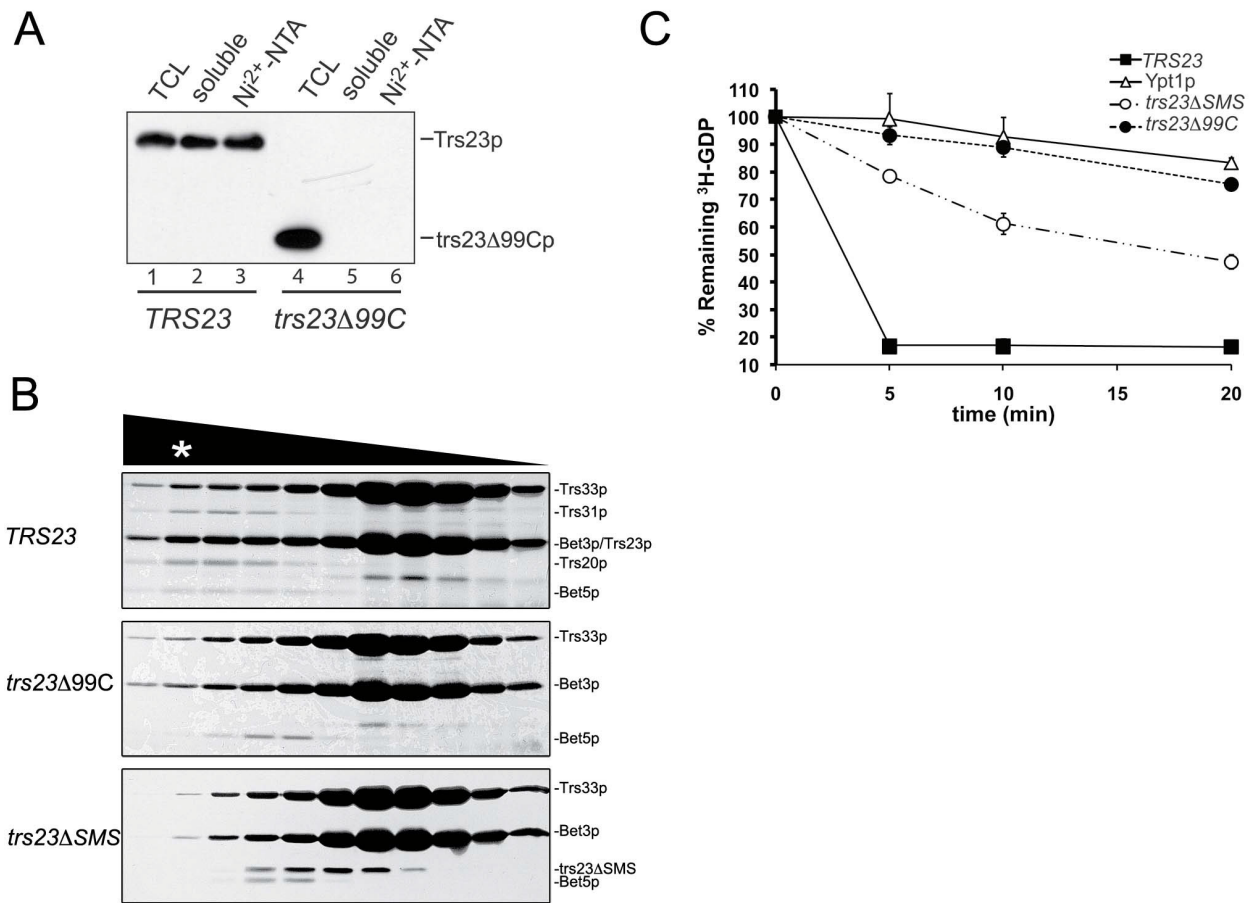


Figure 3.2 Assembly and function of recombinant TRAPP containing the *trs23Δ99C* and *trs23ΔSMS* proteins. (A) Bacterial cells expressing wild type TRAPPI proteins (with His-tagged Bet3p and Trs33p) and Trs23p (lanes 1-3) or *trs23Δ99C* (lanes 4-6) were probed for Trs23 using anti-Trs23p antiserum either in the total cell lysate (TCL; lanes 1 and 4), the soluble fraction (lanes 2 and 5) or in the eluate following a Ni²⁺-NTA agarose purification (lanes 3 and 6). (B) Bacterial cells expressing wild type TRAPPI proteins (where Bet3p is His-tagged) and Trs23p, *trs23Δ99C* or *trs23ΔSMS* as indicated, were first purified with Ni²⁺-NTA agarose and then the eluates were fractionated by size exclusion chromatography on a Superdex 200 column. Fractions from the column were then analyzed by SDS-PAGE and the gel was silver stained. The positions of the TRAPP proteins are indicated to the side of each panel and the position on the column of fully-assembled recombinant TRAPPI is indicated by an asterisk (*). (C) Lysates from the bacterial cells in (B) were assayed for Ypt1p GEF activity as described in Experimental Procedures (wild type (■); *trs23Δ99C* (●); *trs23ΔSMS* (○)). The intrinsic ability of Ypt1p to release nucleotide is also shown (△). Assays represent three replicates and error bars represent ± SEM.

3.3.3 The SMS domain contributes to Trs23p interactions

The lack of efficient assembly of rTRAPPI in the presence of either the trs23 Δ SMS or trs23 Δ 99C proteins suggests that interactions with other TRAPP subunits are abrogated. To test this notion, wild type Trs23p, trs23 Δ SMS and trs23 Δ 99C were expressed as fusion proteins with the Gal4p DNA binding domain. The plasmid expressing these proteins was introduced into yeast containing open reading frames encoding individual TRAPP proteins fused to the Gal4 transcriptional activation domain. Reconstitution of Gal4p-dependent transcription, and hence a protein-protein interaction, was assessed by three criteria: growth of the cells on medium (i) lacking histidine; (ii) lacking both histidine and adenine; (iii) lacking histidine but containing 3-aminotriazole (3AT), a competitive inhibitor of His3p. Wild type Trs23p displayed interactions with Trs31p, Bet5p and Trs20p (Figure 3.3A). Interactions with Trs31p and Bet5p were also seen in the crystal structure of both the yeast and mammalian proteins (Kim *et al.*, 2006; Cai *et al.*, 2008). While an interaction with Trs20p was not detected in the crystal structure, a similar interaction between the mammalian homologs TRAPPC4 and TRAPPC2 was recently reported (Scrivens *et al.*, 2011) and may reflect interactions in higher ordered structures (Yip *et al.*, 2010). The trs23 Δ 99C protein lost all of the interactions seen with the wild type protein, consistent with its inability to support assembly of rTRAPPI. The trs23 Δ SMS protein lost its ability to interact with Bet5p and showed a weakened ability to interact with both Trs31p and Trs20p (Figure 3.3A), suggesting that the SMS domain contributes to these interactions. These differences were not due to reduced expression levels or instability of the mutant proteins (Figure 3.3B). Weakened interactions between trs23 Δ SMS and other TRAPP proteins helps to explain the intermediate GEF activity seen in bacterial lysates containing trs23 Δ SMS (Figure 3.2C) in the absence of detectable amounts of rTRAPPI (Figure 3.2B).

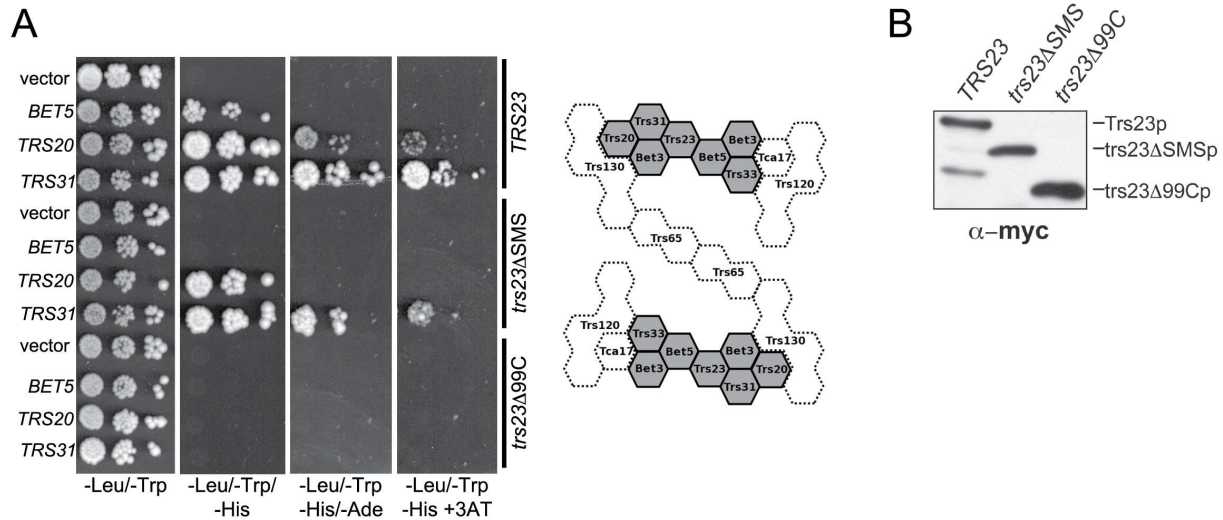


Figure 3.3 The SMS domain of Trs23p contributes to the strength of Trs23p-TRAPP subunit interactions. (A) Wild type Trs23p or the mutants *trs23Δ99C* and *trs23ΔSMS* were expressed in yeast as fusion proteins with the DNA binding domain of Gal4p and mated to yeast strains expressing other TRAPP subunits fused to the transcriptional activation domain of Gal4p. Serial 10-fold dilutions of diploids were plated on SD-leucine/tryptophan, SD-leucine/tryptophan/histidine, SD-leucine/tryptophan/adenine and SD-leucine/tryptophan/histidine containing 5mM 3AT and all plates were incubated at 30°C. A two-dimensional schematic of the TRAPP II complex is shown adjacent to the panel. Shaded in gray is the TRAPPI core of the complex whose crystal structure and organization are known. The position and interactions of the remaining subunits (stippled) are not known but are based on previously published studies on the organization of yeast and mammalian TRAPP complexes (Montpetit and Conibear, 2009; Scrivens *et al.*, 2009; Yip *et al.*, 2010). (B) Lysates were produced from yeast cells expressing Trs23p, or the mutant proteins *trs23ΔSMS* or *trs23Δ99C* from the plasmid pGBKT7. Equal amounts of protein were loaded in each lane and probed with anti-*myc* IgG since the fusion proteins contain a *myc* epitope tag. Identical results were obtained when the blot was probed with anti-Trs23p IgG (not shown).

3.3.4 *trs23ΔSMS* retains Ypt1p GEF activity in yeast lysates

We next explored the level of Ypt1p GEF activity in the yeast mutants *trs23ΔSMS* and *trs23Δ99C*. In lysates prepared from *trs23ΔSMS*, GEF activity was comparable to that of wild type (Figure 3.4A) confirming that this domain is not essential for GEF activity. In contrast, lysates from *trs23Δ99C* were reduced to near background levels and was similar to that of *trs23^{MPR/AWS}* (Figure 3.4A) that was previously shown to be defective *in vitro* (see Cai *et al.*, 2008). These results are similar to those seen *in vitro* (Figure 3.2C) and suggest that the assembly of TRAPP in *trs23ΔSMS* is more efficient *in vivo* compared to *in vitro*.

Furthermore, the stability of TRAPP appears to be largely unaffected in *trs23ΔSMS*, in contrast to *trs23Δ99C* where several subunits are less stable (Figure 3.4B). Reduced levels of TRAPP could account for the growth phenotype seen for *trs23Δ99C*. For these reasons, we focused our attention on the *trs23ΔSMS* mutant which, although has weakened interactions, displays no defects in growth, TRAPP subunit levels or GEF activity in yeast.

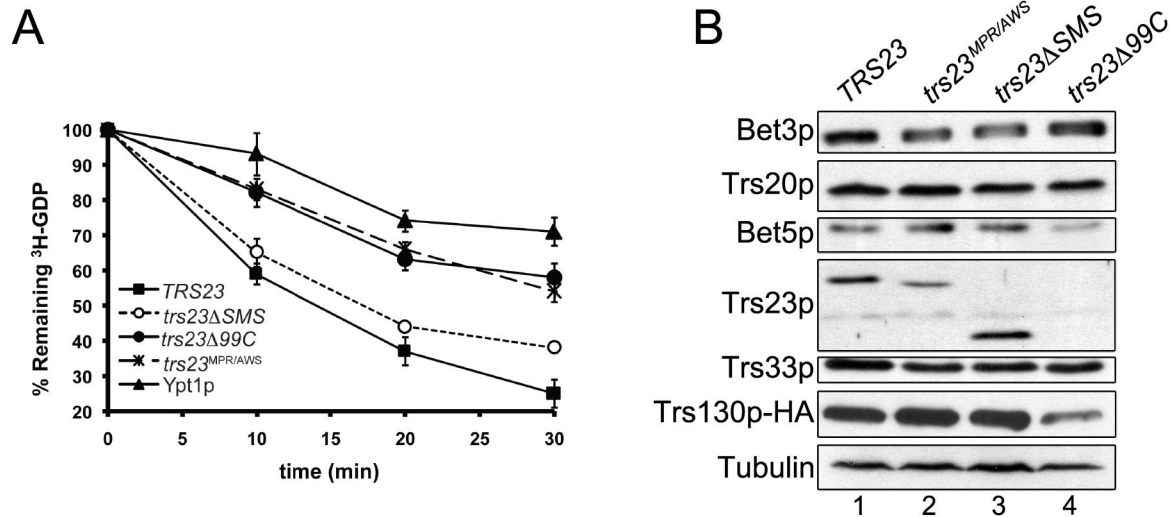


Figure 3.4 GEF activity is unaffected in *S. cerevisiae* containing *trs23ΔSMS*. (A) Lysates from yeast cells expressing wild type Trs23p (■) or the mutant proteins *trs23Δ99C* (●), *trs23ΔSMS* (○) or *trs23^{MPR/AWS}* (×) were prepared and assayed for Ypt1p-directed GEF activity as described in Experimental Procedures. The intrinsic ability of Ypt1p to release nucleotide is also shown (▲). Assay represents three replicates and error bars represent ± SEM. (B) Lysates from wild type (lane 1), *trs23^{MPR/AWS}* (lane 2), *trs23ΔSMS* (lane 3) and *trs23Δ99C* (lane 4) were probed with antibodies recognizing the TRAPP subunits indicated or anti-HA to detect endogenously-tagged Trs130p. Tubulin served as a loading control.

3.3.5 *trs23ΔSMS* contain only a single TRAPP peak at physiological salt

Our results thus far suggest that the *trs23ΔSMS* protein has reduced interactions with TRAPP proteins and only weakly supports the formation of the TRAPP core *in vitro* yet yeast bearing this mutation are not defective in GEF activity. We therefore explored the effects of this mutation on the formation of the three reported yeast TRAPP complexes TRAPPI, II and III. Lysates from wild type and *trs23ΔSMS* were fractionated in physiological salt (150mM) by size exclusion chromatography on a Superose 6 column. This column was chosen since, unlike Superdex 200 that has been used for most previously-reported TRAPP

studies, it readily separates TRAPP^{II} and III (Choi *et al.*, 2011). Consistent with previous studies (Sacher *et al.*, 1998, 2001; Jones *et al.*, 2000; Menon *et al.*, 2006; Montpetit and Conibear, 2009; Choi *et al.*, 2011), Bet3p, Trs23p and Trs33p in wild type lysates are found in two high molecular weight fractions (Figure 3.5A). While these have previously been reported to correspond to TRAPP^{II} and I on a Superdex 200 column, we now show the remarkable result that the highest molecular weight peak (fractions 16/17) contains both the TRAPP^{III}- and II-specific subunits Trs85p and Trs130p, respectively (Figure 3.5A). Only at higher salt concentrations (300mM) do we see these proteins separate into two peaks largely distinct from each other which are indicated as TRAPP^{III} (fractions 16-17) and II (fractions 21-22) (Figure 3.5A). The third TRAPP complex, TRAPP^I, peaks at fractions 30-31 (Figure 3.5A). In lysates from *trs23ΔSMS*, similar results were seen with respect to the peak seen in fractions 16-17, and the salt-induced separation into distinct TRAPP^{III} and II peaks was also noted (Figure 3.5A). However, in *trs23ΔSMS* we no longer detected the TRAPP^I peak that appears in fractions 30-31 in wild type cells. Rather, the TRAPP subunits Bet3p, Trs23p and Trs33p are found in a peak in fractions 33/34 (Figures 3.5A and B). This latter peak has a molecular size of ~67kD which likely corresponds to monomers or very small subcomplexes of these subunits. In addition, we noted the appearance of a sizeable pool of Trs85p in *trs23ΔSMS* that increases under high salt conditions. The complexes seen on this column are likely representative of the cellular pool of TRAPP since the majority of TRAPP was loaded onto the columns at both 150mM and 300mM salt (Figure 3.5C). Collectively, our results demonstrate that, at physiological salt, *trs23ΔSMS* contain just a single TRAPP peak corresponding to the region where TRAPP^{III} fractionates and that under these conditions the TRAPP^{II} peak is not present even in wild type.

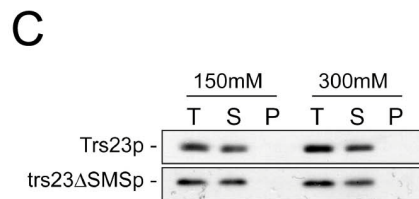
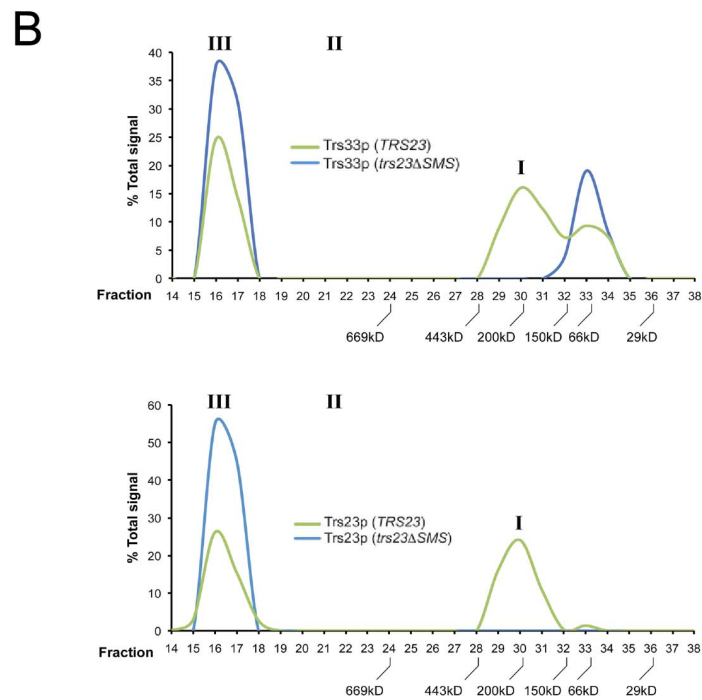
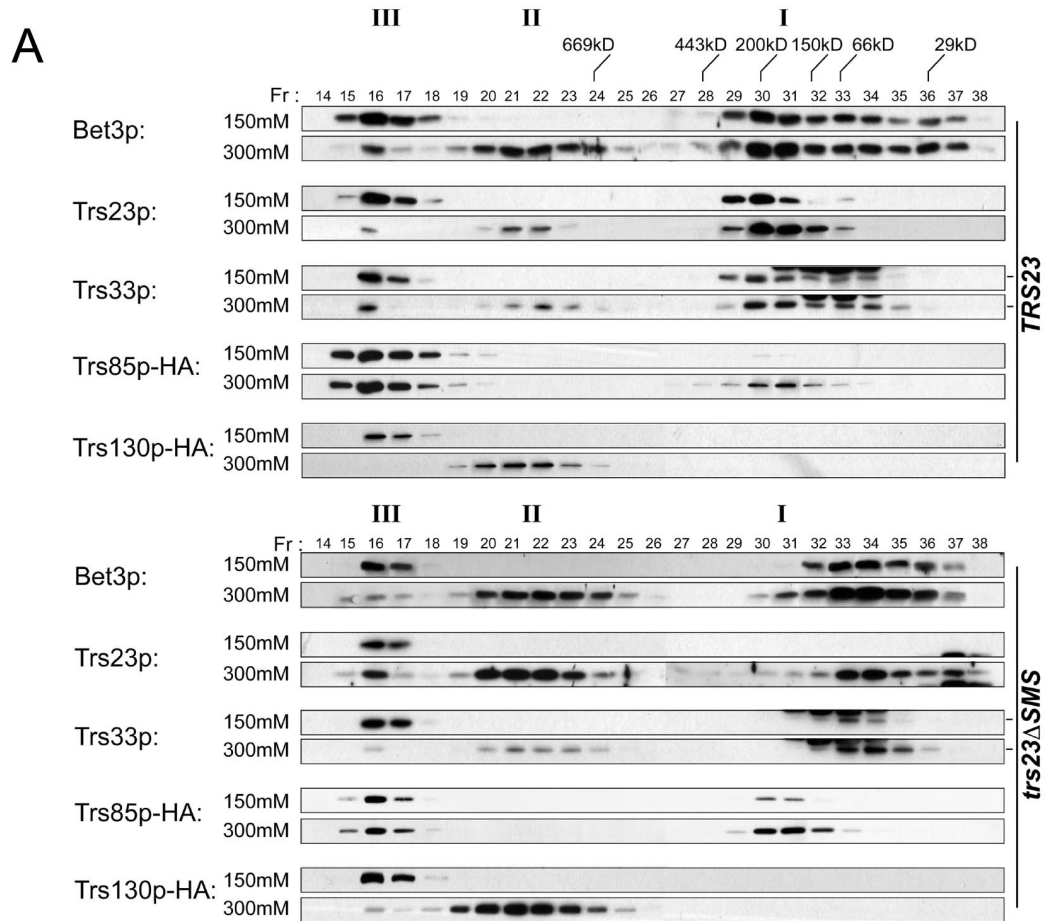


Figure 3.5 (figure legend on next page)

Figure 3.5 A single TRAPP peak is detected in *trs23ΔSMS* at physiological salt concentrations. (A) Lysates from wild type and *trs23ΔSMS* were fractionated on a Superose 6 size exclusion column in buffer containing either 150mM NaCl or 300mM NaCl as indicated. Fractions of 0.5ml were collected and probed with antibodies that recognize Bet3p, Trs33p, Trs23p or HA (to detect endogenously-tagged Trs130p or Trs85p). I, II and III above the wild type and *trs23ΔSMS* blots indicate the location of TRAPPI, II and III, respectively, under conditions where they separate from each other. Molecular size standards are also indicated above the blots. Note that a cross-reactive band appears just above the Trs33p band in fractions 32-34 with the anti-Trs33p antibody and the dash to the right of the Trs33 panels indicates the position of Trs33p. For each subunit shown, samples ranging from fractions 14-38 were fractionated on two separate polyacrylamide gels and processed for Western analysis simultaneously. Exposures for each half of the two gels were identical. (B) The signals for Trs33p (top panel) and Trs23p (bottom panel) from wild type (green) and *trs23ΔSMS* (blue) at 150mM NaCl shown in (A) were quantitated using Image J and plotted as a percentage of the total signal. Note the absence of the TRAPPI peak in *trs23ΔSMS*. (C) Lysates were prepared for fractionation as in (A) at either 150mM or 300mM NaCl. Samples before the centrifugation (T), the pellet fraction following centrifugation (P) and the supernatant (S) that was loaded onto the Superose 6 column were probed for Trs23p in both wild type and *trs23ΔSMS*.

The fact that Trs85p and Trs130p co-fractionated in a single peak at physiological salt in both wild type and *trs23ΔSMS* led us to consider the possibility that there is a single TRAPP complex that is unstable and easily fragments with increasing salt. Alternatively, these two TRAPP complexes could be either oligomerized or bound to other cellular components causing them to co-fractionate. To distinguish between these possibilities we constructed a strain that contains TAP-tagged Trs85p and Trs130p-*myc*. The strain was fractionated under conditions where only the TRAPPIII peak, but not the TRAPPII peak, was detected (50mM NaCl; see Figure 3.13A). The TRAPPIII-containing fraction was then treated with the crosslinking reagent DSP or left untreated before processing for immunoprecipitation. Although crosslinking was efficient (see Figure 3.13B), when Trs85p was immunoprecipitated with anti-TAP IgG we failed to detect co-precipitation of Trs130p-*myc* even though >50% of the cellular Trs85p was immunoprecipitated (Figure 3.6). Since multiple copies of Trs85p were not previously detected in TRAPPIII (Choi *et al.*, 2011) and since at least two copies of Trs130p are present in TRAPPII (Yip *et al.*, 2010), we should have easily been able to detect co-precipitation of Trs130p-*myc* if there was just a single complex in fractions 16-17. Therefore, we conclude that at physiological salt, TRAPPII and III represent distinct complexes that co-fractionate on a Superose 6 column.

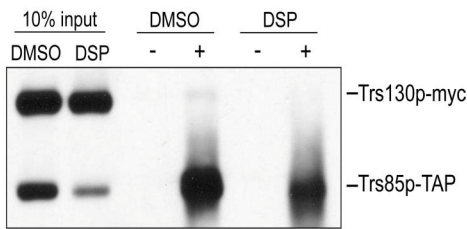


Figure 3.6 TRAPPII and TRAPPIII are distinct complexes. Lysate from wild type cells containing Trs85p-TAP and Trs130p-*myc* were fractionated on a Superose 6 column and fractions 16-17 were collected and split in two. One sample was treated with DMSO while the other sample was treated with the crosslinking reagent DSP for 3 hours on ice. Each sample was then split in two and either treated with (+) or without (-) anti-TAP IgG. The immune complexes were collected on protein A-sepharose beads, fractionated by SDS-PAGE and probed with anti-*myc* IgG. Samples representing 10% of the input are shown.

3.3.6 TRAPPII/III provides Ypt1p GEF activity in *trs23ΔSMS*

The ability of TRAPPI to act as a GEF for Ypt1p is firmly established (Jones *et al.*, 2000; Sacher *et al.*, 2001; Kim *et al.*, 2006; Morozova *et al.*, 2006; Cai *et al.*, 2008). The absence of TRAPPI in *trs23ΔSMS* along with near wild type levels of GEF activity *in vivo*, suggested that an alternate Ypt1p GEF was functioning to support ER-to-Golgi transport. One possibility is that Dss4p, a protein that facilitates nucleotide release from several GTPases including Ypt1p (Esters *et al.*, 2001) and genetically interacts with TRAPP (Jiang *et al.*, 1998), can facilitate nucleotide exchange on Ypt1p in the absence of TRAPPI. If this were the case, we would expect to see a genetic interaction between *DSS4* and *TRS23*. Since *trs23Δ99C* has an obvious growth phenotype, we used this mutant to explore genetic interactions with *DSS4*. Overexpression of *DSS4* did not alleviate either the ts or cs phenotype of *trs23Δ99C* (not shown). In addition, tetrad analysis following a cross between the two haploid mutant yeast strains *dss4Δ* and *trs23Δ99C* did not reveal any growth defect or exacerbation of the growth phenotype seen for *trs23Δ99C* (22 tetrads dissected, co-segregation in 19 colonies). These results argue against Dss4p compensating for the lack of TRAPPI.

Alternatively, TRAPPII or III, the only TRAPP complexes detected in *trs23ΔSMS* at physiological salt, may act as a Ypt1p GEF since previous literature in this area in which

lysates were assayed for GEF activity has been controversial (Jones *et al.*, 2000; Sacher *et al.*, 2001; Morozova *et al.*, 2006; Cai *et al.*, 2008). Yeast lysates from wild type and *trs23ΔSMS* were fractionated by size exclusion chromatography on a Superose 6 column and fractions 16-17 (TRAPP II/III) and 29-31 (where TRAPPI fractionates) were assayed for Ypt1p GEF activity. Indeed, both the TRAPP II/III- and TRAPPI-containing fractions displayed Ypt1p GEF activity in wild type. In contrast, and consistent with the absence of TRAPPI in *trs23ΔSMS*, this mutant only displayed Ypt1p GEF activity in the TRAPP II/III fractions (Figure 3.7). It is noteworthy that although TRAPPIII has been reported to display Ypt1p GEF activity (Lynch-Day *et al.*, 2010), the Trs85p peak near TRAPPI is not active in our assay, suggesting that only the high molecular weight peak of Trs85p possesses this activity. Our results suggest that in the absence of TRAPPI, either TRAPP II or III can provide sufficient Ypt1p GEF activity to maintain cell growth.

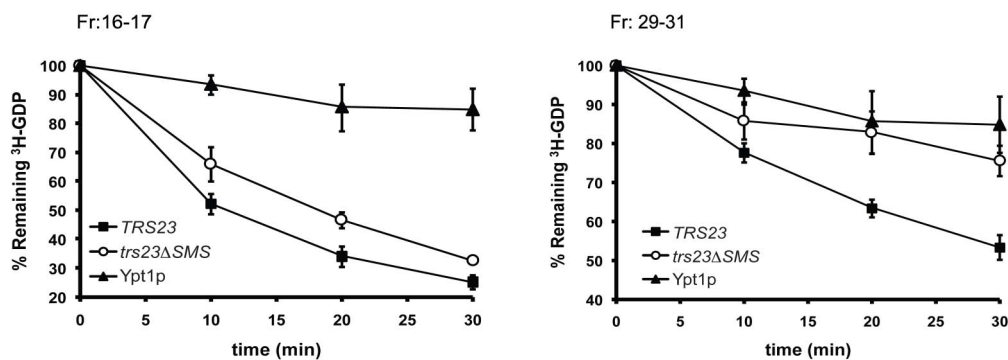


Figure 3.7 Only fractions containing TRAPP II/III display Ypt1p GEF activity in *trs23ΔSMS*. Lysate from wild type (■) or *trs23ΔSMS* (○) was fractionated by size exclusion chromatography on a Superose 6 column in 150mM salt. The fractions enriched in TRAPP II/III (fractions 16-17) and TRAPPI (fractions 29-31) were pooled, concentrated and assayed for Ypt1p GEF activity compared to the intrinsic ability of Ypt1p to release nucleotide. The intrinsic ability of Ypt1p to release nucleotide is also shown (▲). Assays represent three replicates and error bars represent ± SEM.

3.3.7 *trs23ΔSMS* does not display defects in membrane traffic

The only notable defect seen in *trs23ΔSMS* has been the disappearance of its TRAPPI peak. Since TRAPPI is reported to function in ER-to-Golgi transport, we expected that a defect in this stage of membrane traffic would manifest in a growth phenotype. However, this was not seen (see Figure 3.1). In order to more closely assess this mutant for possible defects in membrane traffic we first examined the processing of the vacuolar protease

carboxypeptidase Y (CPY) by pulse-chase analysis. This protein has ER (p1), Golgi (p2) and vacuolar (m) forms that are easily distinguished by SDS-PAGE. As shown in Figure 3.8, *trs23ΔSMS* did not show a noticeable defect in CPY processing. The pattern was similar to wild type and stood in stark contrast to that of *sec18* which displayed the expected block in ER-to-Golgi traffic as evidenced by the failure of the cells to process p1CPY.

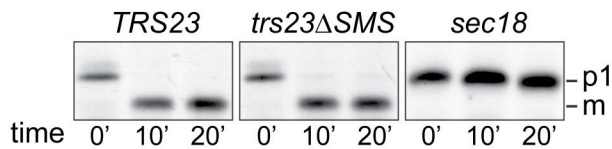


Figure 3.8 CPY trafficking is unaffected in the *trs23ΔSMS* mutant. (A) Wild type, *trs23ΔSMS* and *sec18* yeast were pulse-labeled with ³⁵S-methionine/cysteine and chased for the times indicated below the panels. Carboxypeptidase Y (CPY) was immunoprecipitated from lysates at each time point, fractionated by SDS-PAGE and visualized by autoradiography. The position of the ER (p1) and vacuolar (m) forms of CPY are indicated.

Since Trs23p is a component of TRAPP^{II} that reportedly functions at the late Golgi, we also examined the cells for defects in later stages of the secretory pathway. Snc1p, a protein that cycles between the late Golgi and the plasma membrane, is normally found at steady state on the plasma membrane of unbudded yeast cells or on the emerging bud in a polarized manner when fused to GFP (GFP-Snc1p) (Lewis *et al.*, 2000). Defects in recycling lead to the accumulation of Snc1p inside of the cells or a loss of its polarized distribution. Wild type cells displayed the expected distribution of GFP-Snc1p (Figure 3.9). As was the case with CPY processing, GFP-Snc1p localization was unaffected in *trs23ΔSMS*. This result contrasts with that of *trs85Δ* which showed a strong GFP-Snc1p recycling defect (Figure 3.9) as previously reported (Montpetit and Conibear, 2009).

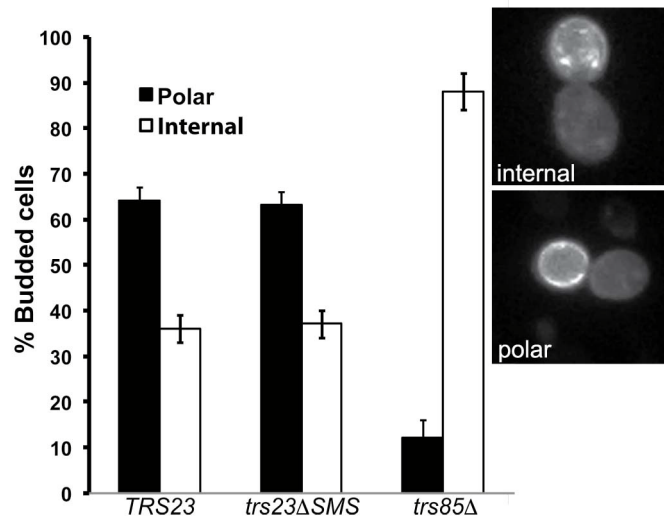


Figure 3.9 Snc1p recycling is unaffected in the *trs23ΔSMS* mutant. Wild type, *trs23ΔSMS* and *trs85Δ* were transformed with a plasmid expressing GFP-Snc1p. The cells were fixed and viewed using an epifluorescence microscope. For quantitation a minimum of 100 cells from three replicates were counted. The error bars represent \pm SEM and representative cells used for quantitation are shown as insets.

To further explore *trs23ΔSMS* for a late secretory pathway defect we examined the localization of the fluorescently-tagged GTPase GFP-Ypt31p. This GTPase normally concentrates in small buds and at the mother/bud neck (Buvelot *et al.*, 2006), which we saw in wild type cells (Figure 3.10). This pattern was unaffected in *trs23ΔSMS*, in contrast to *trs23Δ99C* where it was clearly altered (Figure 3.10).

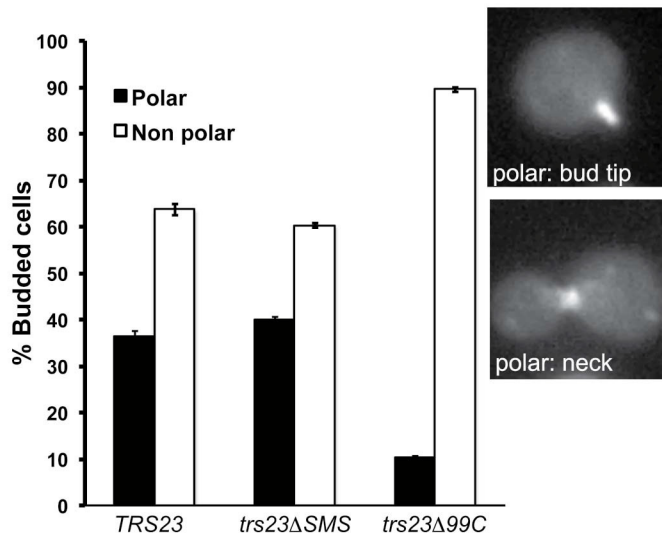


Figure 3.10 Ypt31p is correctly localized in the *trs23ΔSMS* mutant. Wild type, *trs23ΔSMS* and *trs23Δ99C* were transformed with a plasmid expressing Ypt31p-GFP. The cells were fixed and viewed using an epifluorescence microscope. For quantitation a minimum of 100 cells from three replicates were counted. The error bars represent \pm SEM and representative cells used for quantitation are shown as insets.

TRAPPIII has recently been reported to function in autophagy (Lynch-Day *et al.*, 2010). We therefore examined the cytosol-to-vacuole targeting (Cvt) pathway in *trs23ΔSMS* using the marker Ape1p-GFP. This protein is processed by the Cvt pathway and is ultimately cleaved releasing GFP which is detected by Western analysis (Shintani *et al.*, 2002). As shown in Figure 3.11, both wild type and *trs23ΔSMS* were capable of processing Ape1p-GFP. In contrast, and as previously reported (Meiling-Wesse *et al.*, 2005; Nazarko *et al.*, 2005), *trs85Δ* cells were defective in this pathway (Figure 3.11).

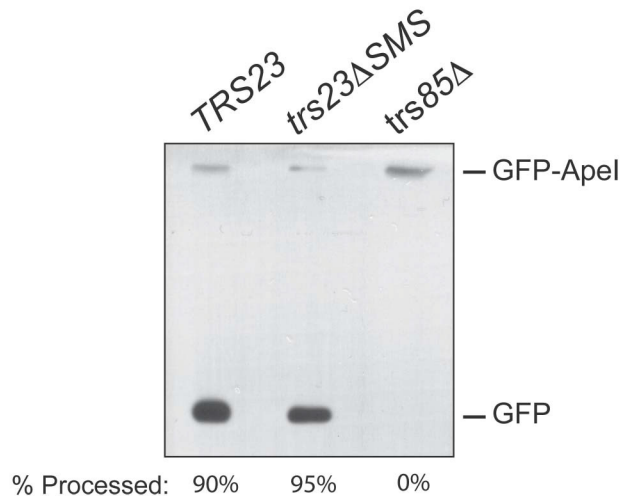


Figure 3.11 The Cvt pathway is normal in the *trs23ΔSMS* mutant. Wild type, *trs23ΔSMS* and *trs85Δ* were transformed with a plasmid expressing Ape1p-GFP, grown in minimal medium without uracil, converted to spheroplasts and lysed. Samples were fractionated by SDS-PAGE and probed with anti-GFP. The percentage of Ape1p-GFP processing, calculated using Image J, is indicated below each lane.

We also examined *trs23ΔSMS* for defects in an *in vitro* assay that reconstitutes ER-to-Golgi transport (Barlowe, 1997). This assay measures the acquisition of Golgi-specific modifications of a marker protein called pro- α -factor. Compared to wild type, *trs23ΔSMS* did not show a defect in transport *in vitro* (Figure 3.12A). As was shown earlier using physiological salt (see Figure 3.5A), lysates from *trs23ΔSMS* prepared in the buffer used for the *in vitro* assay (buffer B88) also showed a single TRAPP peak corresponding to TRAPP^{II/III} (Figure 3.12B). Interestingly, lysates from wild type used for this assay showed a broadening of the TRAPP^I peak suggesting this complex is not stable in this buffer. Collectively, our results suggest that *trs23ΔSMS* does not adversely affect membrane traffic *in vitro* nor *in vivo*.

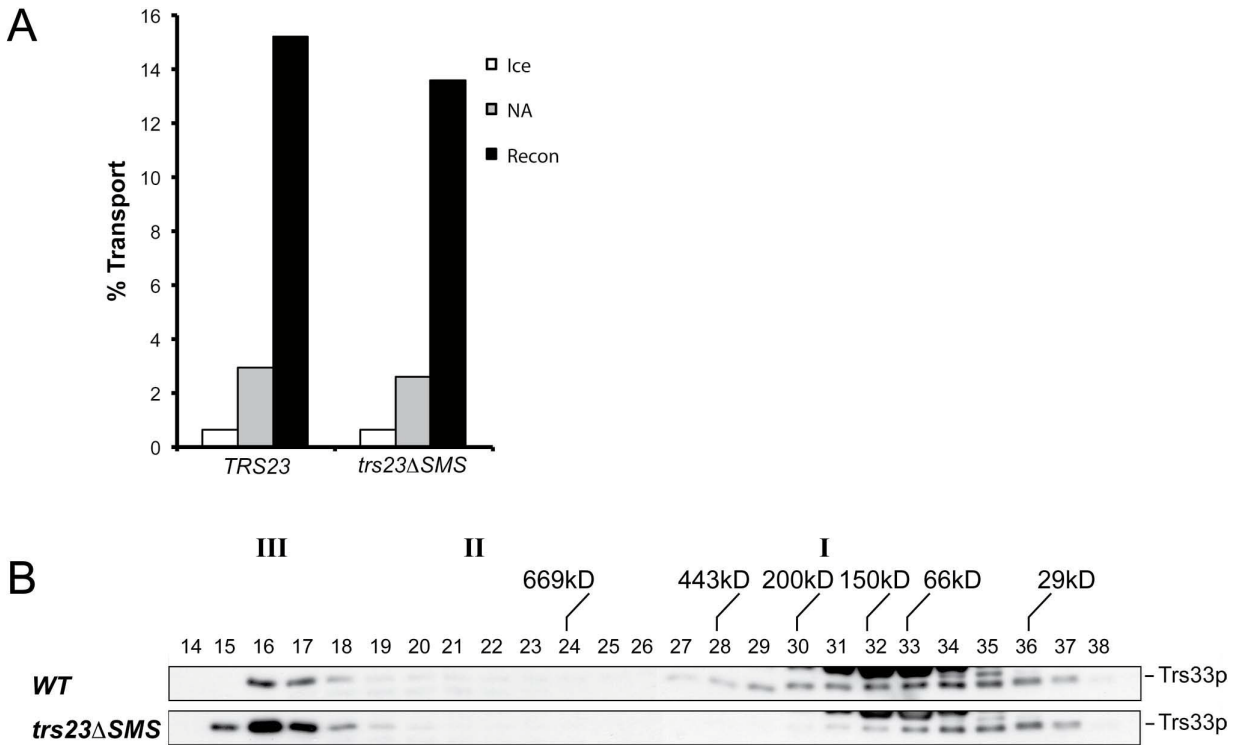


Figure 3.12 Lysates from the *trs23ΔSMS* mutant are competent for *In vitro* ER-to-Golgi trafficking. Reconstitution of ER-to-Golgi traffic was performed as described in Experimental Procedures. Reactions were performed with no additions either on ice (ice) or at 29°C (NA), or fully reconstituted at 29°C (Recon). The results are expressed as percentage of concanavalin A-precipitable pro- α -factor that has received α -1,6-mannose Golgi modifications. The results are the average of duplicates and the range of transport over three independent experiments was 13.6%-15.4% (wild type) and 12.6%-14% (*trs23ΔSMS*). **(B)** Lysates were prepared from wild type and *trs23ΔSMS* in buffer B88 that was used for the *in vitro* transport assay in **(A)** and fractionated on a Superose 6 column in B88. Fractions were probed with anti-Trs33p. I, II and III above the blots indicate the location of TRAPPI, II and III, respectively, under conditions where they separate from each other.

3.3.8 TRAPPI can form from TRAPPII/III *in vitro*

Our results thus far suggest that in the absence of TRAPPI, cells survive with no adverse effects in ER-to-Golgi traffic. This was surprising given that TRAPPI is implicated in this pathway. One explanation is that TRAPPI represents either an intermediate in the assembly of TRAPPII and/or III or is a fragment of either complex since we found that its appearance is salt dependent (Figure 3.13A). To address this we first fractionated a lysate from wild type cells in low (50mM) salt where only the TRAPPII/III peak is detected

(Figure 3.13A). We then incubated this fraction either with or without the crosslinking reagent DSP and fractionated the sample in 300mM salt, conditions where all three TRAPP complexes are detected (see Figure 3.5A). As shown in Figure 3.13B, while the untreated sample did indeed show a TRAPPI peak, the crosslinked sample did not. Importantly, no intermediate peak between TRAPP II/III and TRAPPI was detected in the untreated sample. These results suggest that TRAPPI is a subcomplex of one or both of the larger (TRAPP II and III) complexes that forms in the presence of increasing salt *in vitro*.

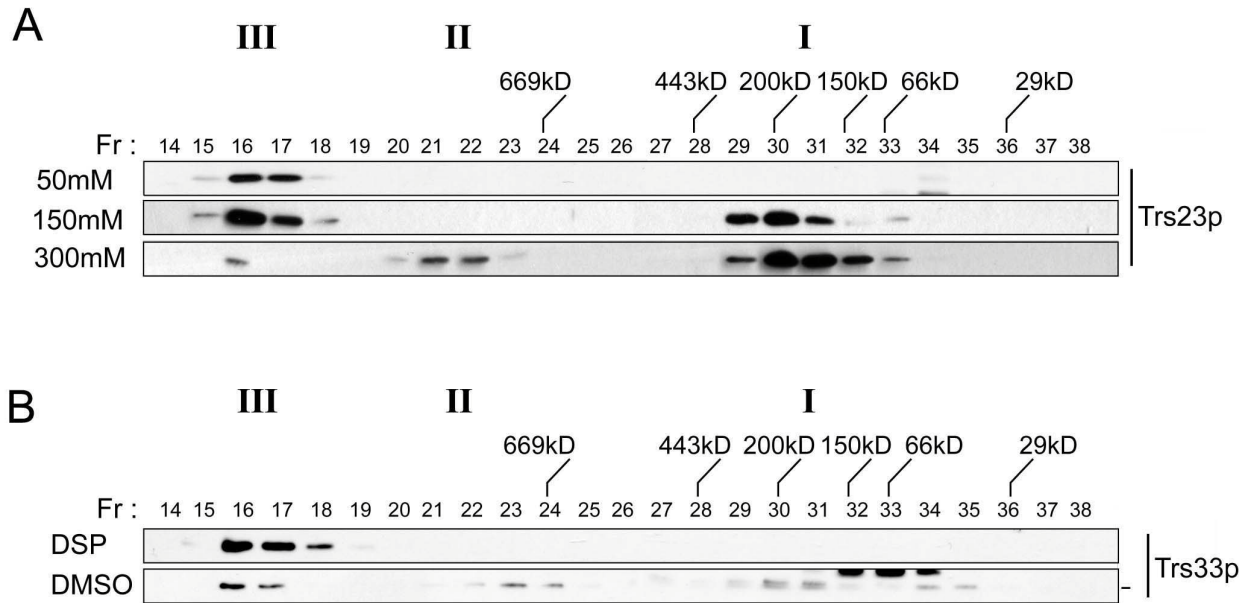


Figure 3.13 TRAPPI can form from TRAPP II/III. (A) Lysates of wild type yeast were prepared in buffer containing 50mM, 150mM or 300mM NaCl and fractionated by size exclusion chromatography on a Superose 6 column in buffer containing identical salt. The fractions were analyzed by Western blotting for the presence of Trs23p. (B) The TRAPP II/III-containing fraction from wild type lysate that was fractionated in the presence of 50mM NaCl was incubated with 2mM DSP or DMSO, quenched with Tris pH 7.5 and re-fractionated on a Superose 6 column in buffer containing 300mM NaCl. Fractions were probed for the presence of Trs33p. Note that a cross-reactive band appears just above the Trs33p band in fractions 32-34 with the anti-Trs33p antibody in the DMSO-treated sample and the dash to the right of the Trs33 panel indicates the position of Trs33p. I, II and III above the wild type and *trs23ΔSMS* blots indicate the location of TRAPPI, II and III, respectively, under conditions where they separate from each other.

3.3.9 TRAPPI appearance is SMS domain-dependent

TRAPPI, as defined by the co-fractionation of the TRAPP core subunits on a gel filtration column, is readily seen in *S. cerevisiae* but not in human cells (Menon *et al.*, 2006; Scrivens *et al.*, 2009, 2011; Yamasaki *et al.*, 2009). We speculated that this may be due to added stability afforded to this complex by the SMS domain of Trs23p. Like the human protein, Trs23p in other yeast such as *P. pastoris* do not have the SMS domain. Thus, if our hypothesis is correct, we would expect that *P. pastoris* would not display a TRAPPI peak. We found that our antibody raised against the human TRAPPC3 protein, the most conserved subunit in TRAPP, was cross-reactive with *P. pastoris* Bet3p providing us with a means to address whether this yeast has a TRAPPI peak. Lysate from *P. pastoris* and *S. cerevisiae* was fractionated by size exclusion chromatography on a Superdex 200 column to better resolve the smaller molecular size region where TRAPPI fractionates. In *S. cerevisiae*, TRAPPI is detected in fraction 13 while TRAPP II/III is detected in fractions 8-9 (Figure 3.14). In the *P. pastoris* lysate, a high molecular weight pool of Bet3p was detected that most likely corresponds to TRAPP II/III (Figure 3.14). Based on the size of the *P. pastoris* TRAPP subunits, a TRAPPI complex would be expected to be only 30kD smaller than the *S. cerevisiae* complex. While a second peak of Bet3p was detected, it eluted in a fraction (fraction 17) with a molecular size much smaller than that expected for TRAPPI and no other peak of *P. pastoris* Bet3p was seen. The absence of a TRAPPI-equivalent was also noted for human cells, whose Trs23p homolog does not contain an SMS domain (Loh *et al.*, 2005; Scrivens *et al.*, 2009, 2011; Yamasaki *et al.*, 2009). This result is consistent with the notion that the SMS domain of Trs23p stabilizes *S. cerevisiae* TRAPPI.

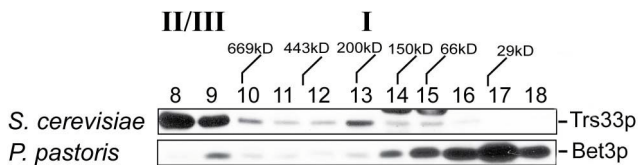


Figure 3.14 *P. pastoris* does not contain a TRAPPI peak. Lysates in 150mM NaCl from *P. pastoris* and *S. cerevisiae* were fractionated by size exclusion chromatography on a Superdex 200 column. The fractions were probed for Trs33p (*S. cerevisiae*) or *P. pastoris* Bet3p using anti-TRAPPC3 IgG. The positions of TRAPP II/III and I are indicated above the top panel.

3.4 Discussion

Here we demonstrate that the *Saccharomycotina*-specific (SMS) domain of *S. cerevisiae* Trs23p is not required for Ypt1p-directed GEF activity but is important for the stable interaction between Trs23p and other TRAPP subunits. Our data suggest that cells devoid of this domain of Trs23p contain two large TRAPP complexes called TRAPP^{II} and III and do not contain the smaller TRAPP^I complex. These cells resemble wild type with respect to four different membrane trafficking assays both *in vivo* and *in vitro* and in terms of their growth characteristics. Based on our study, we suggest that the SMS domain of Trs23p stabilizes fragments (TRAPP^I) of TRAPP^{II} and/or III.

Collectively, our data may suggest that *S. cerevisiae* contain a single Golgi-localized TRAPP complex (TRAPP^{II}) that is capable of supporting ER-to-Golgi traffic. This is based on a number of observations including: (i) removal of the SMS domain of Trs23p in *S. cerevisiae* results in a loss of the TRAPP^I peak with no corresponding reduction in Ypt1p GEF activity or noticeable growth phenotype; (ii) ER-to-Golgi traffic is normal both *in vivo* and *in vitro*; (iii) a TRAPP^I peak can be formed by incubating the TRAPP^{II}/III peak with high salt *in vitro*. Since TRAPP^{II}, but not TRAPP^{III}, localizes to the Golgi we propose that TRAPP^{II} can function in ER-to-Golgi transport. Since we cannot separate TRAPP^{II} from III, we cannot rule out the possibility that TRAPP^{III} is the complex that functions in ER-to-Golgi traffic. In this respect it is noteworthy that depletion of Trs85p, the TRAPP^{III}-specific subunit, was reported to be defective in ER-to-Golgi traffic (Sacher *et al.*, 2001) and autophagy may use membranes derived from the ER (Tooze and Yoshimori, 2010) suggesting the possibility that the role of TRAPP^{III} in autophagy may be an indirect result of its role in ER-to-Golgi traffic.

An important next step will be to characterize the TRAPP^{II} and III superstructures that we report. We have shown an identical fractionation pattern to that seen in Figure 3.5A in the presence of Triton X-100 for the TRAPP^{II} subunit Trs130p (S.B. and M.S., unpublished observation), suggesting that these structures are either bound to detergent-insoluble membranes, they oligomerize to greater than a dimer or are bound to a large protein structure as previously suggested (Sacher *et al.*, 2000). In addition, uncharacterized

subunits may be present in the complex. An alternative explanation for our data is that in the *trs23ΔSMS* cells, TRAPPI is more tightly associated with the TRAPP superstructures and would require higher salt to be liberated. We do not favour this possibility since increasing the salt concentration in *trs23ΔSMS* redistributes TRAPP core proteins from the higher molecular size fractions to a smaller fraction. The resulting peak is significantly smaller than TRAPPI and, at physiological salt, is devoid of Trs23p. It is evident that data addressing the existence and function of TRAPPI (which has only been demonstrated *in vitro*) as an independent TRAPP complex must be cautiously interpreted in light of our *in vitro* data.

Our results implicate the SMS domain of Trs23p in the stability of TRAPPI. The added stability afforded to TRAPPI by the SMS domain may explain why a recombinant form of human TRAPPI could not be assembled like that seen for the *S. cerevisiae* subunits (Kim *et al.*, 2006). Although it remains a formal possibility that small amounts of TRAPPI can support growth with no observable phenotype, given the very low levels of TRAPPI in cells to begin with (Sacher *et al.*, 2000) and the amounts of TRAPPI needed to support ER-to-Golgi transport *in vitro* (Sacher *et al.*, 2001), as well as the lack of GEF activity in the TRAPPI fraction of *trs23ΔSMS* (Figure 3.7) we do not favour this possibility.

Consistent with the notion that TRAPPI may be a fragment of TRAPP II or III is the fact that TRAPPI is not detected in live yeast cells (Montpetit and Conibear, 2009). In addition, it has previously been shown that the relative distribution of core subunits between the two TRAPP peaks on a Superdex 200 size exclusion column (which does not resolve TRAPP II and III) is highly variable but TRAPP II/III levels of these subunits are generally higher than those in TRAPPI (Sacher *et al.*, 2001; Menon *et al.*, 2006; Montpetit and Conibear, 2009; Choi *et al.*, 2011). The only exceptions to this are when high salt (500mM) is used in the preparation of the lysate (Montpetit and Conibear, 2009) or when certain *trs120* or *trs130* (TRAPP II) mutants are used (Menon *et al.*, 2006). The former is consistent with the notion that TRAPPI is an *in vitro*, salt-dependent fragment of TRAPP II and/or III, and the latter is consistent with the role of Trs120p and Trs130p in the overall

architecture of TRAPP^{II} (Yip *et al.*, 2010). The notion that TRAPP^I results from TRAPP^{II}/III is analogous to a recent study that suggested that there were two Trs85p peaks on a size exclusion column (confirmed in the present study), where the low molecular weight peak may represent a breakdown product or an assembly intermediate of the higher molecular weight TRAPP^{III} peak (Choi *et al.*, 2011).

If our suggestion of TRAPP^I being an *in vitro*, salt-dependent fragment of TRAPP^{II}/III is correct, this has strong implications for the role of tethering factors as determinants of specificity and for the mechanism of action of TRAPP in ER-to-Golgi traffic in particular. The Golgi would in fact have a single TRAPP complex (TRAPP^{II}) that could function in traffic at both ends of the organelle. In mammalian cells the early secretory pathway is more complex with a pre-Golgi ERGIC compartment (Schweizer *et al.*, 1990) and the need to transport diverse-sized cargo (Schmidt and Stephens, 2010). Whether the mammalian TRAPP complex functions at both ends of the Golgi is still unknown. However, it has been shown to function in the early secretory pathway (Loh *et al.*, 2005; Yu *et al.*, 2006; Scrivens *et al.*, 2009, 2011; Yamasaki *et al.*, 2009) and only a single complex containing all *S. cerevisiae* TRAPP subunit homologs has been reported, suggesting that if mammalian TRAPP does indeed function at the late Golgi then a single complex would be expected to perform both of these functions. Indeed, parallels between *S. cerevisiae* and human TRAPP proteins with respect to their interactions with vesicle coat proteins have already been made (Cai *et al.*, 2005, 2007b; Yamasaki *et al.*, 2009). We suggest that factors on the vesicles (e.g. GTPases and SNAREs) in combination with coat proteins and tethers contribute to the overall specificity of vesicle transport. This notion helps to explain why some GTPases such as Ypt1p can function at multiple steps in membrane traffic (Bacon *et al.*, 1989; Jedd *et al.*, 1995; Lynch-Day *et al.*, 2010; Sclafani *et al.*, 2010) and why some yeast SNAREs such as Sed5p, Ykt6p and Vti1p can also function in multiple membrane trafficking processes (McNew *et al.*, 1997; von Mollard *et al.*, 1997; Ungermann *et al.*, 1999; Tsui *et al.*, 2001). In this respect, *S. cerevisiae* TRAPP^{II} and mammalian TRAPP would be no different, with the particular combinations of factors and the combined effect of multiple layers of partial specificity dictating the overall specificity of the process.

Whether *S. cerevisiae* TRAPP functions on the Golgi where it interacts with incoming vesicles or binds to vesicles and interacts with a Golgi-localized protein is not clear and needs to be resolved. However, recent studies suggest the latter may be possible (Cai *et al.*, 2005, 2007b; Yamasaki *et al.*, 2009) and the mammalian Bet3p homolog, TRAPPC3, has been shown to be required for homotypic vesicle fusion suggesting that at least this subunit can bind to vesicles independent of the Golgi (Yu *et al.*, 2006). In addition, other MTCs or parts of these complexes such as the exocyst and the COG complex have been reported to localize to vesicles (Boyd *et al.*, 2004; Vasile *et al.*, 2006; Pokrovskaya *et al.*, 2011) leaving open the question of whether MTCs bind first to vesicles or target organelles. If TRAPP were to function analogously, it would have the ability to bind to both COP I and II vesicles.

Given the large size of TRAPP II and III, and the fact that the core subunit Bet3p binds to the inner Sec23/24p layer of the COP II coat, how can we envision TRAPP II or III functioning in ER-to-Golgi transport? The dimensions of a TRAPP II dimer (225Å x 250Å) (Yip *et al.*, 2010) may in theory have access to the Sec23/24p layer since the outer layer, composed of Sec13/31p, has openings of ~300Å (Stagg *et al.*, 2006). However, TRAPP II superstructures, such as those we presently demonstrate to occur at physiological salt, would seem to be prohibitively large to have similar access. In addition, it is unlikely that the openings presented by the COP II cage are completely unobstructed given the density and numbers of proteins that can be found on vesicles (Takamori *et al.*, 2006). In the case of COP II vesicles formed *in vitro*, the extent to which the outer layer of the coat remains intact is unclear (Lord *et al.*, 2011) and it has been suggested that either a portion of each vesicle has lost its outer layer or a portion of the vesicle population has lost its entire outer layer (Conibear, 2011). In this case, the question of access of either TRAPP II or III to the Sec23/24p layer would be mitigated. It is important to stress that the extent to which the vesicle coat remains intact *in vivo* is not known.

Chapter 4: TRAPP^{II} mediates Ypt6p dynamics at the late Golgi

This Chapter is unpublished. I am responsible for the following all figures presented in this Chapter.

4.1. Introduction

Vesicles containing lipids and protein cargo are transported throughout the cell in a highly regulated manner in a process called membrane trafficking. (Palade, 1975; Novick *et al.*, 1980; Balch *et al.*, 1994). Several factors cooperate to ensure that vesicles arrive at the correct compartment, among them small Rab GTPases and tethering factors (Bonifacino and Glick, 2004; Cai *et al.*, 2007a). A number of different Rabs and tethering factors are located throughout the endomembrane system. Rabs act as molecular switches to activate or inactivate membrane trafficking pathways while tethers act to physically anchor vesicles to a specific target membrane (Zerial and McBride, 2001; Seabra and Wasmeyer, 2004; Yu and Hughson, 2010).

Different proteins or complexes act as guanine nucleotide exchange factors (GEFs) to activate specific Rabs by inducing conformational changes that promote the loss of GDP and the uptake of GTP while GTPase accelerating proteins (GAPs) inactivate Rabs by accelerating their intrinsic rate of GTP hydrolysis (Bourne *et al.*, 1990; Bos *et al.*, 2007; Barr and Lambright, 2010). The coordinated recruitment of Rabs and their modifier proteins (GEFs and GAPs) to specific intracellular locations regulates the initiation and termination of membrane trafficking pathways. Rab GEF and Rab GAP cascades have been proposed to proceed in opposite directions and mediate sequential Rab activation and inactivation, respectively (Nottingham and Pfeffer, 2009). Each Rab within these cascades recruits the GEF for the next Rab and the GAP for the previous Rab in the pathway, providing directionality and limiting the localization of Rabs to specific compartments. Examples of these cascades have been described in secretory and endosomal trafficking pathways (Ortiz *et al.*, 2002; Wang and Ferro-Novick, 2002; Rivera-Molina and Novick, 2009; Suda *et al.*, 2013). In addition to Rabs, several other factors have been identified that contribute to the correct localization of Rab GEFs, including vesicle coat proteins and SNAREs (soluble *N*-

ethylmaleimide-sensitive factor attachment protein receptor)(Barr, 2013). In contrast, aside from their interaction with Rabs, very few factors have been identified that mediate the recruitment of Rab GAPs to specific compartments. Rab GEFs are interesting candidates to promote Rab GAP recruitment to the correct location as they are diverse in their structure and composition and are directly involved in Rab activation. A GEF-GAP interaction could also create cross-talk between opposing Rab GAP and Rab GEF cascades, providing an additional layer of control to ensure that Rabs are turned “on” and “off” in a coordinated manner.

Ypt6p is a non-essential Rab in yeast that is implicated in several trafficking pathways including post-Golgi trafficking, endosome to Golgi transport, retrograde transport through the Golgi, ER to early Golgi transport, early Golgi to ER transport, and autophagy (Bensen *et al.*, 2001; Luo and Gallwitz, 2003; Liu *et al.*, 2006; Ohashi and Munro, 2010; Benjamin *et al.*, 2011). Ypt6p is activated by the heterodimeric Ric1p/Rgp1p complex, and inactivated by the GAP protein Gyp6p (Strom *et al.*, 1993; Siniosoglou *et al.*, 2000; Will and Gallwitz, 2001). The GAPs Gyp2p and Gyp3p have also exhibited activity towards Ypt6p *in vitro* (Albert and Gallwitz, 1999). Like Ypt6p, Ric1p, Rgp1p and Gyp6p are all not essential for cell viability (Strom *et al.*, 1993; Siniosoglou *et al.*, 2000).

A Rab GAP cascade was recently described involving the recruitment of Gyp6p by active Ypt31/Ypt32p, a redundant Rab pair localized to the late Golgi, to promote the dissociation of Ypt6p from these membranes (Suda *et al.*, 2013). The multisubunit tethering complex (MTC) TRAPP II acts as a GEF for the early Golgi Rab Ypt1p as well as a putative GEF for the Ypt31/32p Rab pair (Jones *et al.*, 2000; Wang *et al.*, 2000; Morozova *et al.*, 2006; Cai *et al.*, 2008; Lynch-Day *et al.*, 2010; Yip *et al.*, 2010). There is overlap between TRAPP II- and Ypt6p-regulated membrane trafficking pathways as TRAPP II acts in post-Golgi trafficking from the late Golgi to the plasma membrane (PM) and early endosome to late Golgi transport (Sacher *et al.*, 2000, 2001; Cai *et al.*, 2005; Montpetit and Conibear, 2009; Yip *et al.*, 2010; Choi *et al.*, 2011). This Chapter presents evidence that the TRAPP II complex promotes the dissociation of Ypt6p from the late Golgi through the recruitment of the Ypt6p GAP Gyp6p. Destabilization of the TRAPP II complex disrupts its association with

Gyp6p and causes Ypt6p to become enriched at the late Golgi, a phenotype also observed in a *gyp6Δ* mutant. The interaction between TRAPP II, a Ypt1p and putative Ypt31/32p GEF, and the Rab GAP Gyp6p, is a novel mechanism for the recruitment of a GAP to the appropriate membrane and may also be an example of cross talk between a Rab GAP and Rab GEF cascade.

4.2 Materials and methods

Table 4.1 Plasmids used in Chapter 4.

MSB238	<i>pRS425</i>	
MSB247	<i>pRS425-BET5</i>	
MSB248	<i>pRS425-TRS20</i>	
MSB281	<i>pRS425-TRS23</i>	
MSB290	<i>pRS425-BET3</i>	
MSB271	<i>pRS425-TRS31</i>	
MSB250	<i>pRS425-TRS33</i>	
MSB473	<i>pRS425-TCA17</i>	
MSB291	<i>pRS425-TRS65</i>	
MSB284	<i>pRS425-TRS85</i>	
MSB285	<i>pRS425-TRS120</i>	
MSB474	<i>pRS425-TRS130</i>	
MSB1063	<i>pRS315-GFP-YPT6</i>	Received from Ruth Collins (RCB650)
MSB1319	<i>pRS316-ADH1pr-SEC7-mRFP</i>	Received from Akihiko Nakano (Suda <i>et al.</i> , 2013)
MSB1321	<i>pRS306-ADH1pr-mRuby-SED5</i>	Received from Akihiko Nakano (Suda <i>et al.</i> , 2013)

Table 4.2 Yeast strains used in Chapter 4.

MSY135	<i>MATα his3Δ1 leu2Δ0 lys2Δ0 ura3Δ0</i>
MSY540	<i>MATα his3Δ1 leu2Δ0 lys2Δ0 ura3Δ0 ypt6Δ::KanMX</i>
MSY609	<i>MATα his3Δ1 leu2Δ0 lys2Δ0 ura3Δ0 ric1Δ::KanMX</i>
MSY611	<i>MATα his3Δ1 leu2Δ0 lys2Δ0 ura3Δ0 rgp1Δ::KanMX</i>
MSY646	<i>MATα his3Δ1 leu2Δ0 lys2Δ0 ura3Δ0 GYP6-3xHA::HIS3 BY4742.</i>
MSY647	<i>MATα his3Δ1 leu2Δ0 lys2Δ0 ura3Δ0 YEL048cΔ::KanMX GYP6-3xHA::HIS3</i>
MSY658	<i>MATα his3Δ1 leu2Δ0 lys2Δ0 ura3Δ0 ric1Δ::KanMX GYP6-3xHA::HIS3</i>
MSY659	<i>MATα his3Δ1 leu2Δ0 lys2Δ0 ura3Δ0 ypt6Δ::KanMX GYP6-3xHA::HIS3</i>
MSY660	<i>MATα his3Δ1 leu2Δ0 lys2Δ0 ura3Δ0 rgp1Δ::KanMX GYP6-3xHA::HIS3</i>
MSY677	<i>MATα his3Δ1 leu2Δ0 lys2Δ0 ura3Δ0 trs65Δ::KanMX GYP6-3xHA::HIS3</i>
MSY678	<i>MATα his3Δ1 leu2Δ0 lys2Δ0 ura3Δ0 trs85Δ::KanMX GYP6-3xHA::HIS3</i>
MSY679	<i>MATα his3Δ1 leu2Δ0 lys2Δ0 ura3Δ0 trs33Δ::KanMX GYP6-3xHA::HIS3</i>
MSY680	<i>MATα his3Δ1 leu2Δ0 lys2Δ0 ura3Δ0 vps51Δ::KanMX GYP6-3xHA::HIS3</i>
MSY771	<i>MATα his3Δ1 leu2Δ0 lys2Δ0 ura3Δ0 pRS315-GFP-YPT6</i>

MSY772 *MAT* α *his3* Δ 1 *leu2* Δ 0 *lys2* Δ 0 *ura3* Δ 0 *trs65* Δ ::*KanMX* *pRS315-GFP-YPT6*

MSY775 *MAT* α *his3* Δ 1 *leu2* Δ 0 *lys2* Δ 0 *ura3* Δ 0 *ric1* Δ ::*KanMX* *pRS315-GFP-YPT6*

MSY776 *MAT* α *his3* Δ 1 *leu2* Δ 0 *lys2* Δ 0 *ura3* Δ 0 *gyp6* Δ ::*KanMX* *pRS315-GFP-YPT6*

MSY777 *MAT* α *his3* Δ 1 *leu2* Δ 0 *lys2* Δ 0 *ura3* Δ 0 *pRS315-GFP-Ypt6* *pRS316-ADH1pr-SEC7-mRFP*

MSY778 *MAT* α *his3* Δ 1 *leu2* Δ 0 *lys2* Δ 0 *ura3* Δ 0 *trs65* Δ ::*KanMX* *pRS315-GFP-YPT6pRS316-ADH1pr-SEC7-mRFP*

MSY779 *MAT* α *his3* Δ 1 *leu2* Δ 0 *lys2* Δ 0 *ura3* Δ 0 *YEL048c* Δ ::*KanMX* *pRS315-GFP-YPT6pRS316-ADH1pr-SEC7-mRFP*

MSY781 *MAT* α *his3* Δ 1 *leu2* Δ 0 *lys2* Δ 0 *ura3* Δ 0 *ric1* Δ ::*KanMX* *pRS315-GFP-YPT6pRS316-ADH1pr-SEC7-mRFP*

MSY782 *MAT* α *his3* Δ 1 *leu2* Δ 0 *lys2* Δ 0 *ura3* Δ 0 *gyp6* Δ ::*KanMX* *pRS315-GFP-YPT6pRS316-ADH1pr-SEC7-mRFP*

MSY806 *MAT* α *his3* Δ 1 *leu2* Δ 0 *lys2* Δ 0 *ura3* Δ 0 *trs85* Δ ::*KanMX* *pRS315-GFP-YPT6pRS316-ADH1pr-SEC7-mRFP*

MSY786 *MAT* α *his3* Δ 1 *leu2* Δ 0 *lys2* Δ 0 *ura3* Δ 0 *pRS315-GFP-YPT6pRS306-ADH1pr-mRuby-SED5*

MSY787 *MAT* α *his3* Δ 1 *leu2* Δ 0 *lys2* Δ 0 *ura3* Δ 0 *trs65* Δ ::*KanMX* *pRS315-GFP-YPT6pRS306-ADH1pr-mRuby-SED5*

MSY790 *MAT* α *his3* Δ 1 *leu2* Δ 0 *lys2* Δ 0 *ura3* Δ 0 *gyp6* Δ ::*KanMX* *pRS315-GFP-YPT6pRS306-ADH1pr-mRuby-SED5*

MSY800 *MAT* α *his3* Δ 1 *leu2* Δ 0 *lys2* Δ 0 *ura3* Δ 0 *trs65* Δ ::*KanMX* *pRS315-GFP-YPT6pRS316-ADH1pr-SEC7-mRFP pRS313*

MSY801 *MAT* α *his3* Δ 1 *leu2* Δ 0 *lys2* Δ 0 *ura3* Δ 0 *trs65* Δ ::*KanMX* *pRS315-GFP-YPT6pRS316-ADH1pr-SEC7-mRFP pRS313-TRS65*

MSY366 *MAT* α , *trp1-901*, *leu2-3*, *112*, *ura3-52*, *his3-200*, *gal4* Δ , *gal80* Δ , *LYS2::GAL1_{UAS}-GAL1_{TATA}-HIS3*, *GAL2_{UAS}-GAL2_{TATA}-ADE2*, *URA3::MEL1_{UAS}-MEL1_{TATA}-lacZpGADT7-BET5*

MSY367 *MAT* α , *trp1-901*, *leu2-3*, *112*, *ura3-52*, *his3-200*, *gal4* Δ , *gal80* Δ , *LYS2::GAL1_{UAS}-GAL1_{TATA}-HIS3*, *GAL2_{UAS}-GAL2_{TATA}-ADE2*, *URA3::MEL1_{UAS}-MEL1_{TATA}-lacZpGADT7-TRS20*

MSY368 *MAT* α , *trp1-901*, *leu2-3*, *112*, *ura3-52*, *his3-200*, *gal4* Δ , *gal80* Δ , *LYS2::GAL1_{UAS}-GAL1_{TATA}-HIS3*, *GAL2_{UAS}-GAL2_{TATA}-ADE2*, *URA3::MEL1_{UAS}-MEL1_{TATA}-lacZpGADT7-BET3*

MSY369 *MAT* α , *trp1-901*, *leu2-3*, *112*, *ura3-52*, *his3-200*, *gal4* Δ , *gal80* Δ , *LYS2::GAL1_{UAS}-GAL1_{TATA}-HIS3*, *GAL2_{UAS}-GAL2_{TATA}-ADE2*, *URA3::MEL1_{UAS}-MEL1_{TATA}-lacZpGADT7-TRS23*

MSY370 *MAT* α , *trp1-901*, *leu2-3*, *112*, *ura3-52*, *his3-200*, *gal4* Δ , *gal80* Δ , *LYS2::GAL1_{UAS}-GAL1_{TATA}-HIS3*, *GAL2_{UAS}-GAL2_{TATA}-ADE2*, *URA3::MEL1_{UAS}-MEL1_{TATA}-lacZpGADT7-TRS31*

MSY371 *MAT* α , *trp1-901*, *leu2-3*, *112*, *ura3-52*, *his3-200*, *gal4* Δ , *gal80* Δ , *LYS2::GAL1_{UAS}-GAL1_{TATA}-HIS3*, *GAL2_{UAS}-GAL2_{TATA}-ADE2*, *URA3::MEL1_{UAS}-MEL1_{TATA}-lacZpGADT7-TRS33*

MSY372 *MAT* α , *trp1-901*, *leu2-3*, *112*, *ura3-52*, *his3-200*, *gal4* Δ , *gal80* Δ , *LYS2::GAL1_{UAS}-GAL1_{TATA}-HIS3*, *GAL2_{UAS}-GAL2_{TATA}-ADE2*, *URA3::MEL1_{UAS}-MEL1_{TATA}-lacZpGADT7-*

	<i>TRS65</i>
MSY373	<i>MATa, trp1-901, leu2-3, 112, ura3-52, his3-200, gal4Δ, gal80Δ, LYS2::GAL1_{UAS}-GAL1_{TATA}-HIS3, GAL2_{UAS}-GAL2_{TATA}-ADE2, URA3::MEL1_{UAS}-MEL1_{TATA}-lacZpGADT7-TRS85</i>
MSY374	<i>MATa, trp1-901, leu2-3, 112, ura3-52, his3-200, gal4Δ, gal80Δ, LYS2::GAL1_{UAS}-GAL1_{TATA}-HIS3, GAL2_{UAS}-GAL2_{TATA}-ADE2, URA3::MEL1_{UAS}-MEL1_{TATA}-lacZpGADT7-TRS120</i>
MSY375	<i>MATa, trp1-901, leu2-3, 112, ura3-52, his3-200, gal4Δ, gal80Δ, LYS2::GAL1_{UAS}-GAL1_{TATA}-HIS3, GAL2_{UAS}-GAL2_{TATA}-ADE2, URA3::MEL1_{UAS}-MEL1_{TATA}-lacZpGADT7-TRS130</i>
MSY376	<i>MATa, trp1-901, leu2-3, 112, ura3-52, his3-200, gal4Δ, gal80Δ, LYS2::GAL1_{UAS}-GAL1_{TATA}-HIS3, GAL2_{UAS}-GAL2_{TATA}-ADE2, URA3::MEL1_{UAS}-MEL1_{TATA}-lacZpGADT7-TCA17</i>
MSY377	<i>MATa, trp1-901, leu2-3, 112, ura3-52, his3-200, gal4Δ, gal80Δ, LYS2::GAL1_{UAS}-GAL1_{TATA}-HIS3, GAL2_{UAS}-GAL2_{TATA}-ADE2, URA3::MEL1_{UAS}-MEL1_{TATA}-lacZpGADT7</i>
MSY538	<i>MATα, ura3-52, his3-200, ade2-101, trp1-901, leu2-3, 112, met-, gal4D, gal80D, URA3::GAL1_{UAS}-GAL1_{TATA}-lacZ pGBKT7(gateway modified)-GYP6</i>

4.2.1 Strain construction

In wild type and mutant strains *GYP6* was tagged at the carboxy terminus with a hemagglutinin (HA) epitope by genomic insertion of a cassette amplified from pFA6a-3HA-His3MX6 (Longtine *et al.*, 1998). Insertion at the correct location was verified by PCR and Western blot.

4.2.2 Tandem affinity purification (TAP) and mass spectrometry

Yeast cells were grown to log phase in YPD medium and ~20g of cells were collected and flash frozen in liquid nitrogen and stored at -80°C. Pellets were resuspended in an equal volume of lysis buffer (6mM Na₂H₂PO₄/4mM NaH₂PO₄/1% CHAPS/100mM NaCl/2mM EDTA/1mM EGTA/50mM NaF/0.1mM Na₃VO₄/20mM β-mercaptoethanol/1mM PMSF/2mM benzamidine/leupeptin/pepstatin), lysed by bead beating (10s on and 10s off for a total of 10 times) and centrifuged at 21 000g for 25min in a JA25.50 rotor. The resulting supernatant was incubated with 300μL of a 50% slurry of IgG beads for 2 hours at 4°C while nutating. The lysate and bead mixture was transferred to a polyprep column and washed three times with 10mL of wash buffer (10mM Tris-HCl, pH 8.0/100mM NaCl/0.1% CHAPS/1mM DTT), one time with 10mL of TEV-C buffer (10mM Tris-HCl, pH 8.0/100mM NaCl/0.1% CHAPS/0.5mM EDTA/5% glycerol/1mM DTT) and

one time with 200 μ L of TEV-C buffer with 5 μ g/mL of recombinant TEV protease. Beads were then incubated with 1mL of TEV-C buffer with 5 μ g/mL of recombinant TEV protease and for 2h at 16°C while nutating. The eluate combined with two 1mL TEV-C buffer washes was transferred to a new polyprep column and the following was added: 6mL of CAM-B buffer (10mM Tris-HCl pH 8.0/100mM NaCl/0.1% CHAPS/1mM MgOAc₂/1mM imidazole/2mM CaCl₂/5% glycerol/10mM β -mercaptoethanol), 9 μ L of 1M CaCl₂, and 250 μ L of a 50% slurry of calmodulin beads. The mixture was nutated for 2h at 4°C and the beads were washed 3 times with 1.5mL of CAM-B buffer. The beads were incubated with 250 μ L of CAM-E buffer (10mM Tris-HCl pH 8.0/100mM NaCl/0.1% CHAPS/1mM MgOAc₂/1mM imidazole/10mM EGTA/5% glycerol) for 5 min and eluate was collected. A total of five fractions were collected, pooled and TCA precipitated. The total amount of precipitated protein was resuspended in sample buffer and loaded onto an SDS-PAGE gel. Peptides were extracted from gel slices and injected into an LTQ-Orbitrap Velos ETD mass spectrometer. Data was analyzed using SEAQUEST software.

4.2.3 Immunoprecipitations

Yeast strains were grown to log phase in YPD medium approximately 50 OD₆₀₀ units of cells were converted to spheroplasts in spheroplast buffer (1.4M sorbitol/50mM KPi/36mM β -mercaptoethanol/33 μ g/ml zymolyase) for 30 min at 37°C. Spheroplasts were washed with wash buffer (1.4M sorbitol/50mM KPi) and lysed in 1mL of lysis buffer (20mM HEPES, pH. 7.3/150mM NaCl/1mM DTT/2mM EDTA/1% triton/1xPIC) and lysates were cleared by centrifugation at 16000g for 15 min. Lysates were diluted to 1mg/mL and 500 μ L was incubated with or without 0.5 μ g of anti-HA (Sigma clone 7) antibody for 60 min on ice. Lysates were incubated with 20 μ L of a 50% slurry of protein-G beads while nutating at 4°C for 30 min. Beads were washed 2 times with 500 μ L of lysis buffer and eluted by boiling in 25 μ L of sample buffer for 3 minutes. Eluted proteins were separated on an SDS-PAGE gel and detected by Western blot analysis.

4.2.4 Serial dilutions

Yeast strains were inoculated into 3mL of minimal medium and grown in a shaker incubator overnight at 30°C. The OD₆₀₀ was normalized to the lowest value and 10-fold serial dilutions were spotted (2μL) onto minimal selective medium. Yeast were placed at the permissive temperature of 30°C to serve as a growth control and at the restrictive temperatures of 37°C.

4.2.5 Microscopy and Quantification of microscopy

Yeast strains were inoculated into 3mL of minimal medium and grown overnight at 30°C to log phase. Cells were pelleted and resuspended in fresh medium to an OD₆₀₀ of 10-15 and visualized on a Nikon Eclipse TiE inverted epifluorescence microscope using a 100x objective. Images were deconvoluted using AutoQuant X3 software and co-localization between punctae was manually quantified. All images were captured under the same microscope settings and the area of GFP-Ypt6p punctae was measured manually using the Freehand selection tool in ImageJ.

4.2.6 Yeast two hybrid

Genes were cloned into the yeast two hybrid vectors, pGADT7 or pGBKT7, and transformed into AH109 and Y187 yeast strains, respectively. Diploids were selected from matings between AH109 and Y187 strains carrying the appropriate genes on minimal medium not supplemented with leucine or tryptophan. Growth of diploids on medium not supplemented with histidine was used to indicate a positive or negative interaction.

4.2.7 Subcellular fractionation

Cells were grown to log phase overnight and approximately 50 OD₆₀₀ units of cells were spheroplasted (as above). Spheroplasts were resuspended in lysis buffer (50mM Tris-HCl, pH.7.4/200mM sorbitol/1mM EDTA/protease inhibitors), homogenized with a Dounce homogenizer (10 strokes) and lysates were centrifuged at 500g for 5 min. The resulting supernatant was centrifuged at 13 000g for 10 min to generate a pellet (P13) and supernatant (S13). S13 was then centrifuged at 100 000g for 60 min with a TLA100 rotor

to generate a pellet (P100) and a supernatant (S100). Pellets were resuspended in sample buffer and equivalent amounts of pellets and supernatants were loaded onto an SDS-PAGE gel and analyzed by Western blot.

4.3 Results

4.3.1 TRAPP_{II} interacts directly with Gyp6

TRAPP_{II} is a large complex with 10 unique subunits that likely interact with a variety of proteins. To identify what factors the TRAPP_{II} complex interacts with, native yeast TRAPP_{II} was purified from a haploid yeast strain whose endogenous copy of Trs120p was fused to a Tandem Affinity Purification (TAP) tag at the carboxy terminus and co-precipitating proteins were identified by mass spectrometry (Figure 4.1A). In addition to 7 of the 10 TRAPP_{II} subunits, peptides from many proteins were identified including several proteins involved in TRAPP_{II}-associated pathways including cell wall synthesis, endocytosis and exocytosis (Figure 4.1B, Table 4.3). Several of these proteins have been shown to interact either physically or genetically with TRAPP_{II} subunits. Notably, four of the seven COPI coat subunits co-purified with TRAPP_{II}, in support of previous studies showing an association between TRAPP_{II} and COPI vesicles (Cai *et al.*, 2005; Chen *et al.*, 2011). Three GAP proteins functioning in membrane trafficking pathways also co-purified with TRAPP_{II}: the Arf-GAPs Glo3p and Gcs1p, and the Ypt6p Rab-GAP, Gyp6p. Gyp6p has been previously shown to interact with the TRAPP_{II} complex in two independent studies using tandem-affinity purification followed by mass spectrometry, and we chose to characterize this interaction further (Ho *et al.*, 2002; Krogan *et al.*, 2006).

Proteins that co-purified with TRAPP_{II} are likely a combination of proteins interacting directly and indirectly with the complex. To determine whether Gyp6p is directly interacting with the complex, a yeast two-hybrid experiment between full length Gyp6p and all TRAPP_{II} subunits was conducted (Figure 4.1C). Gyp6p interacted solely with Trs130p, suggesting that Gyp6p does in fact interact directly with the TRAPP_{II} complex and it is via the TRAPP_{II} specific subunit, Trs130p.

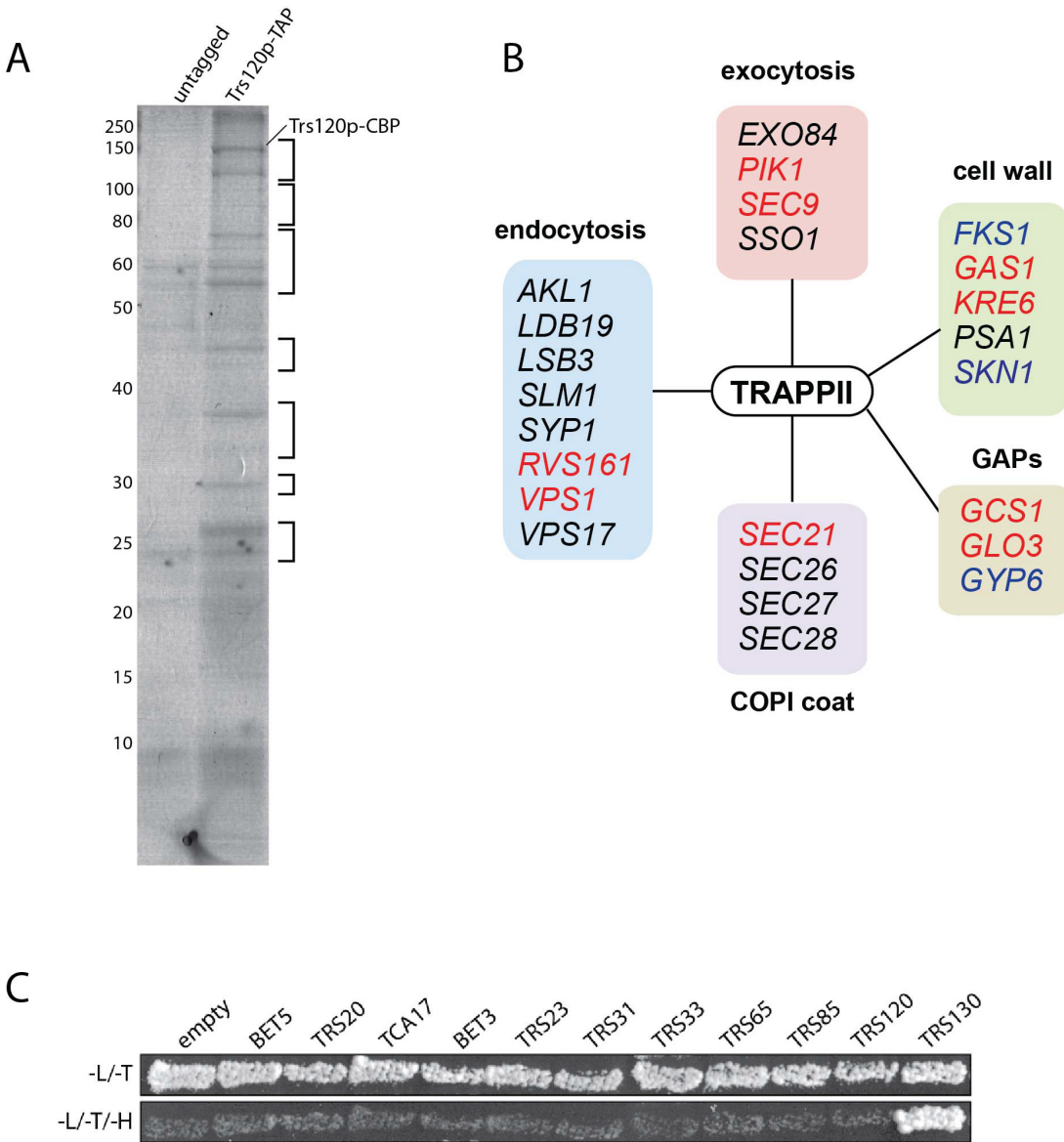


Figure 4.1 Gyp6p interacts with the TRAPP II complex through Trs130p. (A) Trs120p-TAP was purified from cells, separated on an SDS-PAGE gel and stained with blue silver. Peptides were extracted from sections of the stained gel (indicated by square brackets on the side) and analyzed by mass spectrometry. (B) Peptides from various proteins regulating different membrane trafficking pathways were identified as TRAPP II interactors by this method. Genes known to have synthetically lethal interactions with mutations in TRAPP II subunit genes are indicated in red. Proteins reported to physically interact with subunits of the TRAPP II complex are indicated in blue. (C) In a yeast two hybrid assay, Trs130p (fused to the DNA binding domain of Gal4p) is the only TRAPP subunit showing a positive interaction with Gyp6p (fused to the activation domain of Gal4p) indicated by growth on a plate lacking histidine (-H). L/-T = plates lacking leucine and tryptophan; L/-T/-H = plates lacking leucine, tryptophan and histidine.

Accession	Common name	# Peptides	# Unique peptides
YDR407C	<i>TRS120</i>	72	54
YMR218C	<i>TRS130</i>	52	31
YDR472W	<i>TRS31</i>	19	14
YDL055C	<i>PSA1</i>	14	9
YGR166W	<i>TRS65</i>	12	5
YCR009C	<i>RVS161</i>	11	5
YMR307W	<i>GAS1</i>	10	3
YBR059C	<i>AKL1</i>	9	1
YCR030C	<i>SYP1</i>	8	6
YDR238C	<i>SEC26</i>	7	2
YNL267W	<i>PIK1</i>	6	1
YPL232W	<i>SSO1</i>	6	1
YGR143W	<i>SKN1</i>	6	1
YER122C	<i>GLO3</i>	6	3
YKR068C	<i>BET3</i>	6	2
YGR009C	<i>SEC9</i>	5	3
YPR159W	<i>KRE6</i>	5	2
YGL137W	<i>SEC27</i>	5	2
YJL044C	<i>GYP6</i>	5	1
YLR342W	<i>FKS1</i>	4	1
YNL287W	<i>SEC21</i>	4	1
YDL226C	<i>GCS1</i>	4	1
YOR322C	<i>LDB19</i>	3	1
YFR024C-A	<i>LSB3</i>	3	1
YIL105C	<i>SLM1</i>	3	1
YKR001C	<i>VPS1</i>	3	1
YOR132W	<i>VPS17</i>	3	1
YBR102C	<i>EXO84</i>	3	1
YOR115C	<i>TRS33</i>	3	1
YDR246W	<i>TRS23</i>	2	1
YIL076W	<i>SEC28</i>	1	1

Table 4.3 (legend on next page)

Table 4.3 Summary of a subset of TRAPP II interactors by tandem affinity purification and mass spectrometry. Selected genes identified by mass spectrometry are listed in order of greatest # of peptides recovered to smallest and color coded according to their classification in Figure 4.1b (blue = endocytosis; pink = exocytosis; green = cell wall; olive-gray = GAPs; purple = COPI coat) TRAPP subunits recovered from the mass spectrometry analysis are colored in white.

4.3.2 *YPT6* and its GEF interact genetically with TRAPP II subunits

In high throughput screens several genetic interactions have been documented between *YPT6* pathway genes and TRAPP II subunits (Tong *et al.*, 2004; Costanzo *et al.*, 2010; Hoppins *et al.*, 2011). To examine how *YPT6* pathway genes genetically interact with essential and non-essential TRAPP II subunits, a high copy suppression screen was conducted (Figure 4.2). Included in this study were the *RIC1* and *RGP1* genes that encode the subunits of the heterodimeric Ypt6p GEF. TRAPP II subunits expressed in high copy plasmids were transformed into *ypt6Δ*, *ric1Δ* and *rgp1Δ* mutants that are unable to grow at 37°C. The core TRAPP subunit gene, *TRS31*, suppressed temperature sensitivity in all three mutants while another core subunit gene, *BET5*, suppressed the phenotype only in *rgp1Δ*. There was a much stronger phenotypic suppression by *TRS31* in *ric1Δ* and *rgp1Δ* mutants when compared to *ypt6Δ*, indicating that the requirement for active Ypt6p is being bypassed. Overexpression of *YPT1* permits the growth of *ypt6Δ* at restrictive temperatures and rescues trafficking defects associated with this mutant (Li and Warner, 1998; Ye *et al.*, 2014). The suppression of *ric1Δ* and *rgp1Δ* seen with *TRS31* overexpression and *rgp1Δ* with *BET5* overexpression may be indirect and mediated through *YPT1*. Interestingly, overexpression of the TRAPP II specific gene *TRS120* made all three strains very sick even at permissive temperature, with the strongest effect seen in *ric1Δ* and *rgp1Δ* mutants. Overexpression of *TRS33*, a gene important for TRAPP II stability, mirrored the effect of *TRS120*, but to a lesser extent. This effect is specific to the *YPT6* pathway, as overexpression of *TRS120* and *TRS33* had no effect on a wild type strain (data not shown) and the same constructs were able to suppress other mutant phenotypes (Scrivens *et al.*, 2009). Redundant pathways likely exist to compensate for the absence of Ypt6p and one possibility is that Trs120p interacts with proteins required for these redundant pathways and sequesters them when it is overexpressed (Li and Warner, 1998; Benjamin *et al.*, 2011).

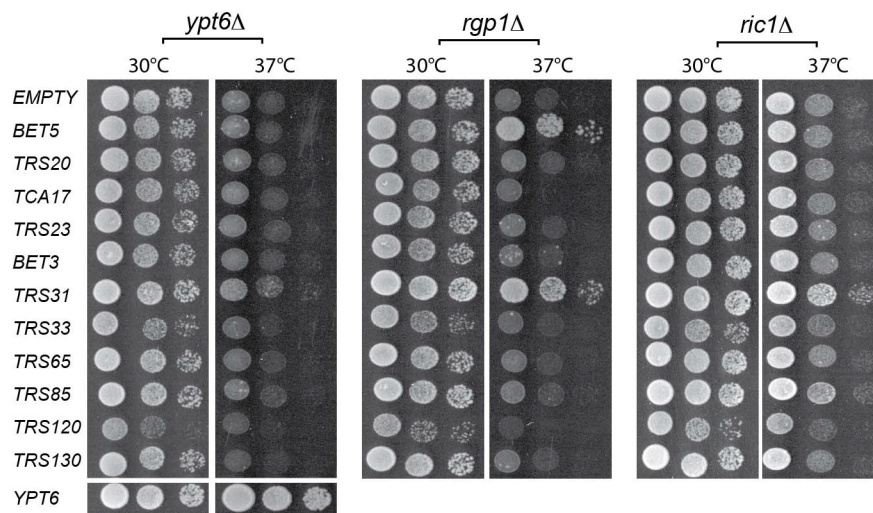


Figure 4.2 TRAPP subunits genetically interact with *YPT6* pathway genes. TRAPP subunits were overexpressed in *ypt6Δ*, *rgp1Δ* and *ric1Δ* strain backgrounds and serial dilutions were plated and grown at permissive (30°C) and restrictive (37°C) temperatures.

4.3.3 The integrity of TRAPP II is important for interacting with Gyp6

In order to continue characterizing the interaction between Gyp6p with TRAPP II, co-immunoprecipitation experiments were conducted in wild type and mutant yeast strains. Of the 10 TRAPP II subunits, Trs33p, Tca17p and Trs65p are non-essential and gel filtration experiments have shown that these subunits are important for complex assembly (Tokarev *et al.*, 2009; Choi *et al.*, 2011). To examine whether the assembly of the TRAPP II complex is important for its interaction with Gyp6p, the endogenous copy of *GYP6* was tagged at the carboxy terminus with a triple hemagglutinin (HA) tag and immunoprecipitated from cell lysates. Bet3p, a core TRAPP subunit, was detected by Western analysis to assay for the presence of TRAPP II (Figure 4.3). In wild type cells, TRAPP II co-precipitates with Gyp6p-HA, confirming Gyp6p as an interacting partner of the TRAPP II complex. This interaction is abrogated in lysates from *trs65Δ*, *tca17Δ* and *trs33Δ* mutants, indicating that proper assembly of the TRAPP II complex is important for its association with Gyp6p (Figure 4.3a). The deletion of *TRS33* and *TCA17* have been shown to destabilize the TRAPP II complex, while deletion of *TRS65* specifically interferes with TRAPP II dimerization and intact TRAPP II monomers can be purified from *trs65Δ* cells (Yip *et al.*, 2010). It is surprising that Gyp6p would not be able to associate with TRAPP II

monomers which contain one copy of Trs130p. It is possible that disrupting TRAPP II dimerization indirectly affects its association with Gyp6p. For example, dimerization may be important for TRAPP II localization to the site of Gyp6p interaction, or be required for upstream events. Deleting the TRAPP III-specific subunit *TRS85* has no effect on the amount of Bet3p co-precipitated with Gyp6p-HA (Figure 4.3A). A small percentage of Bet3p (<0.05%) co-precipitated with Gyp6p-HA despite a very efficient pull-down (not shown), suggesting that the interaction between TRAPP II and Gyp6p is transient, supported by the small number of peptides seen by mass spectrometry (Table 4.3).

Genetic interactions between TRAPP II and *YPT6* pathway genes suggest that the interaction between TRAPP II and Gyp6p may be important for regulating Ypt6p pathways. Gyp6p is a GAP for Ypt6p and to determine whether active Ypt6p must be present for TRAPP II to interact with Gyp6p, the same co-immunoprecipitation experiment was conducted in *ypt6Δ*, *ric1Δ* and *rgp1Δ* mutant strains. TRAPP II and Gyp6p interacted to the same degree in these mutants as wild type, indicating that Ypt6p, active or not, is not required for TRAPP II and Gyp6p to interact (Figure 4.3B). A possible interpretation of this result is that Gyp6p interacts with TRAPP II upstream of its association with Ypt6p.

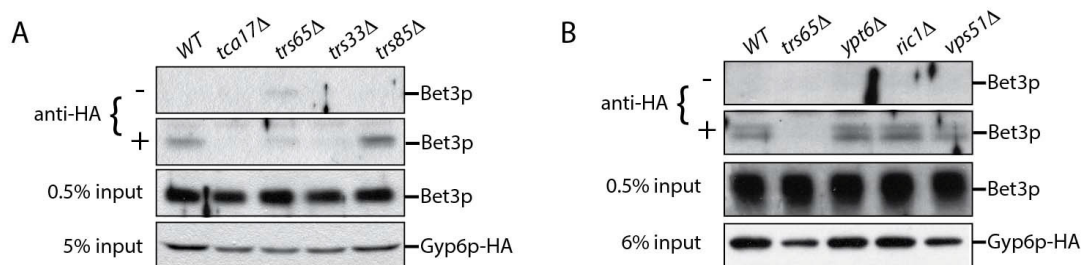


Figure 4.3 TRAPP II co-precipitates with endogenous Gyp6p-HA. (A) A small amount of TRAPP II (Bet3p is used as a marker) co-precipitates with Gyp6p-HA immunoprecipitated from yeast lysates. This interaction is disrupted in mutants (*tca17Δ*, *trs65Δ* and *trs33Δ*) that affect assembly of the TRAPP II but not the TRAPP III (*trs85Δ*) complex. (B) TRAPP II continues to interact with Gyp6p-HA when non-essential components of the Ypt6p pathway are absent. Co-immunoprecipitations were performed in strain backgrounds harboring deletions of either *YPT6*, *RIC1*, or *VPS51*, a Ypt6p-effector.

4.3.4 Ypt6p is enriched at the late Golgi in a *trs65*Δ mutant

Recent work showed that Gyp6p is a putative effector of Ypt32p and in a *gyp6*Δ mutant, Ypt6p remains at the late Golgi for a longer time and has increased co-localization with Ypt32p (Suda *et al.*, 2013). We speculated that TRAPP II is involved in a similar mechanism, and may also recruit Gyp6p to the late Golgi to promote Ypt6p inactivation and dissociation from this organelle. Wild type and mutant strains were transformed with 2 plasmids, one expressing GFP-Ypt6p (Ypt6p) and another expressing Sec7p-mRFP (Sec7p), a marker for the late Golgi. Ypt6p and Sec7p showed a punctate localization pattern, shown in representative fields for each strain (Figure 4.4A). The percentage of co-localized punctae was quantified and in wild type cells, 29% of Ypt6p co-localized with Sec7p (Figure 4.4B), which is consistent with a previous study (Kawamura *et al.*, 2014). Co-localization increased almost 3-fold to 79% in a *trs65*Δ mutant (Figure 4.4B). A less dramatic increase in co-localization was observed in the TRAPP II mutant *tca17*Δ (49%) and in a *gyp6*Δ mutant (61%) (Figure 4.4B). The absence of Trs85p, a TRAPP III-specific subunit, had no effect on co-localization (31%) (Figure 4.4B).

To confirm that the dramatic increase in localization of Ypt6p to the late Golgi observed in *trs65*Δ is caused by the deletion of *TRS65* we attempted to rescue this phenotype. A plasmid expressing the wild type copy of *TRS65* was transformed into the *trs65*Δ strain and co-localization between Ypt6p and Sec7p was quantified. When wild type *TRS65* was introduced into *trs65*Δ cells, the level of co-localization approached wild type levels (39%) suggesting that increased co-localization between Ypt6p and Sec7p was caused by the deletion of *TRS65* (Figure 4.4C).

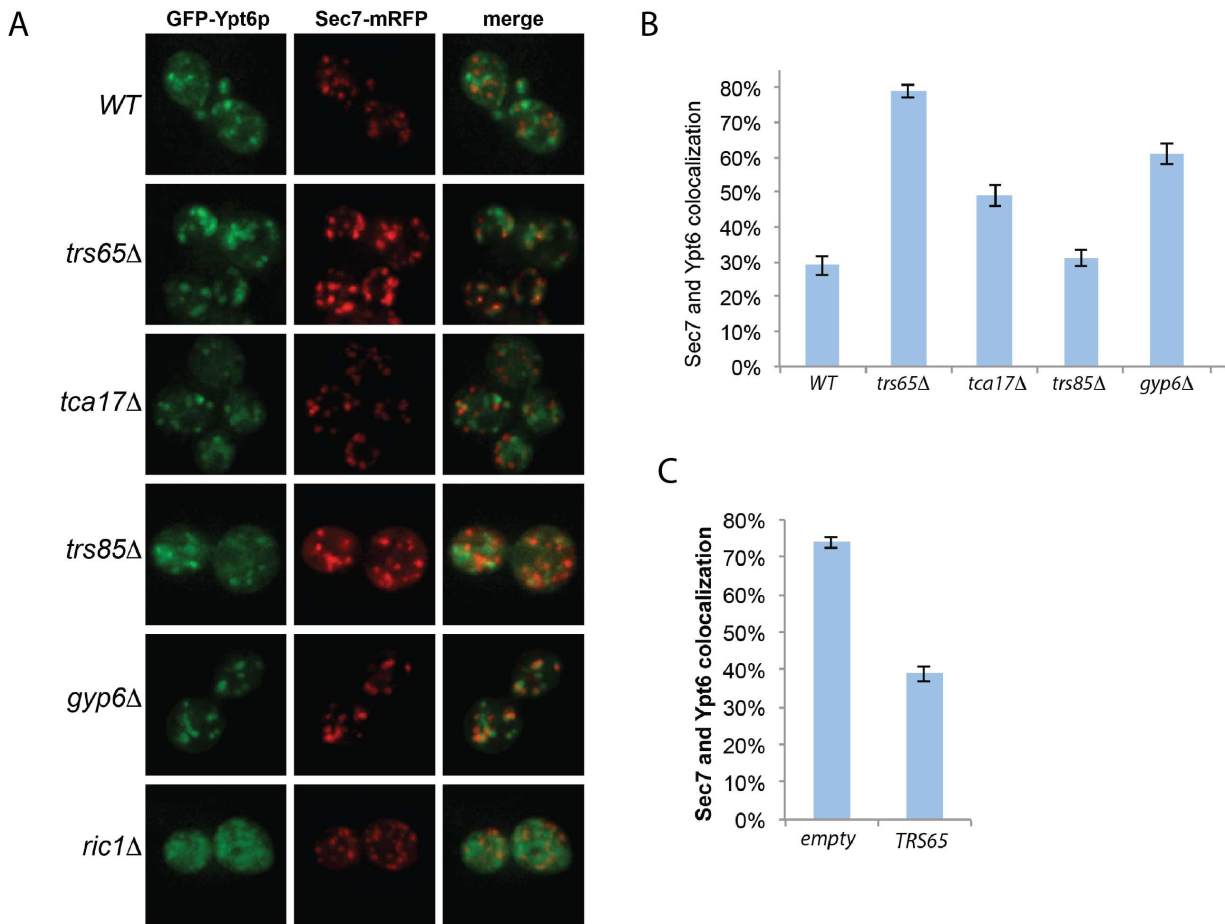


Figure 4.4 GFP-Ypt6p becomes enriched at the late Golgi in a *trs65*Δ mutant. (A) The localization of GFP-Ypt6p was examined in different strain backgrounds and compared to Sec7-mRFP localization, a late Golgi marker. A representative field of 1-2 cells is shown for each strain background. (B) The percentage of GFP-Ypt6p punctae co-localizing with Sec7-mRFP was quantified in each strain. (C) Co-localization of GFP-Ypt6p and Sec7-RFP was quantified in a *trs65*Δ strain transformed with either empty vector (*empty*) or wild type *TRS65*. (For (B) and (C), 56-96 cells, representing 10-15 fields with 3-10 cells each, was counted for each strain. Error bars represent standard error of the mean (SEM)).

Ypt6p localizes to both the early and late Golgi, making it plausible that a portion of the punctae not co-localizing with Sec7p represent early Golgi structures (Suda *et al.*, 2013; Kawamura *et al.*, 2014). To verify this, co-localization between Ypt6p and the early Golgi marker Sed5p was examined (Figure 4.5A). The opposite trend as Sec7p was observed as Ypt6p co-localized with Sed5p more often in wild type (54%) than *trs65*Δ (32%) and *gyp6*Δ (34%) cells (Figure 4.5B). These results, together with the co-localization data for Sec7p, suggest that the punctate localization of Ypt6p is caused by its association with Golgi

compartments, and de-stabilization of TRAPP II oligomers by the deletion of *TRS65* causes an enrichment of Ypt6p at the late Golgi.

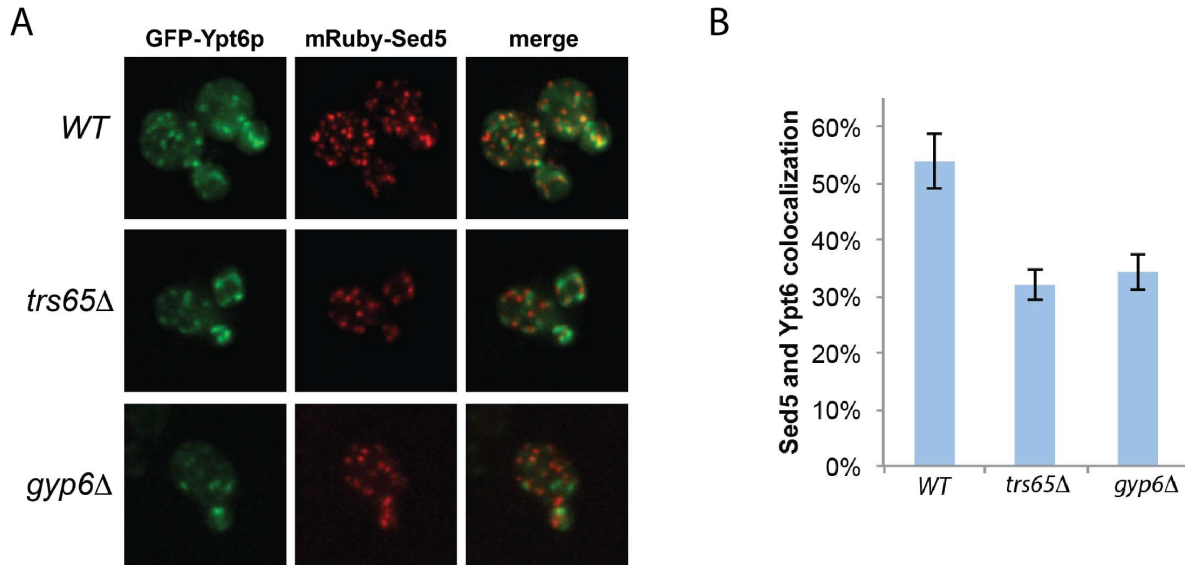


Figure 4.5 Co-localization of GFP-Ypt6p with the early Golgi is decreased in a *trs65Δ* and *gyp6Δ* mutant. (A) The localization of GFP-Ypt6p was examined in wild type (WT), *trs65Δ* and *gyp6Δ* cells and compared to mRuby-Sed5 localization, an early Golgi marker. A representative field of 1-2 cells is shown for each strain. (B) The percentage of GFP-Ypt6p punctae co-localizing with mRuby-Sed5p was quantified in each strain. (31-38 cells representing 5-6 fields of 3-10 cells, were counted for each strain). Error bars represent SEM.

4.3.5 The localization pattern of GFP-Ypt6p varies between wild type and mutant strains

In addition to differences in co-localization with Sec7p, Ypt6p punctae in *trs65Δ* and *gyp6Δ* mutants appear larger and more prominent when compared to wild type. Large variation was seen in the measured area for punctae but interestingly, 21% of punctae in both *trs65Δ* and *gyp6Δ* were larger than $0.5 \mu\text{m}^2$, whereas only 2% of wild type punctae met this criterion (Figure 4.6A). An increased frequency of larger punctae is consistent with an enrichment of Ypt6p to the late Golgi compartment relative to wild type.

Another more striking difference in the distribution of Ypt6p can be observed in *ric1Δ* cells, as GFP-Ypt6p is not punctate but is diffusely localized throughout the cell

(Figure 4.4A). The same phenotype was seen in *rgp1Δ* cells (data not shown). This diffuse localization suggests that Ypt6p is cytosolic but membrane fractionation showed no increase in the ratio of cytosolic to membrane-bound Ypt6p relative to wild type (Figure 4.6B). In the absence of its GEF, Ypt6p does not associate with punctate Golgi structures but does remain associated with membranes. The original study characterizing Ric1p/Rgp1p also observed this localization and hypothesized that inactive Ypt6p localizes to smaller membrane structures such as vesicles (Siniosoglou *et al.*, 2000).

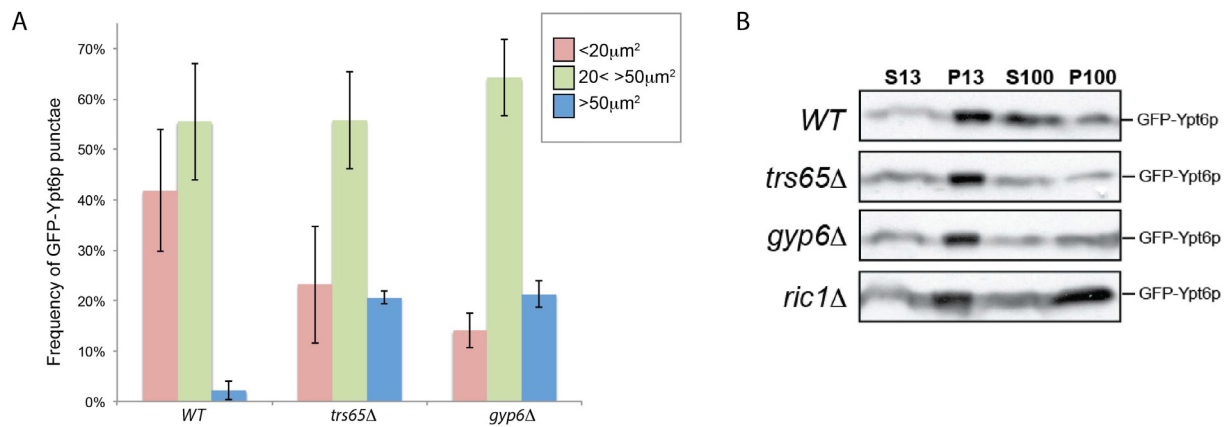


Figure 4.6 Higher frequencies of large punctae are seen in *trs65Δ* and *gyp6Δ* mutants. (A) The area of GFP-Ypt6p punctae was measured with ImageJ, divided into three categories (<0.2 μm², 0.2-0.5 μm² or >0.5 μm²) and the frequency of each category was plotted for *WT*, *trs65Δ* and *gyp6Δ* strains. Between 107 and 154 punctae were counted for two experiments. Error bars represent SEM. (B) Subcellular membrane fractionation was performed in *WT* and mutant strains and GFP-Ypt6p was probed for in each fraction.

4.4 Discussion

Ypt6p is a non-essential Rab protein that has been implicated in several trafficking pathways in both yeast and higher eukaryotes. This study has shown that the TRAPP II complex interacts directly with the Ypt6p GAP Gyp6p, and when this interaction is disrupted *in vivo*, Ypt6p becomes enriched on late Golgi compartments. Several studies have examined the subcellular localization of Ypt6p by microscopy and have found that it localizes to the early/medial/late Golgi compartments, COPI vesicles and late endosomes (Suda *et al.*, 2013; Kawamura *et al.*, 2014). The level of early Golgi localization and late Golgi localization reported varies from ~50 – 80% and ~30% -50%, respectively. The

results in this study fall within this range: in wild type cells Ypt6p punctae localized to the early and late Golgi with a frequency of 54% and 29%, respectively. Ypt6p appears to reside in more than one subcellular compartment, consistent with it regulating several trafficking pathways.

Gyp6p recruitment to different organelles by various protein factors could be a mechanism to promote the exit of Ypt6p from a specific compartment and maintain its homeostatic distribution throughout the cell. In this case, preventing the recruitment of Gyp6p would skew the localization of Ypt6p towards one compartment at the expense of another. This does indeed occur in the TRAPPII mutant *trs65Δ*, as Ypt6p co-localization with the early Golgi is reduced, while it is enriched more than 2-fold at the late Golgi. A similar pattern of re-distribution was observed in a *gyp6Δ* mutant, suggesting that the change in Ypt6p localization in *trs65Δ* is the result of TRAPPII no longer efficiently recruiting Gyp6p to the late Golgi.

The inactivation of Rabs is associated with a non-membrane-bound, cytosolic state, but in the absence of its GEF, the ratio of membrane bound to cytosolic Ypt6p does not change. However, there is a striking difference in Ypt6p localization in *ric1Δ* and *rgp1Δ* mutants compared to wild type. It was recently shown that Ypt6p, Ypt7p and Vps21p re-localize to the ER in the absence of their GEFs, suggesting that GEFs are required for localization to the correct organelle, and not necessarily required for association with membranes (Cabrera and Ungermann, 2013). It is likely that several factors coordinate the spatial and temporal localization of Ypt6p by ensuring that its modifying proteins are also correctly localized.

In addition to the TRAPPII complex (this study), Ypt32p has also been shown to interact with Gyp6p and recruit it to the late Golgi, and the Na⁺/H⁺ exchanger Nhx1p interacts with Gyp6p on late endosomes (Ali *et al.*, 2004; Suda *et al.*, 2013). In both cases, this association was proposed to be important for the regulation of Ypt6p. It is interesting that both TRAPPII and Ypt32p interact with Gyp6p, as TRAPPII is a putative Ypt32p GEF

and has been shown to act upstream of the Rab in autophagy and post Golgi trafficking pathways (Sciorra *et al.*, 2005; Tokarev *et al.*, 2009; Zou *et al.*, 2013). Ypt6p, TRAPPII, and Ypt31p/32p have all been shown to be important for trafficking of the exocytic SNARE Snc1p through the endocytic pathway (Lafourcade *et al.*, 2003; Cai *et al.*, 2005; Chen and Tokarev, 2005). Interestingly, the overexpression of *TRS120* and *TRS33* significantly reduce the viability of *ric1Δ* and *rgp1Δ*, and to a lesser extent *ypt6Δ* cells (this study). Both subunits are important for the function of TRAPPII in endocytic recycling suggesting that both TRAPPII and Ypt32p may interact with Gyp6p to regulate this pathway (Cai *et al.*, 2005; Montpetit and Conibear, 2009). A Rab GAP cascade has already been proposed between Ypt32p and Gyp6p to regulate a not yet specified membrane trafficking pathway (Suda *et al.*, 2013). The double recruitment of Gyp6p by TRAPPII and Ypt32p could act as a positive feedback loop, whereby TRAPPII acts to both recruit Gyp6p directly and indirectly through the activation of Ypt32p. It also remains possible that TRAPPII and Ypt32p interact with Gyp6p to regulate Ypt6p in distinct trafficking pathways that intersect with the late Golgi compartment.

In future experiments, the localization of Ypt6p should be examined in a strain with mutations in both *YPT31/32* and TRAPPII to determine whether there is an additive effect and assess whether they are recruiting Gyp6p within the same pathway. Alternatively, co-localization of Ypt6p with additional markers could be examined. Ypt31p/32p are enriched on secretory vesicles and late Golgi compartments in the bud and bud neck of dividing yeast cells, whereas TRAPPII is associated with Sec7-positive membranes distributed more broadly throughout the cell. Examining co-localization with late secretory pathway markers such as Ypt31p and Sec4p could clarify whether TRAPPII regulates Ypt6p earlier in the secretory pathway than Ypt31/32p.

Chapter 5: Discussion

This thesis provides novel information about the structure of the yeast TRAPP complexes and the contribution of specific subunits, Trs20p and Trs23p in particular, to that structure. This work also provides insight into how a specific mutation in *TRAPPC2* leads to the skeletal disorder SEDT through destabilization of the TRAPPIII complex. Finally, the interaction between TRAPP II and a GAP protein was shown to be important for the regulation of its cognate Rab, and may represent a novel mechanism for how TRAPP coordinates membrane trafficking pathways.

5.1 Distinct TRAPP complexes can be resolved biochemically and functionally

5.1.1 Resolution of the yeast TRAPP complexes is dependent upon lysis conditions

At the onset of this thesis work, the TRAPP complex had been extensively characterized in yeast and two complexes were believed to exist, TRAPPI or the core complex, and a larger TRAPP II complex. A third yeast TRAPP complex, TRAPPIII, was discovered through functional studies and employing a different matrix for gel filtration chromatography (Lynch-Day *et al.*, 2010; Choi *et al.*, 2011). Work in Chapter 3 of this thesis showed that under less stringent lysis conditions (150mM NaCl) TRAPP II and TRAPPIII were not resolved by gel filtration chromatography raising the possibility that TRAPP II/III complexes are part of the same complex and dissociate under more stringent (300mM NaCl) lysis conditions. However the TRAPP II subunit Trs130p and TRAPPIII subunit Trs85p failed to co-precipitate under less stringent lysis conditions, even in the presence of a cross linker, supporting the conclusion that TRAPP II and III are indeed separate complexes with distinct roles in membrane trafficking. A similar combination of experiments showed that equivalent TRAPP II and TRAPPIII complexes also exist in mammalian cells and are distinct complexes carrying out independent functions (Bassik *et al.*, 2013).

Although all subunits from yeast TRAPPI have mammalian homologues, a smaller mammalian TRAPPI complex has not been observed nor reconstituted *in vitro*. Intriguingly, like yeast TRAPP II and III, yeast TRAPPI cannot be resolved by size exclusion

chromatography under less stringent lysis conditions, raising the possibility that it is not a separate complex *in vivo*, but an artifact of lysis. A challenging aspect of this question is that TRAPPI has no unique subunits with respect to TRAPPII and III, making affinity purification experiments not useful in determining whether TRAPPI is a complete complex and not a fragment of TRAPPII or TRAPPIII. Interestingly, when a *Saccharomyces cerevisiae* specific (SMS) domain of the central TRAPPI subunit Trs23p is deleted the TRAPPI complex does not assemble *in vitro* and a peak for TRAPPI is shifted to a much smaller molecular size when yeast lysates are fractionated by size exclusion chromatography (Chapter 3). Importantly, essential functions attributed to the TRAPPI complex in yeast are not compromised in this mutant, suggesting that these functions can be performed by TRAPPII or TRAPPIII. Non-lethal mutations have also been discovered that disrupt the integrity of TRAPPII and TRAPPIII complexes but unlike deletion of the SMS domain, they also compromise the function of these complexes to varying degrees (Montpetit and Conibear, 2009; Choi *et al.*, 2011; Brunet *et al.*, 2013; Taussig *et al.*, 2013). The appearance of an intact TRAPPI complex may be an artifact of lysis: the SMS domain of Trs23p may stabilize the TRAPP core, allowing it to dissociate as an intact unit when yeast cells are lysed whereas the TRAPP core would fall apart in the absence of this domain, such as in mammalian cells (Figure 5.1). Alternatively, TRAPPI in the SMS mutant may be intact *in vivo* and only become destabilized upon cell lysis. Perhaps only trace amounts of intact TRAPPI are adequate for it to satisfy its role within the cell. The possibility that TRAPPI could be an artifact of lysis should be considered when interpreting data from future experiments.

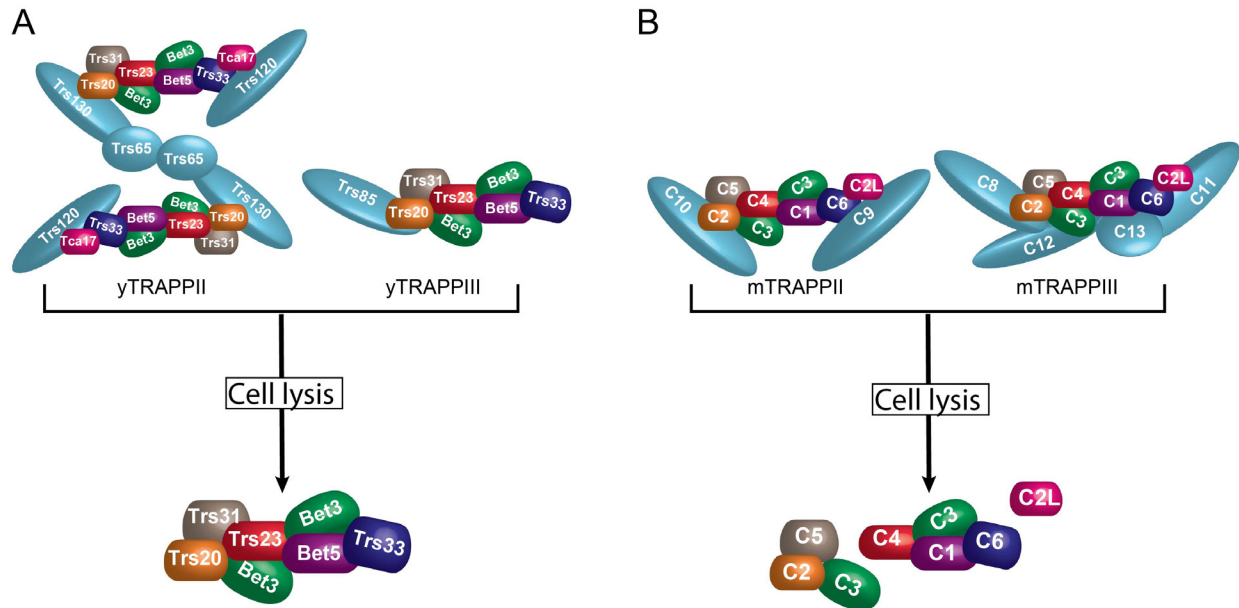


Figure 5.1 The SMS domain of Trs23p stabilizes the TRAPP core in yeast. (A) The appearance of a yeast TRAPP I complex when lysates are separated by size exclusion chromatography may be caused by the TRAPP core being released from the two larger complexes. (B) The mammalian homologue of Trs23p, TRAPPC4, lacks the SMS domain. When mammalian cells are lysed the TRAPP core would not dissociate as an intact fragment.

5.1.2 TRAPP III mediates the tethering of Atg9p vesicles in non-selective and selective autophagy pathways

Evidence presented in Chapter 2 further distinguishes TRAPP II and TRAPP III as two separate complexes and provides insight into how TRAPP III associates with membranes functioning in autophagy. Size exclusion chromatography and sucrose density gradient experiments demonstrated that TRAPP III, but not TRAPP II, remained associated with membranes under equivalent lysis conditions. Furthermore when cells were starved, the association of TRAPP III with membranes was dependent on the presence of Atg9p, a transmembrane protein essential for formation of the PAS. This result suggests that Atg9p mediates the recruitment of TRAPP III to membranes and is consistent with another study showing that the TRAPP III specific subunit, Trs85p, interacts directly with Atg9p and localizes to Atg9p-containing membranes (Kakuta *et al.*, 2012).

Atg17p is a scaffolding protein that is essential for non-selective autophagy and in one report was shown to be required for the localization of TRAPPIII to the PAS under starvation conditions (Wang *et al.*, 2013). The recruitment of TRAPPIII to Atg9p vesicles, and recruitment of TRAPPIII to the PAS by Atg17p is a potential mechanism for TRAPPIII mediated tethering at the PAS (Figure 5.2). PAS-localized Ypt1p can recruit the Atg1p kinase as an effector following Ypt1p activation by TRAPPIII and Atg1p in turn will recruit downstream factors required for the non-selective autophagy pathway (Figure 5.2).

Non-selective autophagy is not completely blocked in a *trs85Δ* mutant suggesting that alternative pathways are functioning alongside TRAPPIII. Atg17p, Atg31p and Atg29p form a crescent shaped complex that interacts directly with the Atg1p kinase and its dimerization is proposed to mediate the homotypic tethering of Atg9p vesicles to form the PAS and autophagosomes (Ragusa *et al.*, 2012). The recruitment of TRAPPIII and Atg1p by Atg17p and activated Ypt1p, respectively, could be a way to reinforce this pathway while not being essential for it to occur. Consistent with this hypothesis, the Atg17p-Atg31p-Atg29p complex is not active in selective autophagy, a process for which the TRAPPIII complex is absolutely required (Ragusa *et al.*, 2012).

Similar to Atg1p, the scaffold protein Atg11p which is required for selective autophagy, has been identified as a Ypt1p effector (Lipatova *et al.*, 2012). Upon activation of Ypt1p by TRAPPIII at the PAS, Atg11p is brought to the PAS and can recruit downstream factors required for the selective autophagy pathway (Figure 5.2). However in nutrient rich conditions TRAPPIII remains associated with membranes in the absence of Atg9p suggesting that a factor(s) other than Atg9p links TRAPPIII to membranes in normal growth conditions (Chapter 5.2). Furthermore, in nutrient rich conditions TRAPPIII still localizes to the PAS but an upstream recruitment factor analogous to Atg17p has not yet been identified (Figure 5.2). Future experiments should focus on identifying what factors are required for recruiting TRAPPIII to membranes and to the PAS.

non-selective macroautophagy

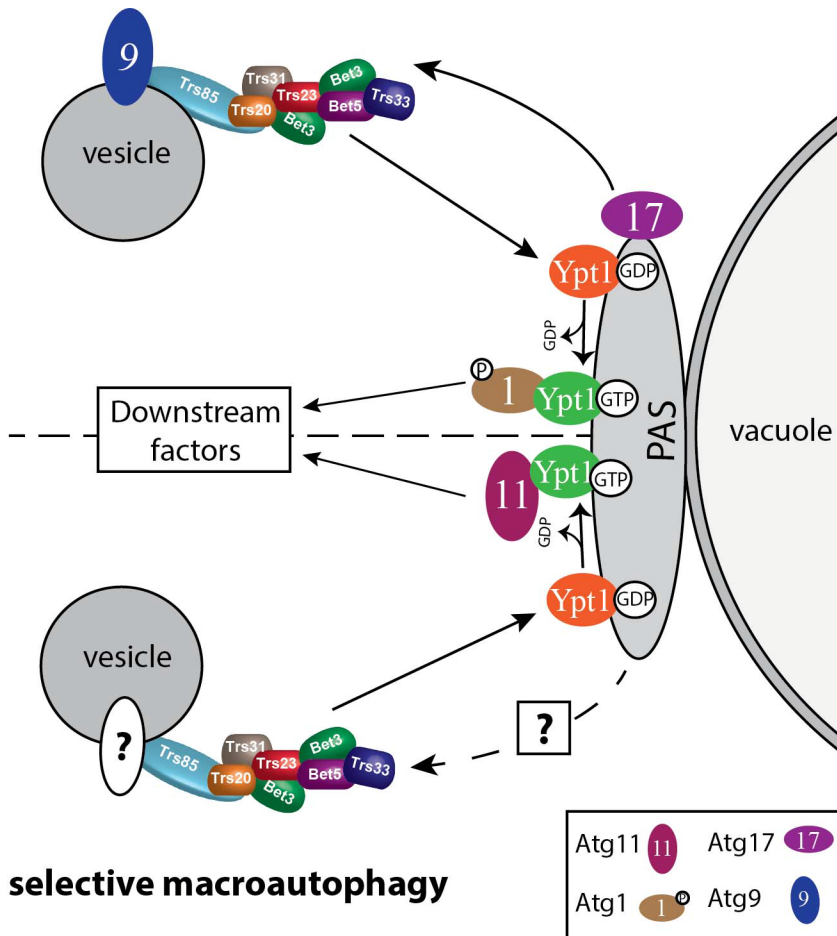


Figure 5.2 Ypt1p recruits effectors specific to non-selective and selective autophagy pathways. TRAPPIII is associated with Atg9p vesicles destined for the PAS. During non-selective autophagy its association with membranes is mediated by Atg9p and is recruited to the PAS by Atg17p. The factors mediating the association of TRAPPIII with membranes and its recruitment to the PAS as part of the selective autophagy pathway have not been identified. In both pathways, TRAPPIII activates Ypt1p at the PAS leading to the recruitment of Atg1p and Atg11p as Ypt1p effectors, during non-selective and selective autophagy respectively.

5.1.3 Bet3p palmitoylation is important for TRAPPIII function

Although Bet3p and its mammalian homologue TrappC3 have been shown to be palmitoylated on a highly conserved residue, this modification is not essential and its purpose was not known. Results in Chapter 2 showed that palmitoylated Bet3p is enriched in the yeast TRAPPIII complex and that this modification is important for the function of TRAPPIII in autophagy. In the absence of this modification autophagy is delayed but not

completely blocked. Bet3p palmitoylation can increase the efficiency of TRAPPIII by several possible mechanisms: (i) it could induce structural changes in the TRAPPIII complex; (ii) it could facilitate interactions with other proteins or aid in recruiting the complex to membrane subdomains. Further experiments are needed to distinguish between these possibilities. It would also be interesting to examine whether palmitoylated TrappC3 is also enriched in mammalian TRAPPIII and whether blocking this modification affects autophagy pathways in mammalian cells. The importance of palmitoylation in other trafficking processes regulated by TRAPPIII should also be examined such as endosomal trafficking in yeast and in ER-Golgi transport in mammals.

5.1.4 A mutation that causes SEDT in humans prevents the association of Trs85p with the TRAPP core in yeast

The understanding that TRAPPII and TRAPPIII are two distinct complexes in yeast was necessary for the work carried out in Chapter 2 where evidence was presented that a mutation in the core subunit, Trs20p, disrupts the assembly of TRAPPIII without impacting the stability of TRAPPII or TRAPPI. The equivalent mutation in humans has been implicated in the skeletal disorder SEDT, providing insight into the etiology of this disease. In yeast, this mutation disrupted the interaction of Trs20p with TRAPPIII and TRAPPII specific subunits but only the integrity of TRAPPIII was compromised in yeast lysates (Chapter 2). Furthermore, cells with this mutation were defective in functions associated with the TRAPPIII complex, including endosomal recycling and autophagy, but did not show any phenotypes previously observed for TRAPPI or TRAPPII mutants. These observations in yeast suggest that the analogous disease-causing mutation in humans may also disrupt TRAPPIII function. Furthermore, a defect in collagen secretion was observed upon the depletion of both *TRAPPC2* and the core subunit *TRAPPC3*, suggesting that TrappC2 regulates collagen export in the context of a TRAPP complex (Venditti *et al.*, 2012). Four complex-specific subunits are present in mammalian TRAPPIII and TRAPPII complexes. Measuring how the depletion of each of these subunits affects collagen secretion could determine whether TrappC2 regulates collagen secretion in the context of either of these complexes.

5.2 TRAPP regulates membrane trafficking pathways by interacting with GTPases and their modifying proteins

The TRAPP core is a GEF for Ypt1p and this activity is required for TRAPP-mediated membrane trafficking pathways. TRAPP complexes have also been shown to interact with other GTPases and their modifier proteins. In human cells, TrappC2 mediates collagen secretion by interacting directly with Sar1, a GTPase that is required for COPII vesicle formation (Venditti *et al.*, 2012). In yeast, the TRAPP II specific subunit Trs65p interacts directly with Gea2p, an Arf1p GEF (Chen *et al.*, 2011). In Chapter 4 I presented evidence that the TRAPP II complex recruits the RabGAP protein Gyp6p to promote Ypt6p dissociation from the late Golgi. Proteins that interact with GTPases are typically classified as GEFs, GAPs or effectors but a separate category of proteins could be responsible for mediating the interaction between GTPases and their modifier proteins. It is not clear whether the interaction of TRAPP with these proteins directly alters their enzymatic activity, and reconstituted *in vitro* experiments would have to be performed to address this possibility. The interaction of TRAPP with these proteins could serve to facilitate the interaction of GTPases with their modifier proteins and vice versa. In the case of Gyp6p, its interaction with TRAPP II seems to be important for recruiting this GAP to a specific compartment (Chapter 4).

Aside from Gyp6p, two additional GAPs, Glo3p and Gcs1p, were identified as potential TRAPP II interactors by pull downs and mass spectrometry (Chapter 4). Glo3p and Gcs1p are ArfGAPs for Arf1p, a GTPase required for the formation of retrograde COPI vesicles (Poon *et al.*, 1996, 1999). Although they have overlapping functions, Glo3p is primarily associated with Golgi-ER transport, while Gcs1p also regulates post Golgi trafficking by acting on the Arf-like GTPase Arl1p (Poon *et al.*, 1999; Robinson and Poon, 2006). In future experiments, it will be important to determine whether TRAPP II interacts directly with these GAP proteins and if so, whether this interaction impacts the dynamics of Arf1p. TRAPP II may regulate membrane trafficking pathways by acting as a GEF for Ypt1p and Ypt31/32p as well as by coordinating the association between Rabs and their modifying proteins. RabGAP and RabGEF cascades have been proposed to mediate the

sequential inactivation and activation of Rabs in membrane trafficking pathways. Additional factors such as MTCs may be necessary to bridge specific RabGAP and RabGEF pairs in these cascades as well as other classes of GTPases, such as Arfs, and their modifying proteins. The requirement for additional factors could provide another layer of regulation to oversee the activation and inactivation of these molecular switches.

5.3 Conclusions and future directions:

In recent years a considerable amount of information has been gathered concerning the structure of TRAPP in yeast and mammals. Three separate yeast complexes have been described which can be separated both physically and functionally, and for each the EM structure has been solved. There is also strong evidence that two distinct TRAPP complexes exist in mammals and their subunit composition is known. Future work should focus on mechanistic studies to gain a better understanding of how the distinct subunit composition and structure of each complex contributes to its function in different membrane trafficking pathways. For example, in yeast the TRAPP II complex forms a dimer but the purpose for this oligomerized state is not yet clear. Furthermore, an interaction between TRAPP II and the COPI coat has been demonstrated but it remains to be seen whether this association is required for the physical tethering of these vesicles.

As in yeast, mammalian TRAPP II and TRAPP III have recently been distinguished as two separate complexes. It will be important to study how these complexes are differentially involved in membrane trafficking processes such as selective and non-selective autophagy, endosomal recycling, and collagen secretion. This thesis work has contributed to further our structural and functional understanding of the yeast TRAPP complexes, which serves as a basis to study how these complexes regulate membrane trafficking pathways in higher eukaryotes such as humans.

Chapter 6: References

- Albert, S., and Gallwitz, D. (1999). Two New Members of a Family of Ypt/Rab GTPase Activating Proteins: Promiscuity of substrate recognition. *J. Biol. Chem.* *274*, 33186–33189.
- Ali, R., Brett, C. L., Mukherjee, S., and Rao, R. (2004). Inhibition of sodium/proton exchange by a Rab-GTPase-activating protein regulates endosomal traffic in yeast. *J. Biol. Chem.* *279*, 4498–4506.
- Angers, C. G., and Merz, A. J. (2011). New links between vesicle coats and Rab-mediated vesicle targeting. *Semin. Cell Dev. Biol.* *22*, 18–26.
- Aridor, M., and Hannan, L. A. (2000). Traffic jam: a compendium of human diseases that affect intracellular transport processes. *Traffic* *1*, 836–851.
- Aridor, M., and Hannan, L. A. (2002). Traffic jams II: an update of diseases of intracellular transport. *Traffic* *3*, 781–790.
- Baba, M., Osumi, M., Scott, S. V., Klionsky, D. J., and Ohsumi, Y. (1997). Two distinct pathways for targeting proteins from the cytoplasm to the vacuole/lysosome. *J. Cell Biol.* *139*, 1687–1695.
- Baba, M., Takeshige, K., Baba, N., and Ohsumi, Y. (1994). Ultrastructural analysis of the autophagic process in yeast: detection of autophagosomes and their characterization. *J. Cell Biol.* *124*, 903–913.
- Bacon, R. A., Salminen, A., Ruohola, H., Novick, P., and Ferro-Novick, S. (1989). The GTP-binding protein Ypt1 is required for transport in vitro: the Golgi apparatus is defective in ypt1 mutants. *J. Cell Biol.* *109*, 1015–1022.
- Baggett, J., and Wendland, B. (2001). Clathrin function in yeast endocytosis. *Traffic* *2*, 297–302.
- Balch, W., McCaffery, J., Plutner, H., and Farquhar, M. (1994). Vesicular stomatitis virus glycoprotein is sorted and concentrated during export from the endoplasmic reticulum. *Cell* *76*, 641–652.
- Barlowe, C. (1997). Coupled ER to Golgi transport reconstituted with purified cytosolic proteins. *J. Cell Biol.* *139*, 1097–1108.
- Barlowe, C. K., and Miller, E. a (2013). Secretory protein biogenesis and traffic in the early secretory pathway. *Genetics* *193*, 383–410.

Barlowe, C., Orci, L., Yeung, T., Hosobuchi, M., Hamamoto, S., Salama, N., Rexach, M. F., Ravazzola, M., Amherdt, M., and Schekman, R. (1994). COPII: a membrane coat formed by Sec proteins that drive vesicle budding from the endoplasmic reticulum. *Cell* 77, 895–907.

Barr, F. (2013). Review series: Rab GTPases and membrane identity: causal or inconsequential? *J. Cell Biol.* 202, 191–199.

Barr, F., and Lambright, D. G. (2010). Rab GEFs and GAPs. *Curr. Opin. Cell Biol.* 22, 461–470.

Barrowman, J., Bhandari, D., Reinisch, K., and Ferro-Novick, S. (2010). TRAPP complexes in membrane traffic: convergence through a common Rab. *Nat. Rev. Mol. Cell Biol.* 11, 759–763.

Barrowman, J., Sacher, M., and Ferro-Novick, S. (2000). TRAPP stably associates with the Golgi and is required for vesicle docking. *EMBO J.* 19, 862–869.

Bassik, M., Kampmann, M., Lebbink, R., Wang, S. C., Hein, M., Poser, I., Weibezahn, J., and Horlbeck (2013). A systematic mammalian genetic interaction map reveals pathways underlying ricin susceptibility. *Cell* 152, 909–922.

Behrends, C., Sowa, M. E., Gygi, S. P., and Harper, J. W. (2010). Network organization of the human autophagy system. *Nature* 466, 68–76.

Ben-Aroya, S., Coombes, C., Kwok, T., O'Donnell, K. A., Boeke, J. D., and Hieter, P. (2008). Toward a comprehensive temperature-sensitive mutant repository of the essential genes of *Saccharomyces cerevisiae*. *Mol. Cell* 30, 248–258.

Benjamin, J. J. R., Poon, P. P., Drysdale, J. D., Wang, X., Singer, R. a, and Johnston, G. C. (2011). Dysregulated Arl1, a regulator of post-Golgi vesicle tethering, can inhibit endosomal transport and cell proliferation in yeast. *Mol. Biol. Cell* 22, 2337–2347.

Bensen, E. S., Yeung, B. G., and Payne, G. S. (2001). Ric1p and the Ypt6p GTPase function in a common pathway required for localization of trans-Golgi network membrane proteins. *Mol. Biol. Cell* 12, 13–26.

Boehm, M., Aguilar, R. C., and Bonifacino, J. S. (2001). Functional and physical interactions of the adaptor protein complex AP-4 with ADP-ribosylation factors (ARFs). *EMBO J.* 20, 6265–6276.

Bonifacino, J. S., and Glick, B. S. (2004). The mechanisms of vesicle budding and fusion. *Cell* 116, 153–166.

Bos, J., Rehmann, H., and Wittinghofer, A. (2007). GEFs and GAPs : Critical Elements in the Control of Small G Proteins. *Cell* 129, 865–877.

- Bourne, H., Sanders, D., and McCormick, F. (1990). The GTPase superfamily- a conserved switch for diverse cell functions. *Nature* *342*, 125-132.
- Boyd, C., Hughes, T., Pypaert, M., and Novick, P. (2004). Vesicles carry most exocyst subunits to exocytic sites marked by the remaining two subunits, Sec3p and Exo70p. *J.Cell Biol.* *167*, 889–901.
- Brodsky, F. M., Chen, C. Y., Knuehl, C., Towler, M. C., and Wakeham, D. E. (2001). Biological basket weaving: formation and function of clathrin-coated vesicles. *Annu. Rev. Cell Dev. Biol.* *17*, 517–568.
- Brunet, S., Noueihed, B., Shahrzad, N., Saint-Dic, D., Hasaj, B., Guan, T. L., Moores, A., Barlowe, C., and Sacher, M. (2012). The SMS domain of Trs23p is responsible for the in vitro appearance of the TRAPPI complex in *Saccharomyces cerevisiae*. *Cell Logist.* *2*, 28–42.
- Brunet, S., and Sacher, M. (2014). In sickness and in health: the role of TRAPP and associated proteins in disease. *Traffic* *15*, 803–818.
- Brunet, S., Shahrzad, N., Saint-Dic, D., Dutczak, H., and Sacher, M. (2013). A trs20 mutation that mimics an SEDT-causing mutation blocks selective and non-selective autophagy: a model for TRAPPIII organization. *Traffic* *14*, 1091–1104.
- Buvelot, F. S. *et al.* (2006). Bioinformatic and comparative localization of Rab proteins reveals functional insights into the uncharacterized GTPases Ypt10p and Ypt11p. *Mol.Cell Biol.* *26*, 7299–7317.
- Cabrera, M., and Ungermann, C. (2013). Guanine nucleotide exchange factors (GEFs) have a critical but not exclusive role in organelle localization of Rab GTPases. *J. Biol. Chem.* *288*, 28704–28712.
- Cai, H., Reinisch, K., and Ferro-Novick, S. (2007a). Coats, tethers, Rabs, and SNAREs work together to mediate the intracellular destination of a transport vesicle. *Dev.Cell* *12*, 671–682.
- Cai, H., Yu, S., Menon, S., Cai, Y., Lazarova, D., Fu, C., Reinisch, K., Hay, J. C., and Ferro-Novick, S. (2007b). TRAPPI tethers COPII vesicles by binding the coat subunit Sec23. *Nature* *445*, 941–944.
- Cai, H., Zhang, Y., Pypaert, M., Walker, L., and Ferro-Novick, S. (2005). Mutants in trs120 disrupt traffic from the early endosome to the late Golgi. *J.Cell Biol.* *171*, 823–833.
- Cai, Y. *et al.* (2008). The structural basis for activation of the Rab Ypt1p by the TRAPP membrane-tethering complexes. *Cell* *133*, 1202–1213.

Calero, M., Chen, C. Z., Zhu, W., Winand, N., Havas, K. A., Gilbert, P. M., Burd, C. G., and Collins, R. N. (2003). Dual Prenylation Is Required for Rab Protein Localization and Function. *Mol. Biol. Cell* 14, 1852–1867.

Chen, S., Cai, H., Park, S.-K., Menon, S., Jackson, C. L., and Ferro-Novick, S. (2011). Trs65p, a subunit of the Ypt1p GEF TRAPP^{II}, interacts with the Arf1p exchange factor Gea2p to facilitate COPI-mediated vesicle traffic. *Mol. Biol. Cell* 22, 3634–3644.

Chen, S., and Tokarev, A. (2005). Ypt31/32 GTPases and their novel F-box effector protein Rcy1 regulate protein recycling. *Mol. Biol. Cell* 16, 178–192.

Chen, Y., and Scheller, R. (2001). SNARE-mediated membrane fusion. *Nat. Rev. Mol. Cell Biol.* 2, 98–106.

Cheong, H., Yorimitsu, T., Reggiori, F., Legakis, J. E., Wang, C. W., and Klionsky, D. J. (2005). Atg17 regulates the magnitude of the autophagic response. *Mol. Biol. Cell* 16, 3438–3453.

Choi, C., Davey, M., Schluter, C., Pandher, P., Fang, Y., Foster, L. J., and Conibear, E. (2011). Organization and assembly of the TRAPP^{II} complex. *Traffic* 12, 715–725.

Conibear, E. (2011). Vesicle transport: springing the TRAPP. *Curr. Biol.* 21, R506–8.

Costanzo, M. *et al.* (2010). The genetic landscape of a cell. *Science* 327, 425–431.

Dunn, W. A. (1990). Studies on the mechanisms of autophagy: formation of the autophagic vacuole. *J. Cell Biol.* 110, 1923–1933.

Esters, H., Alexandrov, K., Iakovenko, A., Ivanova, T., Thoma, N., Rybin, V., Zerial, M., Scheidig, A. J., and Goody, R. S. (2001). Vps9, Rabex-5 and DSS4: proteins with weak but distinct nucleotide-exchange activities for Rab proteins. *J. Mol. Biol.* 310, 141–156.

Faini, M., Beck, R., Wieland, F. T., and Briggs, J. A. (2013). Vesicle coats: structure, function, and general principles of assembly. *Trends Cell Biol.* 23, 279–288.

Fan, S., Feng, Y., Wei, Z., Xia, B., and Gong, W. (2009a). Solution structure of synbindin atypical PDZ domain and interaction with syndecan-2. *Protein Pept. Lett.* 16, 189–195.

Fan, S., Wei, Z., Xu, H., and Gong, W. (2009b). Crystal structure of human synbindin reveals two conformations of longin domain. *Biochem. Biophys. Res. Commun.* 378, 338–343.

Fan, X., and Tang, L. (2013). Aberrant and alternative splicing in skeletal system disease. *Gene* 528, 21–26.

Fasshauer, D., Sutton, R., Brunger, A., and Jahn, R. (1998). Conserved structural features of the synaptic fusion complex: SNARE proteins reclassified as Q- and R-SNAREs. *Proc. Natl. Acad. Sci. U. S. A.* 95, 15781–15786.

- Fotin, A., Cheng, Y., Sliz, P., Grigorieff, N., Harrison, S. C., Kirchhausen, T., and Walz, T. (2004). Molecular model for a complete clathrin lattice from electron cryomicroscopy. *Nature* *432*, 573–579.
- Fromme, J. C., and Schekman, R. (2005). COPII-coated vesicles: flexible enough for large cargo? *Curr. Opin. Cell Biol.* *17*, 345–352.
- Garrett, M., Zahner, J., Cheney, C., and Novick, P. (1994). GDI1 encodes a GDP dissociation inhibitor that plays an essential role in the yeast secretory pathway. *EMBO J.* *1*, 1718–1728.
- Gavin, A., Bösch, M., Krause, R., and Grandi, P. (2002). Functional organization of the yeast proteome by systematic analysis of protein complexes. *Nature* *415*, 141–147.
- Gecz, J., Shaw, M. A., Bellon, J. R., de Barros, L. M., Barros, M. De, and Ge, J. (2003). Human wild-type SEDL protein functionally complements yeast Trs20p but some naturally occurring SEDL mutants do not. *Gene.* *320*, 137–144.
- Gedeon, a K., Colley, a, Jamieson, R., Thompson, E. M., Rogers, J., Sillence, D., Tiller, G. E., Mulley, J. C., and Géc, J. (1999). Identification of the gene (SEDL) causing X-linked spondyloepiphyseal dysplasia tarda. *Nat. Genet.* *22*, 400–404.
- Gedeon, A. K. *et al.* (2001). The molecular basis of X-linked spondyloepiphyseal dysplasia tarda. *Am.J.Hum.Genet.* *68*, 1386–1397.
- Gillingham, A. K., and Munro, S. (2003). Long coiled-coil proteins and membrane traffic. *Biochim. Biophys. Acta* *1641*, 71–85.
- Gonzalez Jr., L. C., Weis, W. I., and Scheller, R. H. (2001). A novel snare N-terminal domain revealed by the crystal structure of Sec22b. *J.Biol.Chem.* *276*, 24203–24211.
- Grosshans, B. L., Ortiz, D., and Novick, P. (2006). Rabs and their effectors: achieving specificity in membrane traffic. *Proc. Natl. Acad. Sci. U. S. A.* *103*, 11821–11827.
- Hanson, P., Roth, R., Morisaki, H., Jahn, R., and Heuser, J. (1997). Structure and conformational changes in NSF and its membrane receptor complexes visualized by quick-freeze/deep-etch electron microscopy. *Cell* *90*, 523–535.
- Hara-Kuge, S., Kuge, O., Orci, L., Amherdt, M., Ravazzola, M., Wieland, F. T., and Rothman, J. E. (1994). En bloc incorporation of coatamer subunits during the assembly of COP-coated vesicles. *J. Cell Biol.* *124*, 883–892.
- Harding, T. M., Morano, K. a, Scott, S. V, and Klionsky, D. J. (1995). Isolation and characterization of yeast mutants in the cytoplasm to vacuole protein targeting pathway. *J. Cell Biol.* *131*, 591–602.

Hehnly, H., and Stamnes, M. (2007). Regulating cytoskeleton-based vesicle motility Heidi. *FEBS Lett.* *581*, 2112–2118.

Ho, Y. *et al.* (2002). Systematic identification of protein complexes in *Saccharomyces cerevisiae* by mass spectrometry. *Nature* *415*, 180–183.

Hoppins, S., Collins, S. R., Cassidy-Stone, A., Hummel, E., DeVay, R. M., Lackner, L. L., Westermann, B., Schuldiner, M., Weissman, J. S., and Nunnari, J. (2011). A mitochondrial-focused genetic interaction map reveals a scaffold-like complex required for inner membrane organization in mitochondria. *J. Cell Biol.* *195*, 323–340.

Hou, H., Subramanian, K., LaGrassa, T. J., Markgraf, D., Dietrich, L. E., Urban, J., Decker, N., and Ungermann, C. (2005). The DHHC protein Pfa3 affects vacuole-associated palmitoylation of the fusion factor Vac8. *Proc.Natl.Acad.Sci.U.S.A.* *102*, 17366–17371.

Jackson, L. P., Kümmel, D., Reinisch, K. M., and Owen, D. J. (2012). Structures and mechanisms of vesicle coat components and multisubunit tethering complexes. *Curr. Opin. Cell Biol.* *24*, 475–483.

Jang, S. B., Kim, Y.-G. G., Cho, Y.-S. S., Suh, P.-G. G., Kim, K.-H. H., and Oh, B.-H. H. (2002). Crystal structure of SEDL and its implications for a genetic disease spondyloepiphyseal dysplasia tarda. *J.Biol.Chem.* *277*, 49863–49869.

Jedd, G., Richardson, C., Litt, R., and Segev, N. (1995). The Ypt1 GTPase is essential for the first two steps of the yeast secretory pathway. *J.Cell Biol.* *131*, 583–590.

Jiang, Y., Scarpa, a, Zhang, L., Stone, S., Feliciano, E., and Ferro-Novick, S. (1998). A high copy suppressor screen reveals genetic interactions between BET3 and a new gene. Evidence for a novel complex in ER-to-Golgi transport. *Genetics* *149*, 833–841.

Jones, S., Newman, C., Liu, F., and Segev, N. (2000). The TRAPP complex is a nucleotide exchanger for Ypt1 and Ypt31/32. *Mol.Biol.Cell* *11*, 4403–4411.

Kakuta, S., Yamamoto, H., Negishi, L., Kondo-Kakuta, C., Hayashi, N., and Ohsumi, Y. (2012). Atg9 vesicles recruit vesicle-tethering proteins, Trs85 and Ypt1, to the autophagosome formation site. *J.Biol.Chem.* *287*, 44261–44269.

Kamada, Y., Funakoshi, T., Shintani, T., Nagano, K., Ohsumi, M., and Ohsumi, Y. (2000). Tor-mediated induction of autophagy via an Apg1 protein kinase complex. *J. Cell Biol.* *150*, 1507–1513.

Kawamata, T., and Kamada, Y. (2008). Organization of the pre-autophagosomal structure responsible for autophagosome formation. *Mol. Biol. Cell* *19*, 2039–2050.

- Kawamura, S., Nagano, M., Toshima, J. Y., and Toshima, J. (2014). Analysis of subcellular localization and function of the yeast Rab6 homologue, Ypt6p, using a novel amino-terminal tagging strategy. *Biochem. Biophys. Res. Commun.* *450*, 519–525.
- Kim, D. W., Sacher, M., Scarpa, A., Quinn, A. M., and Ferro-Novick, S. (1999). High-copy suppressor analysis reveals a physical interaction between Sec34p and Sec35p, a protein implicated in vesicle docking. *Mol.Biol.Cell* *10*, 3317–3329.
- Kim, Y.-G., Raunser, S., Munger, C., Wagner, J., Song, Y.-L., Cygler, M., Walz, T., Oh, B.-H., and Sacher, M. (2006). The architecture of the multisubunit TRAPPI complex suggests a model for vesicle tethering. *Cell* *127*, 817–830.
- Kim, Y.-G., Sohn, E. J., Seo, J., Lee, K.-J., Lee, H.-S., Hwang, I., Whiteway, M., Sacher, M., and Oh, B.-H. (2005). Crystal structure of bet3 reveals a novel mechanism for Golgi localization of tethering factor TRAPP. *Nat. Struct. Mol. Biol.* *12*, 38–45.
- Kirchhausen, T. (2000). Three ways to make a vesicle. *Nat. Rev. Mol. Cell Biol.* *1*, 187–198.
- Klionsky, D. J., Cueva, R., and Yaver, D. S. (1992). Aminopeptidase I of *Saccharomyces cerevisiae* is localized to the vacuole independent of the secretory pathway. *J.Cell Biol.* *119*, 287–299.
- Klumperman, J. (2011). Architecture of the mammalian Golgi. *Cold Spring Harb. Perspect. Biol.* *3*.
- Krogan, N. J. *et al.* (2006). Global landscape of protein complexes in the yeast *Saccharomyces cerevisiae*. *Nature* *440*, 637–643.
- Kummel, D., Heinemann, U., and Veit, M. (2006). Unique self-palmitoylation activity of the transport protein particle component Bet3: a mechanism required for protein stability. *Proc.Natl.Acad.Sci.U.S.A.* *103*, 12701–12706.
- Kümmel, D., Oeckinghaus, A., Wang, C., Krappmann, D., and Heinemann, U. (2008). Distinct isocomplexes of the TRAPP trafficking factor coexist inside human cells. *FEBS Lett.* *582*, 3729–3733.
- Kummel, D., Walter, J., Heck, M., Heinemann, U., and Veit, M. (2010). Characterization of the self-palmitoylation activity of the transport protein particle component Bet3. *Cell Mol.Life.Sci.* *67*, 2653–2664.
- Lafourcade, C., Galan, J.-M., Gloor, Y., Haguenaer-Tsapis, R., and Peter, M. (2004). The GTPase-activating enzyme Gyp1p is required for recycling of internalized membrane material by inactivation of the Rab/Ypt GTPase Ypt1p. *Mol. Cell. Biol.* *24*, 3815–3826.

- Lafourcade, C., Galan, J.-M., and Peter, M. (2003). Opposite roles of the F-box protein Rcy1p and the GTPase-activating protein Gyp2p during recycling of internalized proteins in yeast. *Genetics* 164, 469–477.
- Lee, M. C., and Miller, E. A. (2007). Molecular mechanisms of COPII vesicle formation. *Semin. Dev. Biol.* 18, 424–434.
- Lemmon, S., and Traub, L. (2000). Sorting in the endosomal system in yeast and animal cells. *Curr. Opin. Cell Biol.* 12, 457–466.
- Lewis, M. J., Nichols, B. J., Prescianotto-Baschong, C., Riezman, H., and Pelham, H. R. B. (2000). Specific retrieval of the exocytic SNARE Snc1p from early yeast endosomes. *Mol. Biol. Cell* 11, 23–38.
- Li, B., and Warner, J. (1998). Genetic interaction between YPT6 and YPT1 in *Saccharomyces cerevisiae*. *Yeast* 922, 915–922.
- Liang, Y., and Morozova, N. (2007). The role of Trs65 in the Ypt/Rab guanine nucleotide exchange factor function of the TRAPP II complex. *Mol. Biol. Cell* 18, 2533–2541.
- Lin, R., and Scheller, R. (1997). Structural organization of the synaptic exocytosis core complex. *Neuron* 19, 1087–1094.
- Lipatova, Z., Belogortseva, N., Zhang, X. Q., Kim, J., Taussig, D., and Segev, N. (2012). Regulation of selective autophagy onset by a Ypt/Rab GTPase module. *Proc. Natl. Acad. Sci. U.S.A.* 109, 6981–6986.
- Lipatova, Z., Shah, A. H., Kim, J. J., Mulholland, J. W., and Segev, N. (2013). Regulation of ER-phagy by a Ypt/Rab GTPase module. *Mol. Biol. Cell* 24, 3133–3144.
- Liu, Y.-W., Lee, S.-W., and Lee, F.-J. S. (2006). Arl1p is involved in transport of the GPI-anchored protein Gas1p from the late Golgi to the plasma membrane. *J. Cell Sci.* 119, 3845–3855.
- Loh, E., Peter, F., Subramaniam, V. N., and Hong, W. (2005). Mammalian Bet3 functions as a cytosolic factor participating in transport from the ER to the Golgi apparatus. *J. Cell Sci.* 118, 1209–1222.
- Longtine, M. S., McKenzie III, A., Demarini, D. J., Shah, N. G., Wach, A., Brachat, A., Philippsen, P., and Pringle, J. R. (1998). Additional modules for versatile and economical PCR-based gene deletion and modification in *Saccharomyces cerevisiae*. *Yeast* 961, 953–961.
- Lord, C., Bhandari, D., Menon, S., Ghassemian, M., Nycz, D., Hay, J., Ghosh, P., and Ferro-Novick, S. (2011). Sequential interactions with Sec23 control the direction of vesicle traffic. *Nature* 473, 181–186.

- Losev, E., Reinke, C. a, Jellen, J., Strongin, D. E., Bevis, B. J., and Glick, B. S. (2006). Golgi maturation visualized in living yeast. *Nature* *441*, 1002–1006.
- Luo, Z., and Gallwitz, D. (2003). Biochemical and genetic evidence for the involvement of yeast Ypt6-GTPase in protein retrieval to different Golgi compartments. *J. Biol. Chem.* *278*, 791–799.
- Lynch-Day, M. A., Bhandari, D., Menon, S., Huang, J., Cai, H., Bartholomew, C. R., Brumell, J. H., Ferro-Novick, S., and Klionsky, D. J. (2010). Trs85 directs a Ypt1 GEF, TRAPP^{III}, to the phagophore to promote autophagy. *Proc.Natl.Acad.Sci.U.S.A* *107*, 7811–7816.
- Matsuura-Tokita, K., Takeuchi, M., Ichihara, A., Mikuriya, K., and Nakano, A. (2006). Live imaging of yeast Golgi cisternal maturation. *Nature* *441*, 1007–1010.
- McMahon, H. T., and Mills, I. G. (2004). COP and clathrin-coated vesicle budding: different pathways, common approaches. *Curr. Opin. Cell Biol.* *16*, 379–391.
- McNew, J. A., Sogaard, M., Lampen, N. M., Machida, S., Ye, R. R., Lacomis, L., Tempst, P., Rothman, J. E., and Sollner, T. H. (1997). Ykt6p, a prenylated SNARE essential for endoplasmic reticulum-Golgi transport. *J.Biol.Chem.* *272*, 17776–17783.
- Meiling-Wesse, K., Epple, U. D., Krick, R., Barth, H., Appelles, A., Voss, C., Eskelinen, E.-L., and Thumm, M. (2005). Trs85 (Gsg1), a component of the TRAPP complexes, is required for the organization of the preautophagosomal structure during selective autophagy via the Cvt pathway. *J.Biol.Chem.* *280*, 33669–33678.
- Menon, S., Cai, H., Lu, H., Dong, G., Cai, Y., Reinisch, K., and Ferro-Novick, S. (2006). mBET3 is required for the organization of the TRAPP complexes. *Biochem.Biophys.Res.Commun.* *350*, 669–677.
- Miller, E., Antonny, B., Hamamoto, S., and Schekman, R. (2002). Cargo selection into COPII vesicles is driven by the Sec24p subunit. *EMBO J.* *21*, 6105–6113.
- Mizushima, N., and Klionsky, D. J. (2007). Protein turnover via autophagy: implications for metabolism. *Annu. Rev. Nutr.* *27*, 19–40.
- Von Mollard, G. F., Nothwehr, S. F., and Stevens, T. H. (1997). The yeast v-SNARE Vti1p mediates two vesicle transport pathways through interactions with the t-SNAREs Sed5p and Pep12p. *J.Cell Biol.* *137*, 1511–1524.
- Montpetit, B., and Conibear, E. (2009). Identification of the novel TRAPP associated protein Tca17. *Traffic* *10*, 713–723.
- Morozova, N., Liang, Y., Tokarev, A. A., Chen, S. H., Cox, R., Andrejic, J., Lipatova, Z., Sciorra, V. A., Emr, S. D., and Segev, N. (2006). TRAPP^{II} subunits are required for the specificity switch of a Ypt-Rab GEF. *Nat.Cell Biol.* *8*, 1263–1269.

- Munro, S. (2005). The Golgi apparatus: defining the identity of Golgi membranes. *Curr. Opin. Cell Biol.* *17*, 395–401.
- Nazarko, T. Y., Huang, J., Nicaud, J. M., Klionsky, D. J., and Sibirny, A. A. (2005). Trs85 is Required for Macroautophagy, Pexophagy and Cytoplasm to Vacuole Targeting in *Yarrowia lipolytica* and *Saccharomyces cerevisiae*. *Autophagy* *1*, 37–45.
- Noda, T., Kim, J., Huang, W. P., Baba, M., Tokunaga, C., Ohsumi, Y., and Klionsky, D. J. (2000). Apg9p/Cvt7p is an integral membrane protein required for transport vesicle formation in the Cvt and autophagy pathways. *J. Cell Biol.* *148*, 465–480.
- Nottingham, R. M., and Pfeffer, S. R. (2009). Defining the boundaries: Rab GEFs and GAPs. *Proc. Natl. Acad. Sci. U.S.A.* *106*, 14185–14186.
- Novick, P., Field, C., and Schekman, R. (1980). Identification of 23 complementation groups required for post-translational events in the yeast secretory pathway. *Cell* *21*, 205–215.
- Ohashi, Y., and Munro, S. (2010). Membrane Delivery to the Yeast Autophagosome from the Golgi–Endosomal System. *Mol. Biol. Cell* *21*, 3998–4008.
- Ortiz, D., Medkova, M., Walch-Solimena, C., and Novick, P. (2002). Ypt32 recruits the Sec4p guanine nucleotide exchange factor, Sec2p, to secretory vesicles; evidence for a Rab cascade in yeast. *J. Cell Biol.* *157*, 1005–1015.
- Palade, G. (1975). Intracellular aspects of the process of protein synthesis. *Science* *189*, 347–358.
- Pan, X., Eathiraj, S., Munson, M., and Lambright, D. G. (2006). TBC-domain GAPs for Rab GTPases accelerate GTP hydrolysis by a dual-finger mechanism. *Nature* *442*, 303–306.
- Peplowska, K., Markgraf, D. F., Ostrowicz, C. W., Bange, G., and Ungermann, C. (2007). The CORVET tethering complex interacts with the yeast Rab5 homolog Vps21 and is involved in endo-lysosomal biogenesis. *Dev. Cell* *12*, 739–750.
- Peyroche, a, Paris, S., and Jackson, C. L. (1996). Nucleotide exchange on ARF mediated by yeast Gea1 protein. *Nature* *384*, 479–481.
- Pfeffer, S. R. (2001). Rab GTPases: specifying and deciphering organelle identity and function. *Trends Cell Biol.* *11*, 487–491.
- Pokrovskaya, I. D., Willett, R., Smith, R. D., Morelle, W., Kudlyk, T., and Lupashin, V. V (2011). COG complex specifically regulates the maintenance of Golgi glycosylation machinery. *Glycobiology* *21*, 1554-1569.
- Poon, P., Cassel, D., and Spang, A. (1999). Retrograde transport from the yeast Golgi is mediated by two ARF GAP proteins with overlapping function. *EMBO J.* *18*, 555–564.

Poon, P., Wang, X., and Rotman, M. (1996). *Saccharomyces cerevisiae* Gcs1 is an ADP-ribosylation factor GTPase-activating protein. *Proc. Natl. Acad. Sci. U.S.A.* *93*, 10074–10077.

Ragusa, M., Stanley, R., and Hurley, J. (2012). Architecture of the Atg17 complex as a scaffold for autophagosome biogenesis. *Cell* *151*, 1501–1512.

Reggiori, F., and Klionsky, D. J. (2013). Autophagic processes in yeast: mechanism, machinery and regulation. *Genetics* *194*, 341–361.

Reggiori, F., Wang, C., Nair, U., Shintani, T., Abeliovich, H., and Klionsky, D. J. (2004). Early stages of the secretory pathway, but not endosomes, are required for Cvt vesicle and autophagosome assembly in *Saccharomyces cerevisiae*. *Mol. Biol. Cell* *15*, 2189–2204.

Rivera-Molina, F. E., and Novick, P. J. (2009). A Rab GAP cascade defines the boundary between two Rab GTPases on the secretory pathway. *Proc. Natl. Acad. Sci. U. S. A.* *106*, 14408–14413.

Robinson, M., and Poon, P. (2006). The Gcs1 Arf-GAP mediates Snc1, 2 v-SNARE retrieval to the Golgi in yeast. *Mol. Biol. Cell* *17*, 1845–1858.

Roskoski Jr., R. (2003). Protein prenylation: a pivotal posttranslational process. *Biochem. Biophys. Res. Commun.* *303*, 1–7.

Rossi, G., Kolstad, K., Stone, S., Palluault, F., and Ferro-Novick, S. (1995). BET3 encodes a novel hydrophilic protein that acts in conjunction with yeast SNAREs. *Mol. Biol. Cell* *6*, 1769–1780.

Rothman, J., and Warren, G. (1994). Implications of the SNARE hypothesis for intracellular membrane topology and dynamics. *Curr. Biol.* *4*, 220–233.

Sacher, M. *et al.* (1998). TRAPP, a highly conserved novel complex on the cis-Golgi that mediates vesicle docking and fusion. *EMBO J.* *17*, 2494–2503.

Sacher, M., Barrowman, J., Schieltz, D., Yates, J. R., Ferro-Novick, S., and Yates III, J. R. (2000). Identification and characterization of five new subunits of TRAPP. *Eur. J. Cell Biol.* *79*, 71–80.

Sacher, M., Barrowman, J., Wang, W., Horecka, J., Zhang, Y., Pypaert, M., and Ferro-Novick, S. (2001). TRAPPI implicated in the specificity of tethering in ER-to-Golgi transport. *Mol. Cell* *7*, 433–442.

Sacher, M., Kim, Y.-G., Lavie, A., Oh, B.-H., and Segev, N. (2008). The TRAPP complex: insights into its architecture and function. *Traffic* *9*, 2032–2042.

Schledzewski, K., Brinkmann, H., and Mendel, R. R. (1999). Phylogenetic analysis of components of the eukaryotic vesicle transport system reveals a common origin of adaptor

protein complexes 1, 2, and 3 and the F subcomplex of the coatomer COPI. *Journal of molecular evolution* 48, 770-778.

Schmidt, K., and Stephens, D. J. (2010). Cargo loading at the ER. *Mol.Membr.Biol.* 27, 398-411.

Schweizer, A., Fransen, J. A., Matter, K., Kreis, T. E., Ginsel, L., and Hauri, H. P. (1990). Identification of an intermediate compartment involved in protein transport from endoplasmic reticulum to Golgi apparatus. *Eur.J.Cell Biol.* 53, 185-196.

Sciorra, V. a, Audhya, A., Parsons, A. B., Segev, N., Boone, C., and Emr, S. D. (2005). Synthetic genetic array analysis of the PtdIns 4-kinase Pik1p identifies components in a Golgi-specific Ypt31/rab-GTPase signaling pathway. *Mol. Biol. Cell* 16, 776-793.

Sclafani, A., Chen, S., Rivera-Molina, F., Reinisch, K., Novick, P., and Ferro-Novick, S. (2010). Establishing a role for the GTPase Ypt1p at the late Golgi. *Traffic* 11, 520-532.

Scott, S. V, Baba, M., Ohsumi, Y., and Klionsky, D. J. (1997). Aminopeptidase I is targeted to the vacuole by a nonclassical vesicular mechanism. *J. Cell Biol.* 138, 37-44.

Scott, S. V, Hefner-Gravink, A., Morano, K. A., Noda, T., Ohsumi, Y., and Klionsky, D. J. (1996). Cytoplasm-to-vacuole targeting and autophagy employ the same machinery to deliver proteins to the yeast vacuole. *Proc.Natl.Acad.Sci.U.S.A.* 93, 12304-12308.

Scrivens, P. J., Noueihed, B., Shahrzad, N., Hul, S., Brunet, S., and Sacher, M. (2011). C4orf41 and TTC-15 are mammalian TRAPP components with a role at an early stage in ER-to-Golgi trafficking. *Mol.Biol.Cell* 22, 2083-2093.

Scrivens, P. J., Shahrzad, N., Moores, A., Morin, A., Brunet, S., and Sacher, M. (2009). TRAPPC2L is a novel, highly conserved TRAPP-interacting protein. *Traffic* 10, 724-736.

Seabra, M. C., and Wasmeier, C. (2004). Controlling the location and activation of Rab GTPases. *Curr. Opin. Cell Biol.* 16, 451-457.

Segev, N., Mulholland, J., and Botstein, D. (1988). The yeast GTP-binding YPT1 protein and a mammalian counterpart are associated with the secretion machinery. *Cell* 52, 915-924.

Sekito, T., Kawamata, T., Ichikawa, R., Suzuki, K., and Ohsumi, Y. (2009). Atg17 recruits Atg9 to organize the pre-autophagosomal structure. *Genes.Cells.* 14, 525-538.

Serafini, T., Orci, L., Amherdt, M., Brunner, M., Kahn, R. a, and Rothman, J. E. (1991). ADP-ribosylation factor is a subunit of the coat of Golgi-derived COP-coated vesicles: a novel role for a GTP-binding protein. *Cell* 67, 239-253.

Shaw, M. A., Brunetti-Pierri, N., Kadasi, L., Kovacova, V., Van, M. L., De, B. D., Salerno, M., and Gecz, J. (2003). Identification of three novel SEDL mutations, including mutation in the rare, non-canonical splice site of exon 4. *Clin.Genet.* *64*, 235–242.

Shintani, T., Huang, W.-P. P., Stromhaug, P. E., and Klionsky, D. J. (2002). Mechanism of cargo selection in the cytoplasm to vacuole targeting pathway. *Dev.Cell* *3*, 825–837.

Short, B., Haas, A., and Barr, F. a (2005). Golgins and GTPases, giving identity and structure to the Golgi apparatus. *Biochim. Biophys. Acta* *1744*, 383–395.

Siniooglou, S., Peak-Chew, S. Y., and Pelham, H. R. B. (2000). Ric1p and Rgp1p form a complex that catalyses nucleotide exchange on Ypt6p. *Eur. Mol. Biol. Organ. J.* *19*, 4885–4894.

Solinger, J. a, and Spang, A. (2013). Tethering complexes in the endocytic pathway: CORVET and HOPS. *FEBS J.* *280*, 2743–2757.

Sollner, T., Whiteheart, S. W., Brunner, M., Erdjument-Bromage, H., Geromanos, S., Tempst, P., and Rothman, J. E. (1993). SNAP receptors implicated in vesicle targeting and fusion. *Nature* *362*, 318–324.

Stachowiak, J., Brodsky, F., and Miller, E. (2013). A cost-benefit analysis of the physical mechanisms of membrane curvature. *Nat. Cell Biol.* *15*, 1–18.

Stagg, S. M., Gurkan, C., Fowler, D. M., LaPointe, P., Foss, T. R., Potter, C. S., Carragher, B., and Balch, W. E. (2006). Structure of the Sec13/31 COPII coat cage. *Nature.* *439*, 234–238.

Stamnes, M. a, and Rothman, J. E. (1993). The binding of AP-1 clathrin adaptor particles to Golgi membranes requires ADP-ribosylation factor, a small GTP-binding protein. *Cell* *73*, 999–1005.

Stevens, T., Esmon, B., and Schekman, R. (1982). Early stages in the yeast secretory pathway are required for transport of carboxypeptidase Y to the vacuole. *Cell* *30*, 439–448.

Strom, M., Vollmer, P., Tan, T., and Gallwitz, D. (1993). A yeast GTPase-activating protein that interacts specifically with a member of the Ypt/Rab family. *Nature* *361*, 736–737.

Suda, Y., Kurokawa, K., Hirata, R., and Nakano, A. (2013). Rab GAP cascade regulates dynamics of Ypt6 in the Golgi traffic. *Proc. Natl. Acad. Sci. U.S.A.* *110*, 18976–18981.

Suda, Y., and Nakano, A. (2012). The yeast Golgi apparatus. *Traffic* *13*, 505–510.

Suzuki, K., Kirisako, T., Kamada, Y., Mizushima, N., Noda, T., and Ohsumi, Y. (2001). The pre-autophagosomal structure organized by concerted functions of APG genes is essential for autophagosome formation. *EMBO J.* *20*, 5971–5981.

Sztul, E., and Lupashin, V. (2006). Role of tethering factors in secretory membrane traffic. *Am. J. Physiol. Cell Physiol.* *290*, C11–26.

Sztul, E., and Lupashin, V. (2009). Role of vesicle tethering factors in the ER-Golgi membrane traffic. *FEBS.Lett.* *583*, 3770–3783.

Tai, G., Lu, L., Wang, T. L., Tang, B. L., Goud, B., Johannes, L., and Hong, W. (2004). Participation of the syntaxin 5/Ykt6/GS28/GS15 SNARE complex in transport from the early/recycling endosome to the trans-Golgi network. *Mol.Biol.Cell* *15*, 4011–4022.

Takamori, S. *et al.* (2006). Molecular anatomy of a trafficking organelle. *Cell* *127*, 831–846.

Tan, D., Cai, Y., Wang, J., Zhang, J., Menon, S., Chou, H.-T., Ferro-Novick, S., Reinisch, K. M., and Walz, T. (2013). The EM structure of the TRAPP III complex leads to the identification of a requirement for COPII vesicles on the macroautophagy pathway. *Proc. Natl. Acad. Sci. U. S. A.* *110*, 19432–19437.

Taussig, D., Lipatova, Z., and Segev, N. (2013). Trs20 is required for TRAPP III complex assembly at the PAS and its function in autophagy. *Traffic* *15*, 327–337.

Taylor, R., Chen, P.-H., Chou, C.-C., Patel, J., and Jin, S. V (2012). KCS1 deletion in *Saccharomyces cerevisiae* leads to a defect in translocation of autophagic proteins and reduces autophagosome formation. *Autophagy* *8*, 1300–1311.

Thumm, M., Egner, R., Koch, B., Schlumpberger, M., Straub, M., Veenhuis, M., and Wolf, D. H. (1994). Isolation of autophagocytosis mutants of *Saccharomyces cerevisiae*. *FEBS Lett.* *349*, 275–280.

Tiller, G. E., Hannig, V. L., Dozier, D., Carrel, L., Trevarthen, K. C., Wilcox, W. R., Mundlos, S., Haines, J. L., Gedeon, A. K., and Gecz, J. (2001). A recurrent RNA-splicing mutation in the *SEDL* gene causes X-linked spondyloepiphyseal dysplasia tarda. *Am.J.Hum.Genet.* *68*, 1398–1407.

Tochio, H., Tsui, M. M., Banfield, D. K., and Zhang, M. (2001). An autoinhibitory mechanism for nonsyntaxin SNARE proteins revealed by the structure of Ykt6p. *Science* *293*, 698–702.

Tokarev, A. A., Taussig, D., Sundaram, G., Lipatova, Z., Liang, Y., Mulholland, J. W., and Segev, N. (2009). TRAPP II complex assembly requires Trs33 or Trs65. *Traffic* *10*, 1831–1844.

Tong, A. H. Y. *et al.* (2004). Global mapping of the yeast genetic interaction network. *Science* *303*, 808–813.

Tooze, S. A., and Yoshimori, T. (2010). The origin of the autophagosomal membrane. *Nat.Cell Biol.* *12*, 831–835.

- Tsui, M. M., Tai, W. C., and Banfield, D. K. (2001). Selective formation of Sed5p-containing SNARE complexes is mediated by combinatorial binding interactions. *Mol.Biol.Cell* 12, 521–538.
- Tsukada, M., and Ohsumi, Y. (1993). Isolation and characterization of autophagy-defective mutants of *Saccharomyces cerevisiae*. *FEBS Lett.* 333, 169–174.
- Turnbull, A. P. *et al.* (2005). Structure of palmitoylated BET3: insights into TRAPP complex assembly and membrane localization. *EMBO J.* 24, 875–884.
- Ungermann, C., von Mollard, G. F., Jensen, O. N., Margolis, N., Stevens, T. H., and Wickner, W. (1999). Three v-SNAREs and two t-SNAREs, present in a pentameric cis-SNARE complex on isolated vacuoles, are essential for homotypic fusion. *J.Cell Biol.* 145, 1435–1442.
- Valdivia, R. H., Baggott, D., Chuang, J. S., and Schekman, R. W. (2002). The yeast clathrin adaptor protein complex 1 is required for the efficient retention of a subset of late Golgi membrane proteins. *Dev.Cell* 2, 283–294.
- Vasile, E., Oka, T., Ericsson, M., Nakamura, N., and Krieger, M. (2006). IntraGolgi distribution of the Conserved Oligomeric Golgi (COG) complex. *Exp.Cell Res.* 312, 3132–3141.
- Venditti, R. *et al.* (2012). Sedlin Controls the ER Export of Procollagen by Regulating the Sar1 Cycle. *Science* 337, 1668–1672.
- Wan, J., Roth, A. F., Bailey, A. O., and Davis, N. G. (2007). Palmitoylated proteins: purification and identification. *Nat.Protoc.* 2, 1573–1584.
- Wang, J., Menon, S., Yamasaki, A., Chou, H.-T., Walz, T., Jiang, Y., and Ferro-Novick, S. (2013). Ypt1 recruits the Atg1 kinase to the preautophagosomal structure. *Proc. Natl. Acad. Sci. U. S. A.* 110, 9800–9805.
- Wang, W., and Ferro-Novick, S. (2002). A Ypt32p exchange factor is a putative effector of Ypt1p. *Mol. Biol. Cell* 13, 3336–3343.
- Wang, W., Sacher, M., and Ferro-Novick, S. (2000). TRAPP Stimulates Guanine Nucleotide Exchange on Ypt1p. *J.Cell Biol.* 151, 289–296.
- Weber, T., Zemelman, B., and McNew, J. (1998). SNAREpins: minimal machinery for membrane fusion. *Cell* 92, 759–772.
- Whyte, J. R. C., and Munro, S. (2002). Vesicle tethering complexes in membrane traffic. *J. Cell Sci.* 115, 2627–2637.
- Whyte, J. R., and Munro, S. (2001). The Sec34/35 Golgi transport complex is related to the exocyst, defining a family of complexes involved in multiple steps of membrane traffic. *Dev. Cell* 1, 527–537.

Will, E., and Gallwitz, D. (2001). Biochemical characterization of Gyp6p, a Ypt/Rab-specific GTPase-activating protein from yeast. *J. Biol. Chem.* *276*, 12135–12139.

Williams, A. L., Ehm, S., Jacobson, N. C., Xu, D., and Hay, J. C. (2004). rsly1 binding to syntaxin 5 is required for endoplasmic reticulum-to-Golgi transport but does not promote SNARE motif accessibility. *Mol.Biol.Cell* *15*, 162–175.

Xu, D., and Hay, J. C. (2004). Reconstitution of COPII vesicle fusion to generate a pre-Golgi intermediate compartment. *J. Cell Biol.* *167*, 997–1003.

Xu, Y., Martin, S., James, D. E., and Hong, W. (2002). GS15 forms a SNARE complex with syntaxin 5, GS28, and Ykt6 and is implicated in traffic in the early cisternae of the Golgi apparatus. *Mol.Biol.Cell* *13*, 3493–3507.

Yamamoto, H., Kakuta, S., Watanabe, T. M., Kitamura, A., Sekito, T., Kondo-Kakuta, C., Ichikawa, R., Kinjo, M., and Ohsumi, Y. (2012). Atg9 vesicles are an important membrane source during early steps of autophagosome formation. *J. Cell Biol.* *198*, 219–233.

Yamamoto, K., and Jigami, Y. (2002). Mutation of TRS130, which encodes a component of the TRAPP II complex, activates transcription of OCH1 in *Saccharomyces cerevisiae*. *Curr. Genet.* *42*, 85–93.

Yamasaki, A., Menon, S., Yu, S., Barrowman, J., Meerloo, T., Oorschot, V., Klumperman, J., Satoh, A., and Ferro-Novick, S. (2009). mTrs130 Is a Component of a Mammalian TRAPP II Complex, a Rab1 GEF That Binds to COPI-coated Vesicles. *Mol. Biol. Cell* *20*, 4205–4215.

Ye, M., Chen, Y., Zou, S., Yu, S., and Liang, Y. (2014). Ypt1 suppresses defects of vesicle trafficking and autophagy in Ypt6 related mutants. *Cell Biol. Int.* *38*, 663–674.

Yip, C. K., Berscheminski, J., and Walz, T. (2010). Molecular architecture of the TRAPP II complex and implications for vesicle tethering. *Nat. Struct. Mol. Biol.* *17*, 1298–1304.

Yu, I. M., and Hughson, F. M. (2010). Tethering factors as organizers of intracellular vesicular traffic. *Annu. Rev. Cell Dev. Biol.* *26*, 137–156.

Yu, S., Satoh, A., Pypaert, M., Mullen, K., Hay, J. C., and Ferro-Novick, S. (2006). mBet3p is required for homotypic COPII vesicle tethering in mammalian cells. *J. Cell Biol.* *174*, 359–368.

Zerial, M., and McBride, H. (2001). Rab proteins as membrane organizers. *Nat. Rev. Mol. Cell Biol.* *2*, 107–117.

Zong, M., Wu, X. gang, Chan, C. W. L., Choi, M. Y., Chan, H. C., Tanner, J. A., and Yu, S. (2011). The adaptor function of TRAPPC2 in mammalian TRAPPs explains TRAPPC2-associated SEDT and TRAPPC9-associated congenital intellectual disability. *PLoS One.* *6*, e23350.

Zou, S. *et al.* (2012a). Trs130 Participates in Autophagy Through GTPases Ypt31/32 in *Saccharomyces cerevisiae*. *Traffic* *14*, 233-246.

Zou, S., Liu, Y., Zhang, X. Q., Chen, Y., Ye, M., Zhu, X., Yang, S., Lipatova, Z., Liang, Y., and Segev, N. (2012b). Modular TRAPP complexes regulate intracellular protein trafficking through multiple Ypt/Rab GTPases in *Saccharomyces cerevisiae*. *Genetics* *191*, 451–460.

Zou, S., Chen, Y., Liu, Y., Segev, N., and Yu, S. (2013). Trs130 participates in autophagy through GTPases Ypt31/32 in *Saccharomyces cerevisiae*. *Traffic* *14*, 233–246.